PB-239 864

IN-STACK TRANSMISSOMETER MEASUREMENT OF PARTICULATE OPACITY AND MASS CONCENTRATION

E. Reisman, et al

Philco-Ford Corporation

Prepared for:

National Environmental Research Center

November 1974

DISTRIBUTED BY:

NTIS

National Technical Information Service
U. S. DEPARTMENT OF COMMERCE

BIBLIOGRAPHIC DATA SHEET	1. Report No. EPA-650/2-74-120	2.	PB 239 864

4. Title and Subtitle
In-Stack Transmissometer Measurement of Particulate Opacity and Mass Concentration

5. Report Date
November 1974

6.

7. Author(s)
E. Reisman, W. D. Gerber, N. D. Potter

8. Performing Organization Rept. No.

9. Performing Organization Name and Address
Philco-Ford Corporation
Aeronutronic Division
Newport Beach, California 92663

10. Project/Task/Work Unit No.

11. Contract/Grant No.
EPA 68-02-1229

12. Sponsoring Organization Name and Address
EPA, Chemistry and Physics Laboratory
National Environmental Research Center
Research Triangle Park, North Carolina 27711

13. Type of Report & Period Covered
Final Report

14.

15. Supplementary Notes
APTIC # 75084

16. Abstracts The objectives of the program were to evaluate the light transmission approach to monitoring particulate pollution and to determine the reliability and degree of correlation of the transmissometer and other particulate measurement methods in a variety of industrial environments. The six industrial environments were as follows: (1) A petroleum refinery catalytic cracking unit catalyst regenerator, (2) Sewage treatment plant incinerator for sludge burning, (3) Asphaltic concrete plant (hot mix), (4/5) Secondary brass and lead smelter, (6) Oil fired power plant.
The scope of work required that a commercially available transmissometer be tested at each site for 30 days and its performance evaluated as a continuous monitor of the in-stack opacity, plume opacity and in-stack mass concentration. The mass concentrations were measured directly with the EPA particulate sampling train (Method 5, Federal Register Vol. 30, No. 247, December 23, 1971). The plume opacity was measured by one of several objective methods such as telephotometry of contrasting targets through the plumes or sun photometry through the plumes. Data were also obtained on the spectral transmission characteristics and size distribution of the particulate emissions of the plants.

17. Key Words and Document Analysis. 17a. Descriptors

Pollution Monitoring
Mass concentration
Plume opacity
Transmissometry
Particulates
Optical Monitoring
Impactors
EPA Train
Stack Monitoring
Stationary Source
In-stack Monitoring
Sampling
Sun Photometer
Telephotometer
Particle Size
Effluents

17b. Identifiers/Open-Ended Terms

Reproduced by
NATIONAL TECHNICAL INFORMATION SERVICE
US Department of Commerce
Springfield, VA. 22151

PRICES SUBJECT TO CHANGE

17c. COSATI Field/Group 0401 0606 0610 1708 2006

18. Availability Statement
Release unlimited

19. Security Class (This Report) UNCLASSIFIED

20. Security Class (This Page UNCLASSIFIED

21. No. of Pages 116

22. Price $5.25/2.25

FORM NTIS-35 (10-70)

USCOMM-DC 40329-P71

EPA-650/2-74-120

IN-STACK TRANSMISSOMETER MEASUREMENT OF PARTICULATE OPACITY AND MASS CONCENTRATION

by

E. Reisman, W. D.Gerber, and N. D. Potter

Philco-Ford Corporation
Aeronutronic Division
Newport Beach, California 92663

Contract No. 68-02-1229
ROAP No. 26AAM
Program Element No. 1AA010

EPA Project Officer: W. D. Conner

Chemistry and Physics Laboratory
National Environmental Research Center
Research Triangle Park, North Carolina 27711

Prepared for

OFFICE OF RESEARCH AND DEVELOPMENT
U.S. ENVIRONMENTAL PROTECTION AGENCY
WASHINGTON, D.C. 20460

November 1974

This report has been reviewed by the Environmental Protection Agency and approved for publication. Approval does not signify that the contents necessarily reflect the views and policies of the Agency, nor does mention of trade names or commercial products constitute endorsement or recommendation for use.

ABSTRACT

The objectives of the program were to evaluate the light transmission approach to monitoring particulate pollution and to determine the reliability and degree of correlation of the transmissometer and other particulate measurement methods in a variety of industrial environments.

The six industrial environments were as follows:

1. A petroleum refinery catalytic cracking unit catalyst regenerator.

2. Sewage treatment plant incinerator for sludge burning.

3. Asphaltic concrete plant (hot mix).

4/5. Secondary brass and lead smelter.

6. Oil fired power plant.

The scope of work required that a commercially available transmissometer be tested at each site for 30 days and its performance evaluated as a continuous monitor of the in-stack opacity, plume opacity and in-stack mass concentration.

The mass concentrations were measured directly with the EPA particulate sampling train (Method 5, Federal Register Vol. 30, No. 247, December 23, 1971).

The plume opacity was measured by one of several objective methods such as telephotometry of contrasting targets through the plumes or sun photometry through the plumes. Data were also obtained on the spectral transmission characteristics and size distribution of the particulate emissions of the plants.

CONTENTS

SECTION		PAGE
I	INTRODUCTION	1
II	SITE SELECTION AND PREPARATION	3
	1. Site Selection	3
	2. Pollution Control Agency	3
	3. Site Preparation	4
III	TEST SITES	7
	1. Site #1 - Asphalt Plant	7
	2. Site #2 - Water Pollution Control Plant	8
	3. Site #3 - Oil Refinery	11
	4. Sites 4 and 5 - Brass and Lead Secondary Smelters	14
	5. Site #6 - Oil-Fired Power Plant	18
IV	INSTRUMENTATION	24
	1. Sampling Devices	24
	2. Optical Devices	29
V	TEST RESULTS	34
	1. Asphaltic Concrete Plant	34
	2. Sludge Incinerator	45
	3. Refinery Catalytic Cracker Regenerator	52
	4. Brass and Lead Smelter	57
	5. Oil Fired Power Plant	72
VI	SUMMARY AND CONCLUSIONS	79
	REFERENCES	86
APPENDIX		
A	RAW DATA AND NOMOGRAPHS	87
B	TABULATION FORMS	93
C	SUMMARY TABLES OF METHOD 5 TEST DATA	100

Preceding page blank

ILLUSTRATIONS

FIGURE		PAGE
3-1	Sketch of Asphaltic Concrete Plant Test Site	9
3-2	Instrument and Sampling Port Locations at Asphaltic Concrete Plant Test Site	10
3-3	Sketch of Sludge Incinerator Test Site	12
3-4	Instrument and Sampling Port Locations at Sludge Incinerator Test Site	13
3-5	Sketch of Refinery Catalytic Cracker Regenerator Test Site	15
3-6	Instrument and Sampling Port Locations at Refinery Catalytic Cracker Regenerator Test Site	16
3-7	Sketch of Brass and Lead Smelter Test Site	19
3-8	Instrument and Sampling Port Locations at Brass and Lead Smelter Test Site	20
3-9	Sketch of Oil Fired Power Plant Test Site	22
3-10	Instrument and Sampling Port Locations at Oil Fired Power Plant Test Site	23
5-1	Comparison of Particle Size Distributions in the Emissions of an Asphaltic Concrete Plant with Controlled Baghouse Leaks	35
5-2	Opacity - Mass Concentration Relationship of the Asphaltic Concrete Plant Emissions	37
5-3	Comparison of the Plume and In-Stack Opacities of the Asphaltic Concrete Plant Emissions	38
5-4	Comparison Between Optical Density Measurements Made with White Light and Monochromatic Radiation at 0.4 Microns on Asphaltic Concrete Plant Emissions	39
5-5	Comparison Between Optical Density Measurements Made with White Light and Monochromatic Radiation at 1.25 Microns on Asphaltic Concrete Plant Emissions . . .	40
5-6	Comparison Between Optical Density Measurements Made with White Light and Monochromatic Radiation at 2.2 Microns on Asphaltic Concrete Plant Emissions . . .	41

ILLUSTRATIONS (Continued)

FIGURE		PAGE
5-7	Comparison Between Optical Density Measurements Made with White Light and Monochromatic Radiation at 11.6 Microns on Asphaltic Concrete Plant Emissions	42
5-8	Summary of Optical Density Measurements Made on Asphaltic Concrete Plant Emissions with White Light and Monochromatic Radiation at Four Wavelengths	44
5-9	Particle Size Distribution of the Sludge Incinerator Emissions	47
5-10	Opacity - Mass Concentration Relationship of the Incinerator Plant Emissions	48
5-11	Comparison of the Plume and In-Stack Opacities of the Sludge Incinerator Emissions	50
5-12	Summary of Optical Density Measurements Made on Sludge Incinerator Emissions with White Light and Monochromatic Radiation at Four Wavelengths	51
5-13	Particle Size Distributions of the Refinery Catalytic Cracker Regenerator Emissions	53
5-14	Opacity-Mass Concentration Relationship of the Refinery Catalytic Cracker Regenerator Emissions	54
5-15	Comparison of the Plume and In-Stack Opacities of the Refinery Catalytic Cracker Regenerator Emissions	56
5-16	Comparison Between White-Light and 0.4 Micron Monochromatic Optical Density Measurements of the Refinery Catalytic Cracker Regenerator Emissions	58
5-17	Comparison Between White-Light and 1.25 Micron Monochromatic Optical Density Measurements of the Refinery Catalytic Cracker Regenerator Emissions	59
5-18	Comparison Between White-Light and 2.2 Micron Monochromatic Optical Density Measurements of the Refinery Catalytic Cracker Regenerator Emissions	60

ILLUSTRATIONS (Continued)

FIGURE		PAGE
5-19	Summary of Optical Density Measurement Made on Refinery Catalytic Cracker Regenerator Emissions with White Light and Monochromatic Radiation of three Wavelengths	61
5-20	Particle Size Distribution of the Lead Smelter Emissions . .	63
5-21	Particle Size Distribution of the Brass Smelter Emissions .	65
5-22	Opacity - Mass Concentration Relationship of the Brass Smelter Emissions.	66
5-23	Opacity - Mass Concentration Relationship of the Lead Smelter Emissions.	67
5-24	Comparison of the Plume and In-Stack Opacities of the Brass and Lead Smelter Emissions	68
5-25	Comparison Between Monochromatic and White-Light Optical Density Measurements of the Brass Smelter Emissions	69
5-26	Comparison Between Monochromatic and White-Light Optical Density Measurements of the Lead Smelter Emissions	71
5-27	Comparison of In-Duct and In-Stack Opacity Measurements of the Oil-Fired Power Plant Emissions	78
A-1	Aerodynamic Diameter Nomograph of Anderson Impactor	88
A-2	Impactor Density Correction Nomograph	89
A-3	Temperature Correction Nomograph of Anderson Impactor . . .	90
A-4	Typical Transmissometer Recording from Circular Chart . . .	91
A-5	Typical Transmissometer Recording from Linear Chart	92

TABLES

TABLE		PAGE
2-1	Installation and Operation Procedures	6
5-1	Weight Gain per Impactor Stage from Oil Fired Power Plant Emissions	74
5-2	Opacity-Mass Concentration Measurements of the Oil Fired Power Plant Emissions	76
B-1	Example Tabulation of Probe Data	94
B-2	Example Calculations from Probe Data	95
B-3	Example Tabulation of Impactor Particle Data	96
B-4	Example Tabulation of Transmissometer Data	97
B-5	Example Tabulation of Sun Photometer Opacity Data	98
B-6	Example Tabulation of Telephotometer Opacity Data	99
C-1	Summary of Method 5 Test Data, Asphaltic Concrete Plant . .	101
C-2	Summary of Method 5 Test Data, Sludge Incinerator	102
C-3	Summary of Method 5 Test Data, Refinery Catalytic Cracker Regenerator	103
C-4	Summary of Method 5 Test Data, Brass and Lead Smelter . . .	104
C-5	Summary of Method 5 Test Data, Oil-Fired Power Plant . . .	105

ACKNOWLEDGMENT

We wish to give special recognition to Mr. D. S. Goodsell, a member of our technical team. He devoted much of his own time and ingenuity to each field exercise and handled a major share of the logistics associated with the transitional phases of our program.

We would also like to express our appreciation to the managerial and supervisory staffs at each site. Their assistance, cooperation, and patience greatly contributed to the expediency and efficiency of our program.

Finally, we would like to thank William D. Conner, the Project Officer, for his numerous suggestions and his active interest throughout the course of the program.

SECTION I

INTRODUCTION

In the next few years, increasing numbers of industrial stacks will come under new laws requiring permanent installation of stack-mounted monitoring equipment[1]. While the cost of such equipment might normally be expected to create a strong negative attitude in industry, we found that the reverse was generally true. The people responsible for pollution control at each industry are most anxious to obtain an instrument which can provide them with:

1. A minimum-maintenance, reliable warning system.
2. A permanent record of performance.
3. Legal evidence in cases of civil suit.
4. Freedom from visual inspection techniques.

The EPA has prescribed standards for stack particulates both in terms of opacity and mass concentration. It would be ideal if a single instrument would monitor both quantities for all possible types of sites. It is probably more realistic to accept the fact that each industrial species has its own characteristic particulate problems and may need both its standards and monitoring instrumentation specially tailored.

The report which follows covers a one year program conducted at six different types of industrial sites. At each site a variety of monitoring procedures were initiated and measurements made for a period of 30 days or longer. The sites selected were typical examples of a given industry.

1. Asphaltic Concrete Plant[2]
2. Sludge Incinerator[3]
3. Catalytic Cracker Regenerator[4]

4/5. Brass/Lead Smelter[5]

6. Oil-fired Power Plant[6]

Since, at nearly every site, the management preferred that the companies remain anonymous, the company identities and specific locations have been omitted from this report. All features relevant to the study, such as the plant facilities, their capacity and function, the pollution control equipment, etc., are discussed in great detail.

Section II of this report covers the general subject of site selection and preparation, beginning with the initial contacts with management and corporate officers and extending to the numerous engineering details associated with the facility modification required to implement the program.

The facilities at each site, their operational procedures and productivity, are discussed in Section III. The details of the pollution control systems are also covered.

At every site, numerous sampling and optical measurements were made. The sampling procedure included determinations of the mass concentration and the particle size distribution. The optical studies included stack opacity measurements with a commercial transmissometer, remote plume opacity measurements with any of several non-subjective techniques and an auxiliary optical stack monitoring approach. These are discussed in Section IV.

The experimental results are described in Section V and the general conclusion in Section VI.

SECTION II

SITE SELECTION AND PREPARATION

In retrospect, the magnitude of this phase of the program was the most difficult to properly estimate. Each facility presented its own problems and these had to be solved one at a time as they were encountered.

1. SITE SELECTION

The first task was to locate several sites for each of the industrial types under consideration. Since the program covered a full year and required a great deal of outdoor work, a moderate climate was mandatory. Next in order of consideration was the accessability of the facility, the complications likely to be encountered on site and most important of all, the degree of interest indicated by the participating company.

In all cases, the plant manager was contacted by phone and he would generally request that his engineering supervisors or the environmental control engineer be supplied with all the technical details and goals of the program. This was done both by phone and letter. If the project was not refused at this point, a meeting with the manager was scheduled and generally included those members of the engineering staff who would be involved or affected by our test program. After the meeting, we would generally be given a tour of the site and at that time make our first estimate of the engineering problems likely to be encountered. The final approval was generally obtained by submitting a request in writing to the corporate office.

2. POLLUTION CONTROL AGENCY

Once a site location was selected, we would contact the local pollution control agency and meet with representatives from both the engineering and enforcement branches to explain the details of our program. We would generally invite them to visit the facility during the period when our tests would be in progress. This was naturally done with the approval of the site management. The local agencies were uniformly interested in the program and very cooperative. They provided the necessary variance if a test required a deviation from minimum opacity.

3. SITE PREPARATION

While each site was different, we soon realized the many problems associated with site preparation were basic in nature and, if we attempted to save time by ignoring them or accepting limited solutions, we would generally encounter delays, breakdowns or mistakes which would ultimately prove more time consuming. It became clear that the most efficient approach was to prepare the site adequately before beginning the measurements.

The need for adequate platforms and scaffolding existed at all sites. In order to function efficiently over the long hours of testing for periods of a month or longer, the test crew needed a secure and stable work area at the level selected to perform the measurements. The areas had to be large enough to accommodate the necessary instruments and accessories and still have enough space to move around safely. In general, the length of the probe train controlled the amount of space required.

In general, if the work level was close to the ground or just above the roof, we would construct a wooden platform designed to fit the site. If the work level was significantly above ground level, we would utilize commercial scaffolding. Working levels ran from 6.1 meters (20 feet) to 48.6 meters (158 feet) above the ground. In all cases we found it expedient to provide rain, wind and weather protection for men and equipment through use of tarps, fiberglass panels and plywood.

Although power in the form of a single outlet was sometimes available near our working area, our total requirements ran from 40 to 60 amps at 110 volts, thus requiring four nominal lines. Since some of the load was intermittent, we attempted to separate the loads (particularly the instruments) and found it best to run our own lines from the nearest main. Separate circuit breakers were added to the existing box or a sub-panel was installed if required. Generally, the power cables were about 61 to 91 meters (200 to 300 feet long, requiring #10 conductors. It was found expedient, when installing the power cables, to also install a complete set of signal cables which handled all the inputs to the recorders, including sync signals and event markers, as well as remote switches, buzzers and communication lines.

At each site we found it valuable to create a clean and secure work area at ground level near the base of the working platform. This space was used to house all the recorders, provide office space for data reduction, provide secure storage when the site was not operating, and support the analytical work of probe and impactor. A small office trailer was generally adequate when furnished with a few chairs, desks and tables.

The problem of adequate communications between the various work areas was a constant problem. High noise levels on the platform made normal conversation difficult and tended to dominate the output of intercoms and walkie-talkies. Call buzzers were installed to overcome part of this problem. The main communication channel between platform and trailer was finally selected as a two-way active intercom, utilizing directional mikes, loudspeakers and headset options. The link intermittently required between isolated sections of the platform was provided in a less satisfactory manner by sound-powered field-phone equipment. The most troublesome link was between the trailer and the remote point of measuring plume opacity. This was generally provided by walkie-talkies, but was often of poor quality due to the massive steelwork usually associated with these industrial sites. The final line of communication between us and the plant personnel was generally accomplished on foot.

At each site, we needed to locate a variety of local craftsmen. It was necessary to modify existing port facilities and in many cases install new ports. This required the services of welders or cement cutters, depending on the nature of the duct work and stacks. On some occasions, we needed the services of a sheet metal worker and, at other times, the services of a local machine shop; at still another time, the services of a skilled carpenter. The necessary material had to be procured from local hardware stores, lumber yards, etc. All of these tasks, particularly the procurement of material and services, including the solicitation of bids and the attendant paperwork, proved to be very time-consuming. It normally took from two to three weeks for an experienced crew of three (depending on the level of outside contractor help) to implement the site and be ready for testing.

Our installation and operation procedures followed a set pattern following our arrival at the site (see Table 2-1).

TABLE 2-1

INSTALLATION AND OPERATION PROCEDURES

1. Begin scaffolding (negotiated at site previous week)
2. Obtain trailer and furniture
3. Install equipment in trailer
4. Draw power and signal cables
5. Install ports
6. Install platform weather protection
7. Install commercial transmissometer and accessories; begin collection of data
8. Bring all required instrumentation up to platform
9. Build all necessary braces, brackets and stands, etc., needed at platform level
10. Install EPA train and accessories; begin preliminary sampling
11. Set up auxiliary optical systems; begin data collection
12. Decide on plume opacity locations and techniques; begin preliminary data collection
13. Begin full measurement program baseline operation (normal conditions)
14. Begin measurements under non-normal operating conditions
15. Preliminary data reduction
16. Special measurements
17. Dismantling site
18. Cleanup

SECTION III

TEST SITES

1. SITE #1 - ASPHALT PLANT

An asphalt plant located in Southern California was used as the first site in this experimental program. It is technically known as an Asphaltic Concrete Batch Mixing Plant, providing either hot or cold batching. The plant is composed of a stockpile of graded aggregates, a conveyor-fed drier kiln, an asphalt heating kettle, and a plug mill. The kiln unit is fueled by natural gas and is rated at 31.9 MW (109 X 10^6) BTU/hr.).

The pollution control equipment was installed by Joy Manufacturing Company in December of 1972. It is a bag-house installation comprised of 30 Dacron bags measuring 15 mm (6 in.) diameter and 9.15 m (30 ft.) in length. The design calls for a volume of air flow through the system of 21.2 m^3 sec^{-1} (45000 CFM). The bags are sequentially cleaned on a continuous cycle using an air-blast technique.

The plant was designed for an output of 2.3 X 10^3 kg/batch (2.5 ton/batch), and 1.8 X 10^5 kg/hour (200 ton/hour), although normal operation is contingent upon orders and truck arrivals, reducing the nominal daily output considerably. In operation, a prescribed mix of aggregate is fed to the kiln drier, where it is tumbled while heated to establish correct moisture content. It is then fed, together with the hot asphalt, into the plug-mill where it is thoroughly mixed and eventually loaded into trucks.

The flow system feeding the bag house is such as to include combustion products and processing fumes, including the smoke from the receptor truck while being loaded and immediately thereafter. The principle source of particulates, however, is the "fines" from the aggregate operations.

The investigative ports were cut into the ducting between the bag house and the blower feeding the stack. On this site only was the experimental study made on the negative side of the blower. In order to vary the range of mass concentration, two bags were removed and replaced by plates containing capped openings of different sizes. Baghouse leaks of various magnitudes were then simulated by uncapping a selected combination of openings.

Figures 3-1 and 3-2 show the general layout of the ducting and the port locations established for the probe train and the optical devices being studied.

2. SITE #2 - WATER POLLUTION CONTROL PLANT

The Water Pollution Control Plant selected for this site is located in California. The plant utilizes a disposal procedure known technically as a "total mix, activated sludge process, with a secondary waste-water treatment plant incorporating ocean disposal, sludge incineration, and grease digestion". The plant is designed for a capacity of 20.9 X 10^6 liters/day (4.6 X 10^6 gal/day). Peak loads of 27.3 X 10^6 liters/day (6 X 10^6 gal/day) are accommodated, with a nominal average throughput of 13.6 X 10^6 liters/day (3 X 10^6 gal/day).

The primary plant was built in 1953 and updated in 1968, with a two-stage sludge digestion system and ultimate ocean disposal of all waste. Under a federal Water Pollution Control Administration grant, a new secondary treatment plant with sludge incineration was put on-line in August, 1970.

The 14-foot diameter, two-feed inlet, six-stage multiple-hearth sludge incinerator was built by the BSP Division of Envirotech Corporation and employs an impinger plate scrubber for emission control. The furnace utilizes natural gas combustion to augment the self-sustained flame with oxidation efficiency optimized by a controlled induced draft providing 75 - 100% excess air. Associated equipment permits additional control of sludge moisture content prior to entering the incinerator.

The steps involved in treatment can be summarized as follows: Pre-treatment of incoming sewage includes pre-chlorination, pre-aeration, and grinding, followed by the primary sedimentation treatment. In the primary tank, the sewage settles into three layers; the sludge on the bottom, the grease on top and the fluid in the middle. By skimming and scraping, liquid and solid layers are separated. The liquid waste passes to a secondary treatment tank where it is aereated, mixed and treated biologically with bacteria in a process known as activated sludge. The liquid then moves to a secondary clarifier and is chlorinated again prior to delivery to the ocean. The sludge and grease pass through a cyclone where the sand is removed and then are deposited in a thickening tank. The grease is skimmed from the tank and passes to a

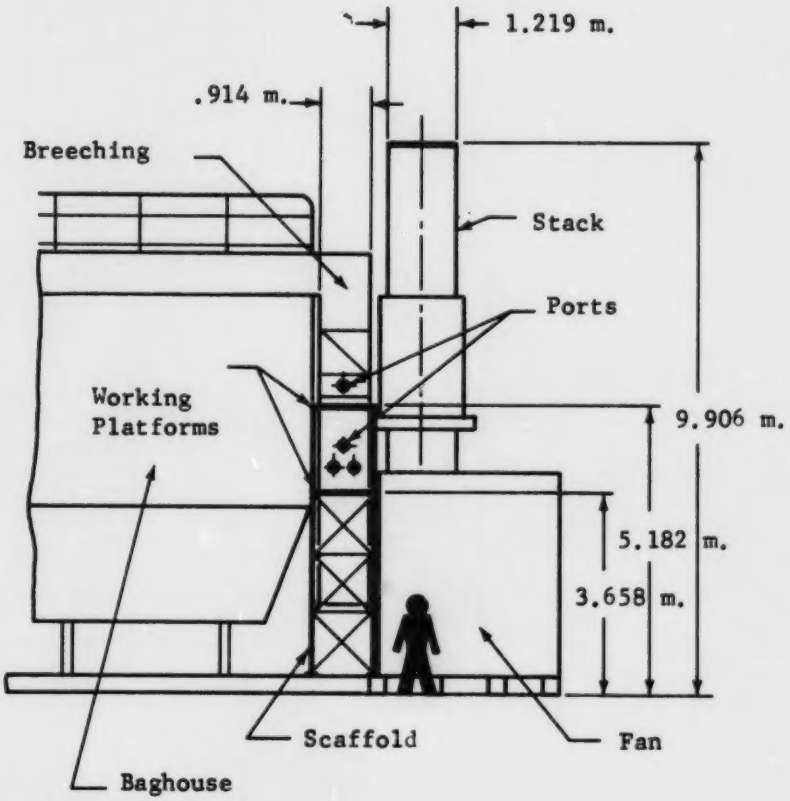

FIGURE 3-1

SKETCH OF ASPHALTIC CONCRETE PLANT TEST SITE

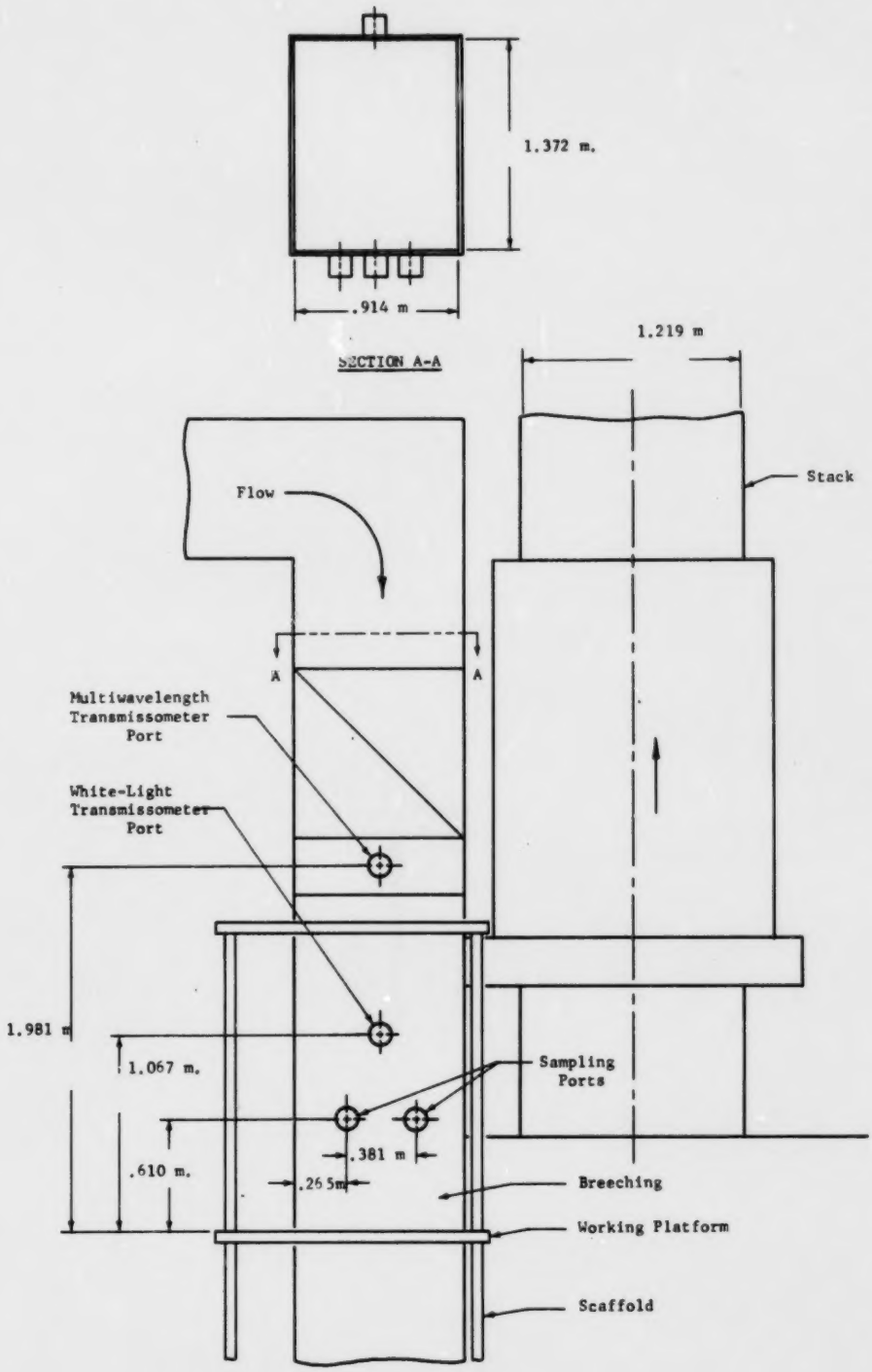

FIGURE 3-2

INSTRUMENT AND SAMPLING PORT LOCATIONS AT ASPHALTIC CONCRETE PLANT TEST SITE

digesting tank. From here the grease can be fed to the furnace to augment combustion. The sludge is dried by a centrifuge and is fed to the top hearth of the furnace where it is further dried as it works its way down to the combustion area. The sludge is incinerated with an automatic process control regulating feed rates, moisture content, percentage of excess air, flame augmentation, etc. The waste gases from the furnace pass through a wet scrubber that serves to remove particulates and lowers the temperature of the flue gases. As a result of the processing involved and the pollution control equipment utilized, a very low level of particulate emission is present in the stack gases under normal operating conditions.

To permit experimental studies to be made of particulate matter in the exhaust gases, a platform was erected surrounding the stack. An 8-foot extension was added to the stack to provide the necessary ports for the instruments employed. The permanent hood, normally installed over the stack, was replaced by a temporary hood which could be removed during the tests to minimize flow disturbances. A conical flow-director was installed at the base of the stack to establish a more appropriate flow profile and more evenly distribute the particulate matter across the stack cross-section. In order to achieve a broad range of mass concentrations, the scrubber was operated inefficiently and the manual override controls were used to defeat the automatic incincerator process control system. Port locations and the general geometry of the site are indicated in Figures 3-3 and 3-4.

3. SITE #3 - OIL REFINERY

The oil refinery studies were conducted at a medium-sized plant located in California. Although a number of refining processes are employed at this site, our study was confined to the exhaust gases resulting from the Fluid Catalytic Cracker operation.

This unit was originally installed in 1943 and has been upgraded several times to provide its current output of 14,000 Bbls/day. In 1973, an Electrostatic Precipitator was installed to reduce particulate emission. This dual unit consists of two banks of three sections each, designed and installed by Research Cotrell. Each section operates at 32 KVA, and the gas throughput capacity of each bank is 2110 m^3/min (74,500 cu. ft/min).

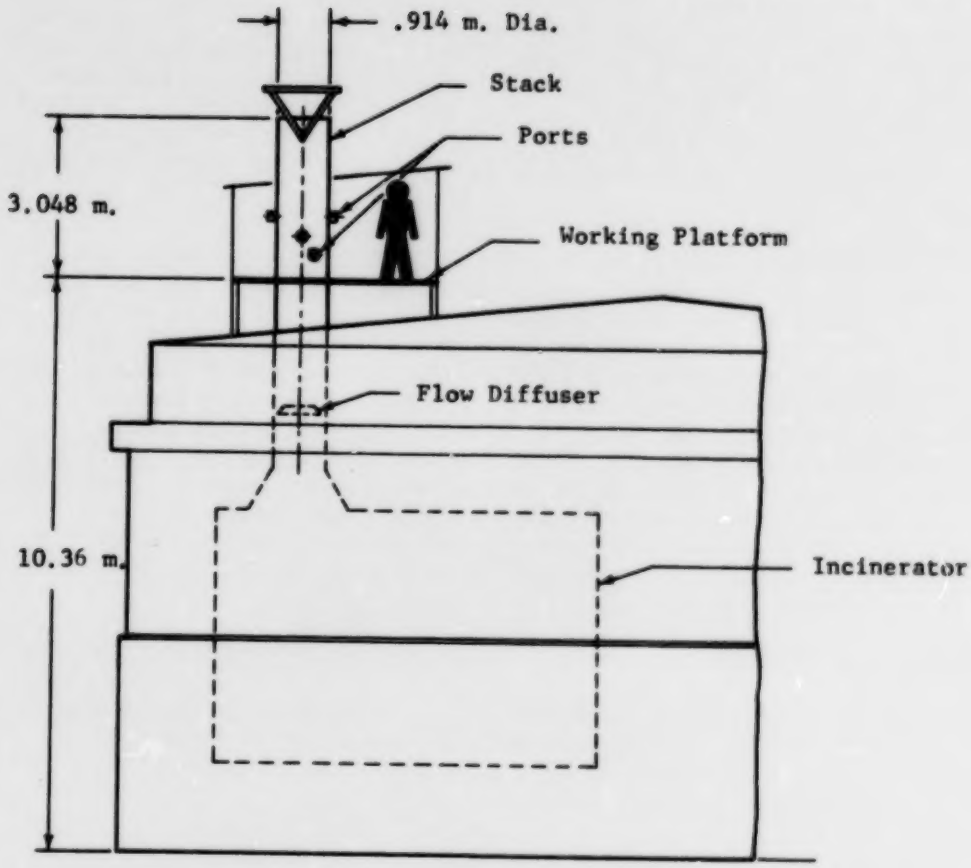

FIGURE 3-3

SKETCH OF SLUDGE INCINERATOR TEST SITE

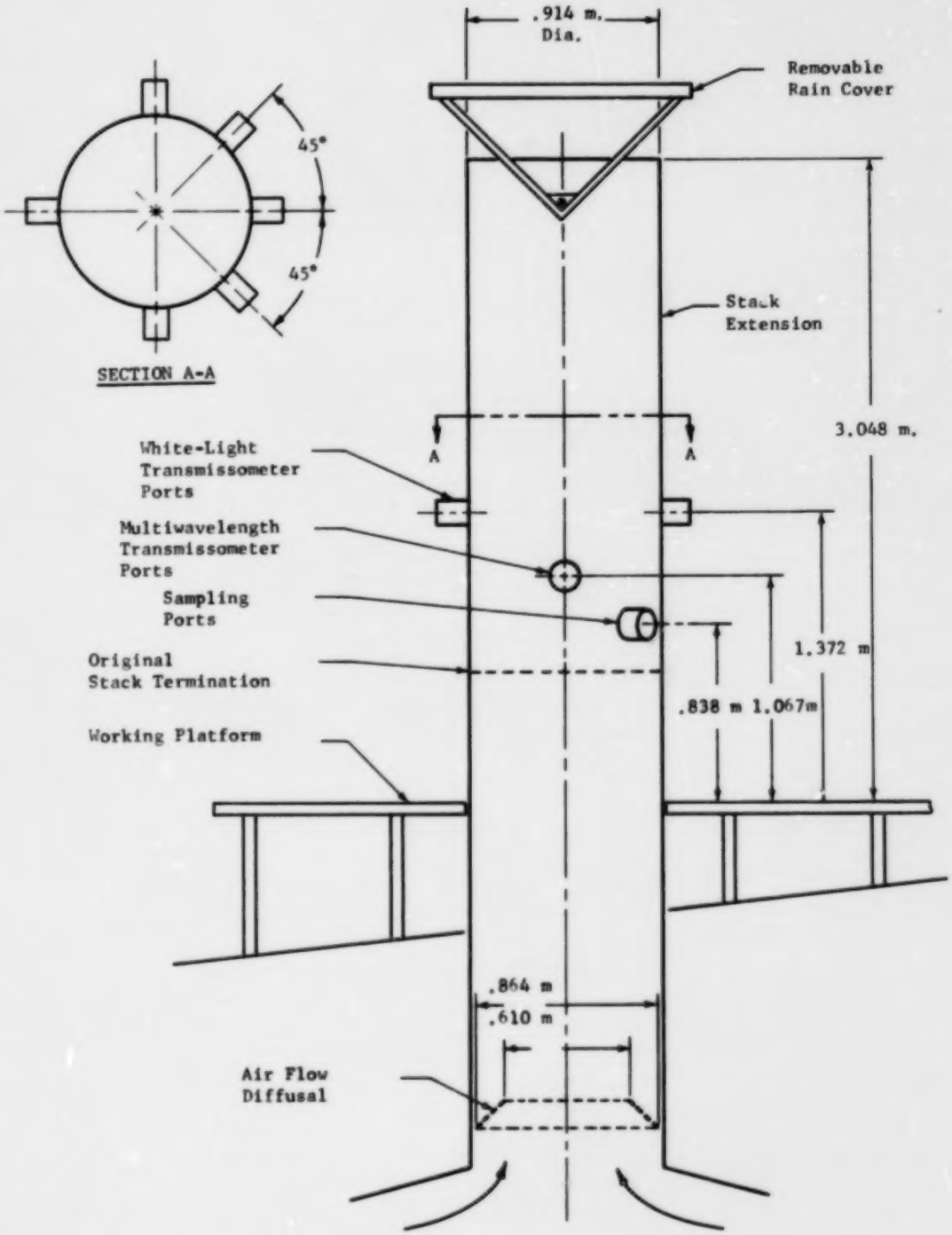

FIGURE 3-4

INSTRUMENT AND SAMPLING PORT LOCATIONS AT SLUDGE INCINERATOR TEST SITE

The system is designed to split the load equally into both banks under normal conditions, but the capability of each is sufficient to permit the entire flow to be routed through one. This was the operational condition in effect during the experimental study. Each section of a bank is separately controlled, making it possible to alter the efficiency of a unit. It was thus possible to vary the level of mass concentration during the course of the study.

A brief description of the overall refining operation follows. Crude oil is introduced into a reactor vessel along with the required amount of catalyst. Upon completion of the reaction, the exhaust gases are processed through several dual-cyclone units to remove the catalytic material which is now in the form of a "coke". This coke is subsequently burned in a regenerator permitting a high rate of recovery of the catalyst which is then recycled. A "minimum air" condition is maintained in the regeneration process such that the resulting exhaust gas is primarily carbon monoxide. This exhaust gas, along with the unreclaimed catalyst it is carrying, is utilized as the fuel in a "CO Boiler" where steam is generated for general plant useage. Excess air is added for optimum conversion of CO_2, and "Refinery gas" is used to augment the CO supply if required. Finally, these flue gases are passed through the precipitator and out the stack.

In order to perform the measurements in a region of minimum flow disturbance, an 85-foot scaffold was erected around the stack. Ports were cut to accommodate the optical and sampling measurements being made. A sketch of the site is shown in Figures 3-5 and 3-6 indicating the geometries involved.

4. SITES 4 AND 5 - BRASS AND LEAD SECONDARY SMELTERS

The plant selected for the combined sites of 4 and 5 was located on the west coast and operates solely as a secondary refining plant for the reclamation of scrap metals.

The plant was built in the thirties and presently consists of seven discrete smelting furnaces in addition to a variety of other processing equipment. In the "Red Metals" area (i.e., brass, bronze, etc.), there are four Rotary Brass Smelting furnaces including two 1.81×10^3 kg (2-ton) units built by U.S. Furnace Company (size 4B), one 1.36×10^4 kg (15-ton) unit manufactured by Lindberg, and one 1.81×10^4 kg (20-ton) system which was built in-house. The "white metal" section includes a 2.26×10^4 kg (25-ton) Lead Dross Reverbratory Furnace and

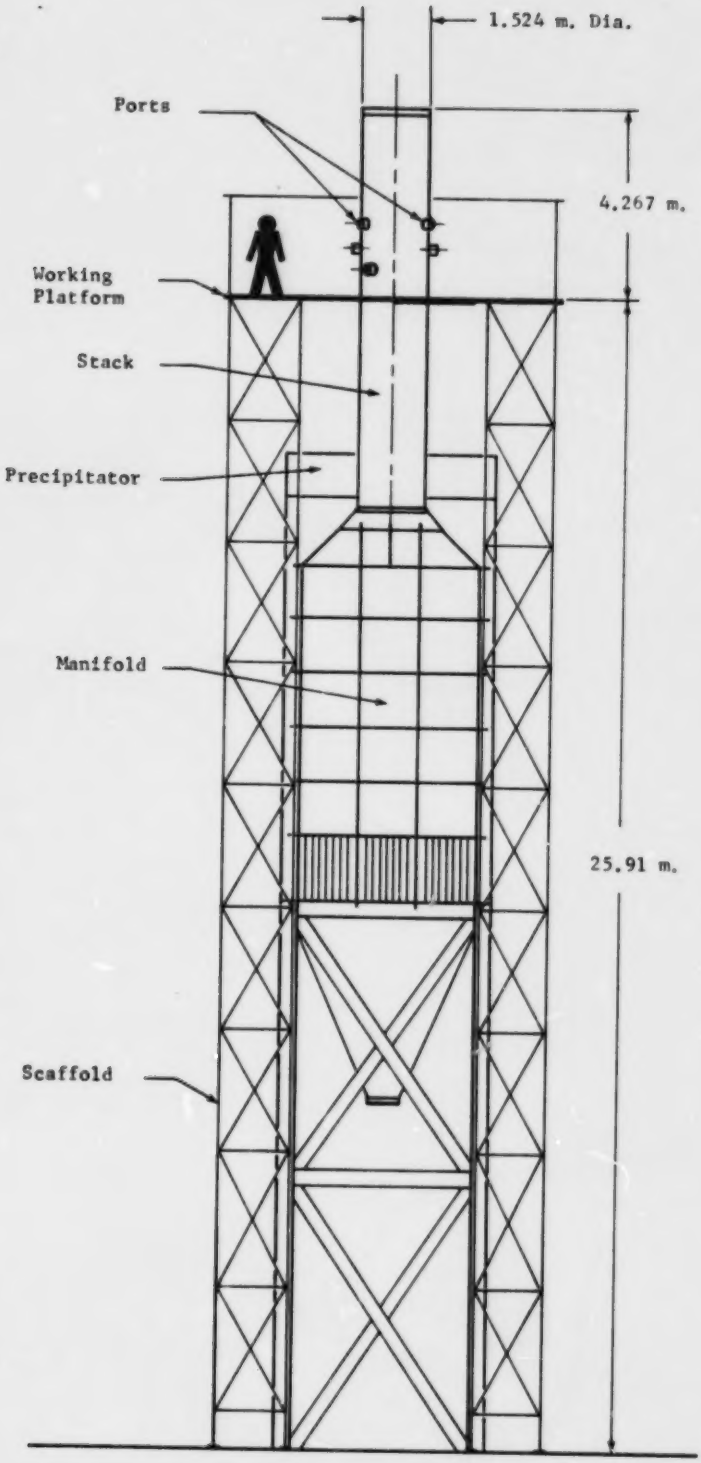

FIGURE 3-5

SKETCH OF REFINERY CATALYTIC CRACKER REGENERATOR TEST SITE

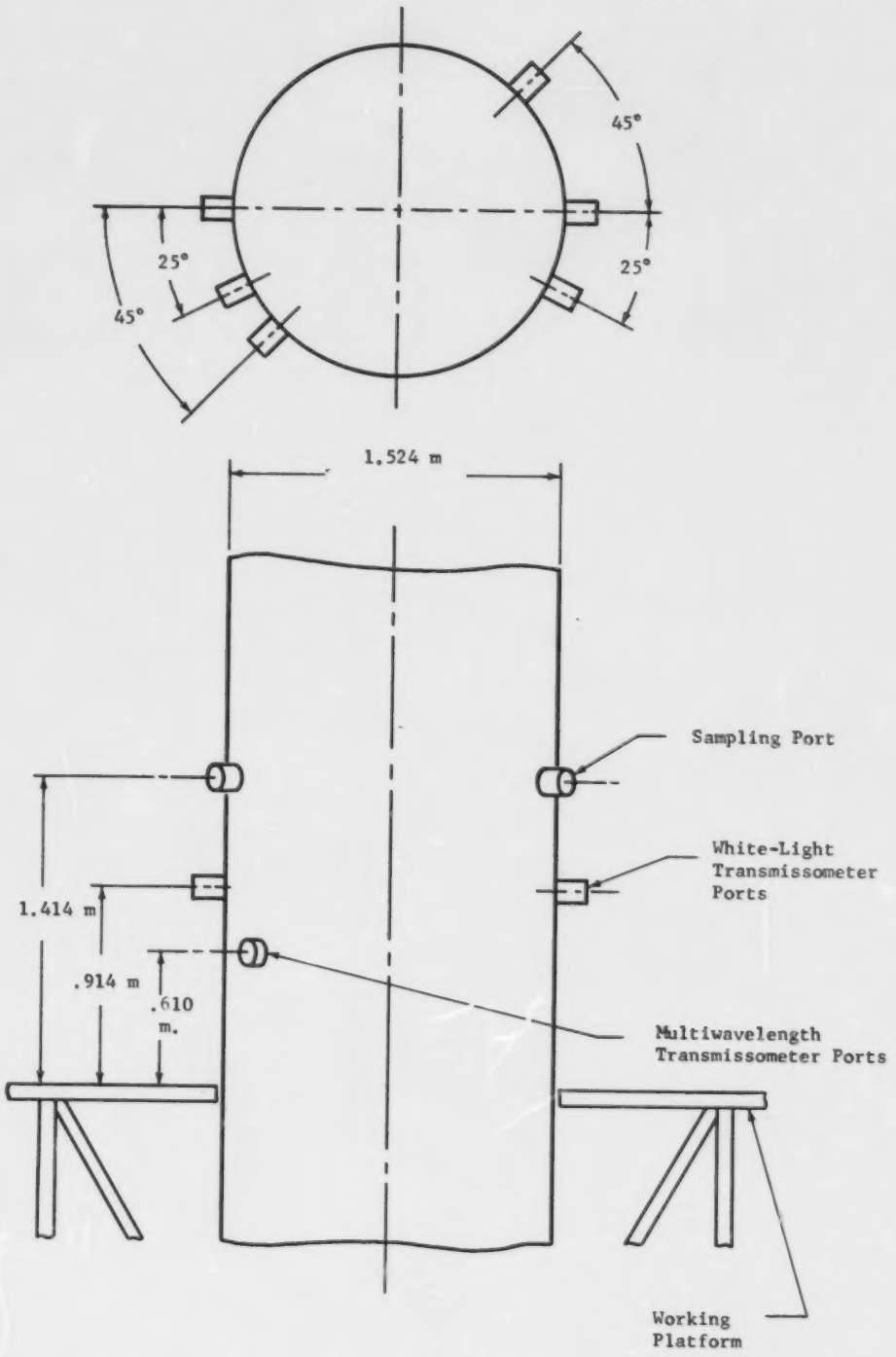

FIGURE 3-6

INSTRUMENT AND SAMPLING PORT LOCATIONS AT REFINERY CATALYTIC CRACKER REGENERATOR TEST SITE

two 3.16×10^4 kg (35-ton) Lead Refining Kettles. All furnaces are fired by No. 2 Diesel fuel, with the exception of the lead kettles which use natural gas. There are more operations within the plant, but these are the only ones feeding the stack upon which the experiment was conducted. Subject to the availability of scrap, the plant runs 24 hours a day, five days a week. The plant activities are scheduled week by week. Because of the limited number of personnel available for three shifts, the weekly emphasis moves back and forth between brass and lead. Generally, when the large brass smelters are operating, the lead smelters are not, and vice-versa.

The smoke and effluent from all of the processes mentioned above pass through baghouses for reclamation as well as air pollution control. Built in 1939 for lead reclamation, the baghouse was segmented in 1962 such that four sections service the red-metal operations and three sections service the lead. On the former, a 75 KW (100 HP) 99.1 m^3/minute (3500 CFM) blower provides the required flow, while a 18.7 KW (25 HP) 50.9 m^3/minute unit is installed in the lead side. Each section contains 33 dacron bags, each of which is 45.7 cm (18 inches) in diameter and 9.14 m (30 feet) long.

In operation, various grades of scrap brass, bronze, copper, etc. are briquetted and then used to charge the furnaces. The melting period includes fluxing with borax, glass, etc. to establish slag viscosity, after which the slagging operation is completed. Rabbling (stirring), sampling, and laboratory analysis is then performed. Proper additives are dictated by the analysis, followed by a blowing phase employed to burn out impurities such as iron. Casting occurs upon the attainment of specifications.

The lead cycle is similar, starting with drosses of lead, solder, type metal, etc. feeding a reverbatory furnace. After the basic melting, the lead is transferred to the refining kettles where further fluxing and blow-down operations occur. It is cast from the kettles into pigs, bars, billets, etc. In both the brass and lead operations, the principal source of pollutants occur during the charging, fluxing, and blowing operations.

The stack at this site is of concrete construction, three hundred feet (91.4 m) in height. Due to the accessability problems involved, the sampling ports were established in the breeching duct between the bag-house and the stack, approximately 15.2 m (fifty feet) above ground level. Five ports were approximately equally spaced vertically to appropriately accommodate the flow profile at a plane located approximately 3/5 of the distance toward the stack. The diagram of Figures 3-7 and 3-8 indicate the geometries involved.

In order to vary the amount of particulate in the exhaust gases, one bag in each of the white and red metal sections was detached and replaced by an adjustable leak plate. When, on occasion, both brass and lead operations occurred simultaneously, the leakage controls thus achieved permitted us to establish a predominance of one particular side of the bag-house, insofar as stack particulates were concerned.

5. SITE #6 - OIL-FIRED POWER PLANT

The oil-fired power plant selected for this portion of the program was located in Southern California. The factors which influenced the selection were the complexity of the scaffolding required to reach a level of four to five stack diameters above the feed ducts, the size of the unit, its operational schedule and the general interest of their engineering staff in monitoring a program.

The unit which was finally chosen was originally placed into operation in 1957. It incorporates a Babcock and Wilcox natural circulation boiler operating at 1.53×10^5 gm/cm^2 (2180 PSI) and providing 5.18×10^5 Kg/hr. (1.14×10^6 lb/hr.) of steam. Input to the boiler is 468 MW (1.6×10^9 BTU/hour), providing an output of 175 MW. Either gas or oil may be used, but it is normally fired by oil with a gravity between API 9.8 and 4.1, a viscosity of 175 to 1500, a sulfur content of 1.3 - 1.7%, and an ash content of 0.04 - 0.05%. The generators employed are tandem-compound, triple-flow, reheat turbines made by General Electric Company.

During normal conditions, the level of operation is controlled by a central dispatcher who regulates all the units under his control with regard to load demand on the distribution grid. During a typical 24-hour operation period, the output usually varies between 20 MW at night to 175 MW at peak consumption. Under proper circumstances, advanced arrangements can be made to remove the unit from the dispatcher's control, thereby permitting a scheduled series of operation conditions for purposes of particulate studies.

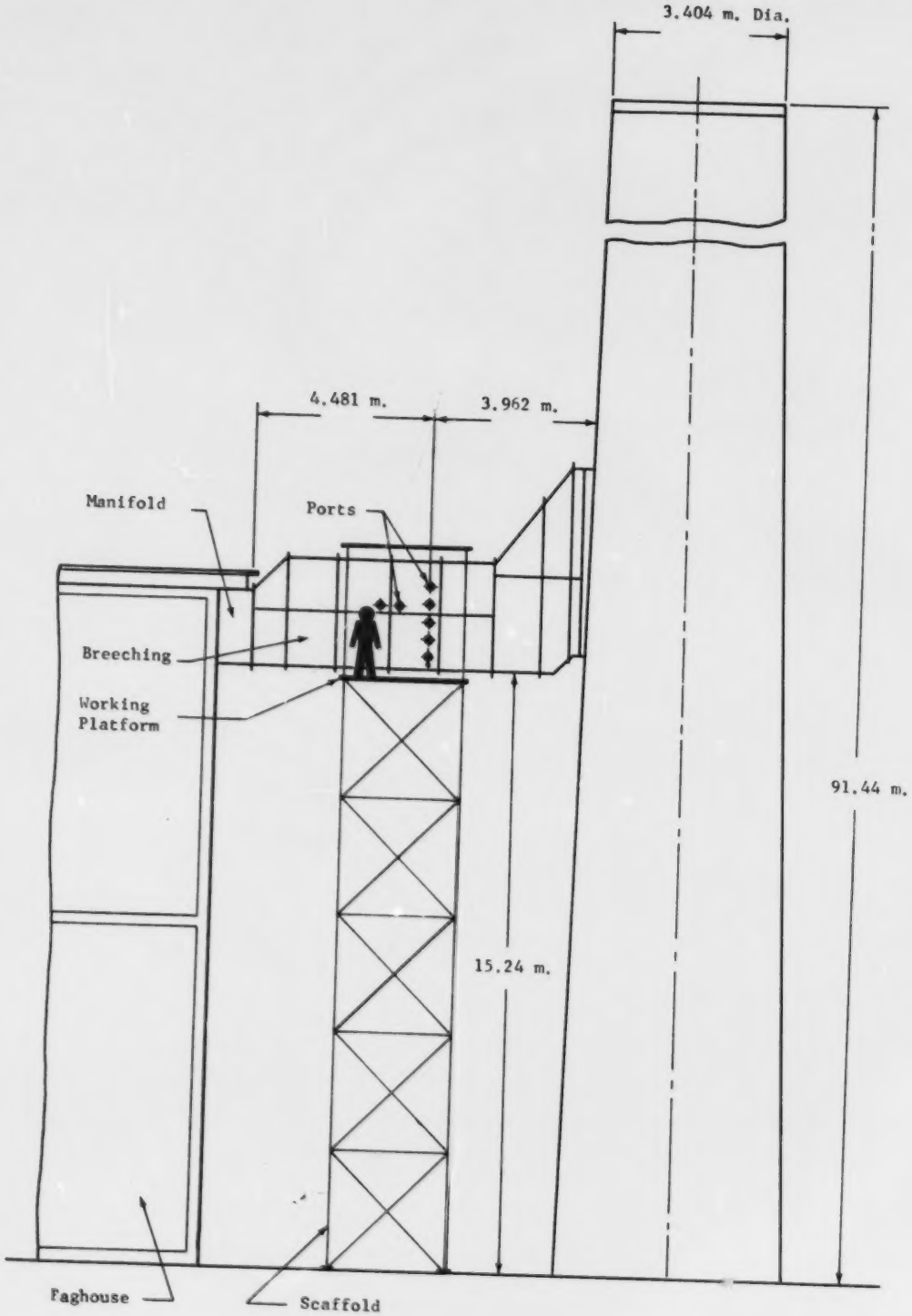

FIGURE 3-7

SKETCH OF BRASS AND LEAD SMELTER TEST SITE

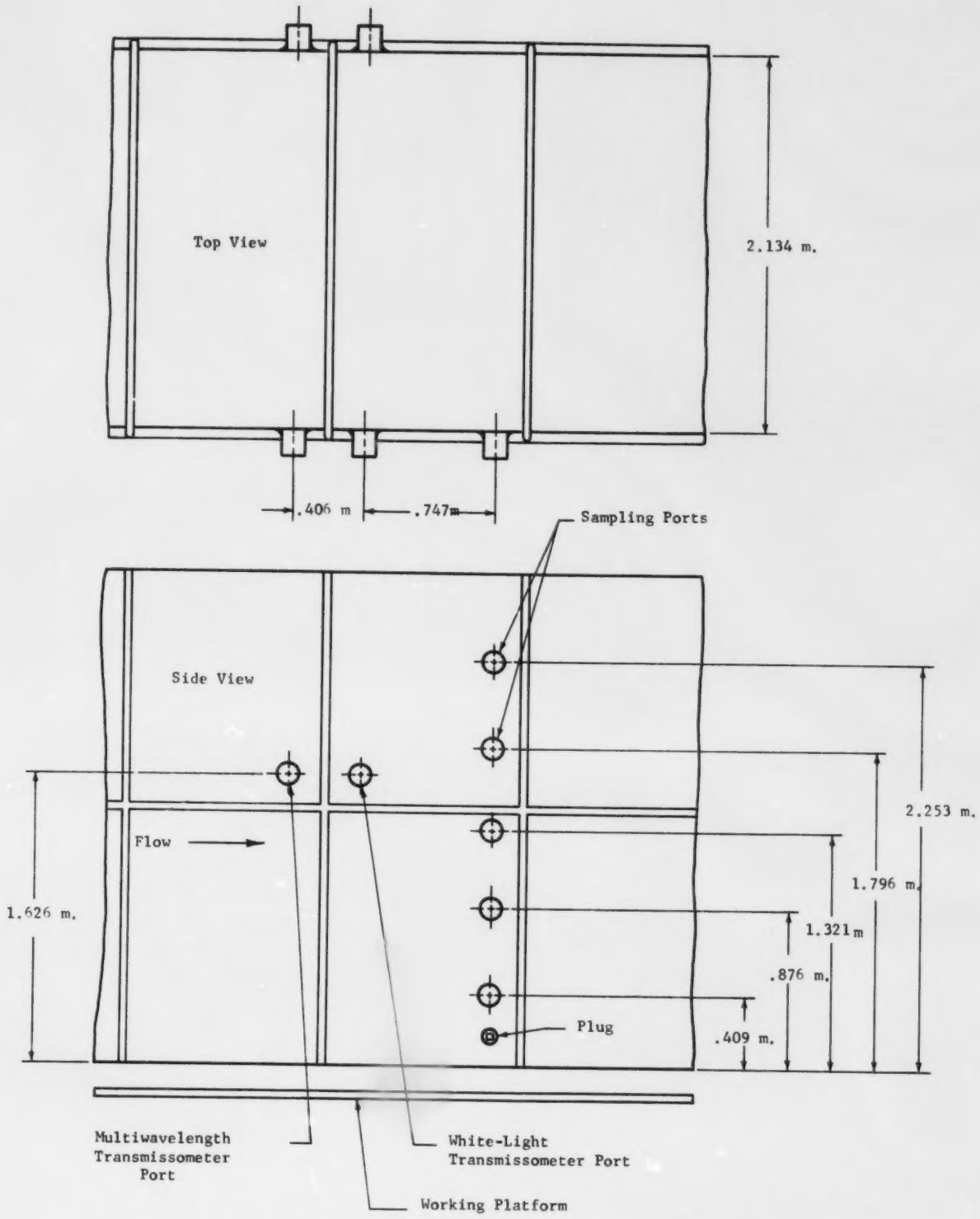

FIGURE 3-8

INSTRUMENT AND SAMPLING PORT LOCATIONS AT BRASS AND LEAD SMELTER TEST SITE

With the exception of modified operational procedures (excess air and reduction in number of burners operated) for the purposes of NOX control, there are no pollution control techniques employed.

A scaffold was erected completely around the stack beginning at its base which is located approximately 27.4 m (90 feet) above the ground. A working platform was placed about 20.7 m (68 feet) above the base. A skeleton structure one level above the platform was used to provide anchorage for wind and weather protection materials.

The stack is of concrete construction, approximately 22.8 cm (9 inches) thick at the level of the experimental ports, with a diameter at that point of approximately 3.8 m (12 feet, 8 inches). Two ports for the white-light transmissometer, two for the multi-wavelength transmissometer, and four for gas train sampling probe were cut at convenient working levels above the platform. In addition, a pair of ports were cut in the breeching duct very near the plane of intersection with the stack for accommodation of a second correlating, white-light transmissometer. The I.D. of the duct at this point was approximately 3.76 m (12 feet, 4 inches).

Port locations and general geometry of the site are shown in Figures 3-9 and 3-10.

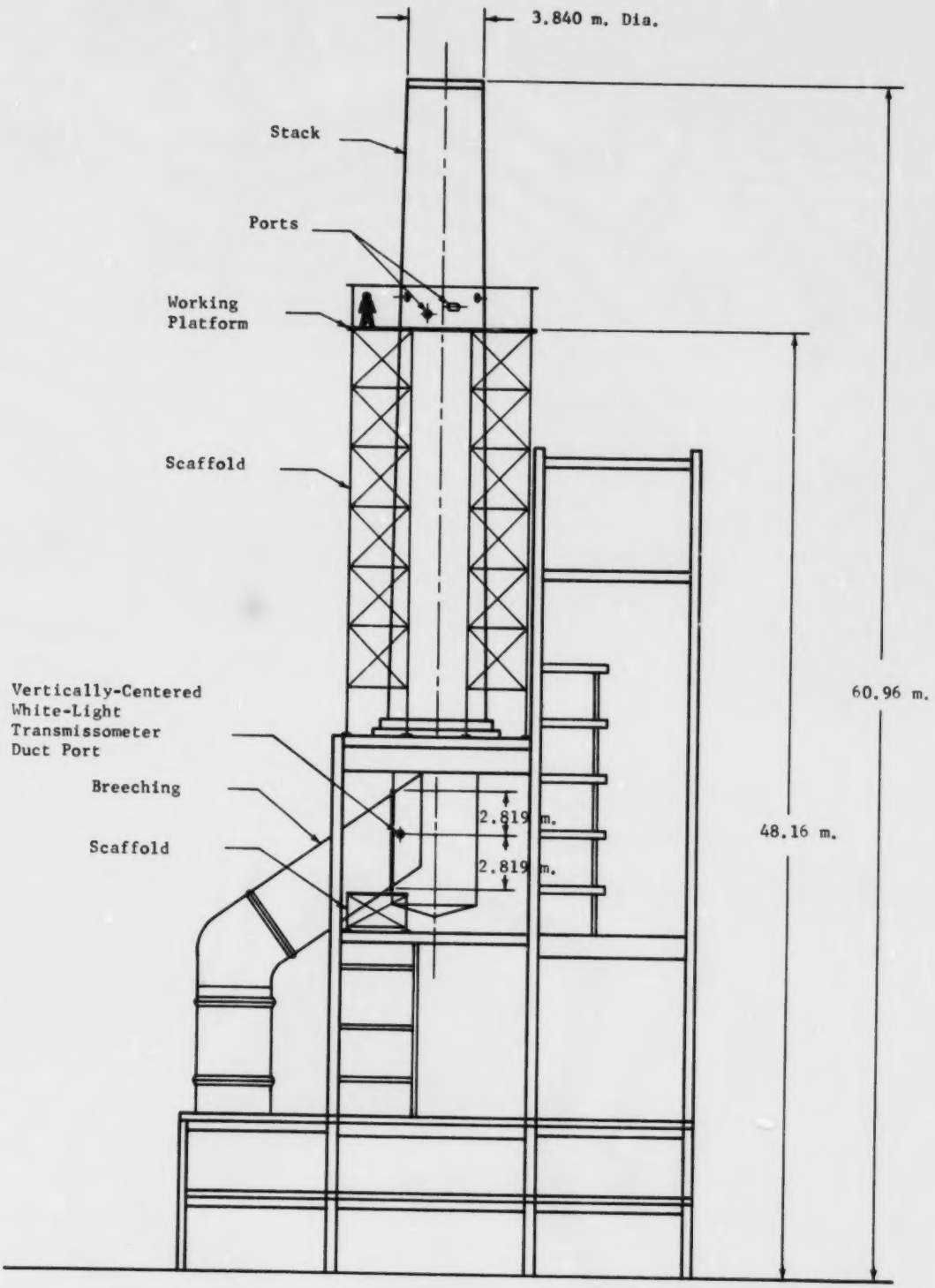

FIGURE 3-9

SKETCH OF OIL FIRED POWER PLANT TEST SITE

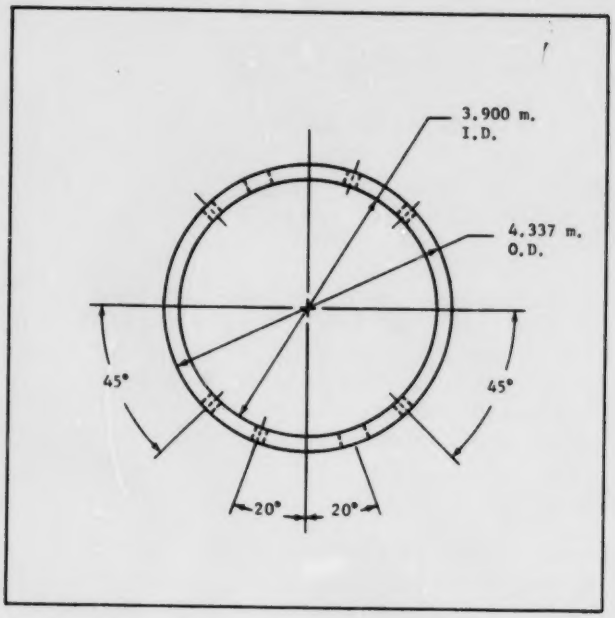

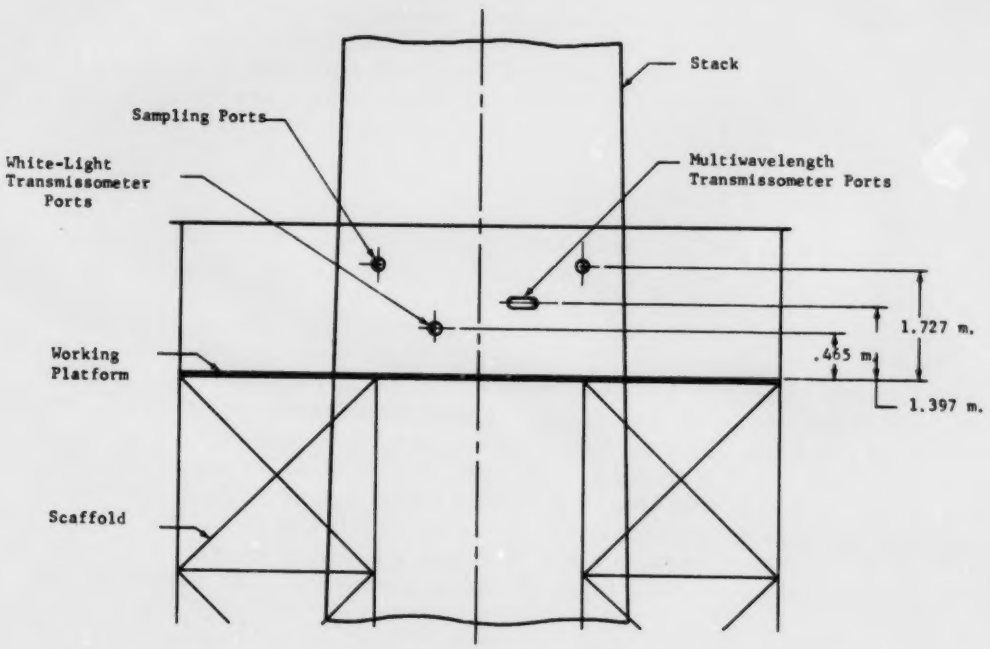

FIGURE 3-10

INSTRUMENT AND SAMPLING PORT LOCATIONS AT OIL FIRED POWER PLANT TEST SITE

SECTION IV

INSTRUMENTATION

1. SAMPLING DEVICES

A. EPA Train*

The particulate loading in the stacks was inferred from isokinetic measurements made with the EPA Train. Sampling was accomplished by inserting a heated probe into the flow of the stack and sampling the gas in the recommended manner[7]. The entire instrument is made up of four main parts. The heated probe, the oven and filter housing, the chilled impinger train, and the meter, pump, and control console.

(1) The Probe

The probe itself is made up of two coaxial tubes, the outer tube which serves as a protective stainless steel sheath, and the inner tube. The latter was of stainless steel or Pyrex glass, depending on the corrosiveness of the gas stream. The inner tube was fitted with a heating element to insure that the gas stream temperature entered the oven at a temperature of at least 121°C (250°F). The temperature was measured with a resistance thermometer element near the exit of the tube. The entrance of the probe was a stainless steel "gooseneck" tip which had a sharpened leading edge so as to minimize any flow disturbance. A Pitot tube and a resistance thermometer was attached to the probe to monitor the stack gas flow rate and temperature.

(2) The Filter and Oven

The probe is connected to a filter holder by ball and socket joints. The filter holder is contained in an oven which maintains the filter at a minimum temperature of 107°C (225°F). The temperature of the oven was monitored by a resistance thermometer. The filter paper itself is of glass fiber to withstand the high temperature. In order to ensure that this paper (Western Precipitation Part No. 2710), which is relatively alkaline, did not absorb acidic gases such as CO_2, SO_2, and especially SO_3, it was washed first with dilute hydrochloric acid and then deionized water. The washings were repeated several times, until the water rinse, when free of chloride, was also of neutral pH. This prevented collecting acid gases and counting them as particulates. The filter papers from each site were tested for the sulfate and sulfite with negative results in all cases but one, the oil-fired steamplant, as discussed below.

*Emission Parameter Analyzer obtained from Joy Manufacturing Corporation.

(3) The Impinger Train

The filtered gases are cooled and dried by passage through a set of four impingers which are interconnected with ball and socket joints. The first two impingers contain a measured volume of water, the third is empty, and the final impinger contains a weighed quantity of silica gel. Resistance thermometers monitor the temperature of the gas both as it enters and leaves the train.

(4) The Control Box

The cooled dry gas exiting the impinger train is led through a 7.6 m (25 foot) umbilical cord to the control box. This umbilical cord also connects a meter readout to each of the resistance thermometers, and the pitot tube to a Magnahelic gauge. The integrated gas flow is read on a dry gas meter. The instantaneous flow rate is estimated from an orifice plate and a second Magnahelic gauge. The pump and flow control valves are housed in the control box.

(5) Procedure

Insofar as possible, ports were located several diameters from flow disturbances. In locating the ports and determining the number of points sampled per traverse, figures 1-1, 1-2, and 1-3 and Table 1-1 presented in The Federal Register (reference 7, pp 24882, 3) were used. Figure 1-1 of reference 7 is used to determine the number of traverse points for sampling, depending on the proximity of the sampling site to disturbances in the gas flow. (For circular stacks, the number of points is increased to an exact multiple of four.) Figure 1-2 (ref. 7) illustrates that the traverse points should be on two perpendicular diameters in a circular stack. Sampling is done at centroids of equal areas. For circular stacks and ducts, Table 1-1 (ref. 7) provides the fraction of stack diameter at which the centroids of concentric rings are located. The cross-section of rectangular ducts and stacks is divided into equal areas as indicated in figure 1-2 (ref. 7).

As a first step, the stack was measured and a scan of the flow profile and gas temperature was made. These data determined the required number of traverse points to be sampled in order to obtain data representative of the overall particulate concentration in the stack.

Prior to each measurement, the probe and tip were cleaned. A clean, weighed filter paper was installed in the filter holder in the oven. Exactly two hundred milliliters of de-ionized water were divided between the first two impingers and 200 grams of silica gel were placed in the last impinger. Ice water was placed around the impinger train. The probe train was leak-checked, and initial data were recorded in a table as shown in Table B-1. The run was initiated and a time mark generated to permit correlation of the probe data with the optical data. For each point on the traverse, the minimum sampling time was five minutes and for each run, the nominal minimum time was two hours. At each point, the data was recorded as indicated on Table B-1, with the exception that it was not necessary to record the temperatures in the last five columns for each point. Immediately upon movement of the probe to a new sampling position during the traverse, the gas velocity and the stack temperature were read and the sampling rate, as read on the orifice gauge, was adjusted to maintain isokinetic sampling.

At the completion of each traverse the pump was stopped, a time mark was generated, the probe was moved to the next port, the pump was restarted and another time mark was sent out*. This was repeated until the run was completed.

At the end of the run, the probe was disconnected from the filter holder and oven, and carefully, to avoid losing any particulates, put aside in a safe place. The impinger train was dismantled. The silica gel was poured into a jar and saved for weighing, the volume of water in the first three impingers was measured, and the filter paper was removed to a labeled petri dish for subsequent weighing. After the probe had cooled so it could be handled, its exterior was carefully cleaned and then the interior was rinsed with chloroform and acetone. The probe washings were placed in a closed jar for subsequent evaporation of solvents and weighing of the particulates. These operations were usually conducted on the platform to minimize the time required to complete the runs, and it was necessary to exercise considerable caution to avoid the introduction of extraneous dust or loss of some of the particulate sample. For most sites, the particulates were weighed in our home laboratory using a single-pan, semi-micro balance capable of precision to 1×10^{-5} gram and accuracy to 3×10^{-5} gram. A balance of equal precision and accuracy was used on site at the sludge incineration plant. The particulate samples from the brass and lead foundry were weighed on a chainomatic, two-pan balance of one decade less precision and accuracy.

After the probe washings and the filter and the silica gel had been weighed, the results of the experiment were computed in the usual way. This is illustrated in Table B-2.

---

*A time mark consists of a signal from the platform to all recorders as well as a voice message explaining the mark. The explanation is entered on charts by hand.

B. Impactor Measurements

The size distribution of particles in the stacks were analyzed by sampling by an Anderson source test Cascade impactor[8]. The sampling procedures are very similar to those employed in determining the particle loading in the stack. The number of sampling points per run and the time of sampling per point were the same. Sampling was done isokinetically.

For these measurements, the same "gooseneck" probe tip, probe, filter, impinger train, and control box were used as with the EPA train. Here, however, an Anderson Stack Sampling Head was inserted between the gooseneck and the heated probe.

The Andersen Stack Sampling Head consists of a stainless steel case and 1/2" female pipe fittings. It is designed to be inserted directly into the stack (standard 3 inch opening) where high temperature and/or corrosive conditions may exist.

The Sampler contains nine jet plates each having a pattern of precision-drilled orifices. The nine plates, separated by 2.5 millimeter stainless steel spacers, divide the sample into eight fractions or particle size ranges. The jets on each plate are arranged in concentric circles which are offset on each succeeding plate. The size of the orifices is the same on a given plate, but is smaller for each succeeding downstream plate. Therefore, as the sample is drawn through the Sampler at a constant flow rate, the jets of air flowing through any particular plate direct the particulates toward the collection area on the downstream plate directly below the circles of jets on the plate above. Since the jet diameters decrease from plate to plate, the velocities increase such that, whenever the velocity imparted to a particle is sufficiently great, its inertia will overcome the aerodynamic drag of the turning airstream and the particle will be impacted on the collection surface. Otherwise, the particle remains in the airstream and proceeds to the next plate.

Since the particle deposit areas are directly below the jets, seven of the plates act as both a jet stage and a collection plate. The entire sampler head is made of 304 stainless steel.

---

*Purchased from Anderson 2000 Inc., Atlanta, Ga.

According to the manufacturer, the Andersen Stack Sampler has been calibrated by several independent laboratories in order to arrive at the current respective size cuts for each stage. Figure A-1 is a plot of D_p versus flow rate through the Stack Sampler at 70°F for each of the seven stages of the sampler. D_p is the aerodynamic diameter of a spherical, unit density particle that has a 50% probability of being collected on the stage.

Figure A-2 shows the correction factor for determining D_p for particles of other than unit density. The unit density aerodynamic diameter as determined from Figure A-1 is multiplied by the factor from Figure A-2 to determine the aerodynamic diameter for that density. The aerodynamic sizes can be equated to the physical sizes if the particles are spherical. Caution is required, however, in equating aerodynamic size to physical dimensions for non-spherical particles.

Figure A-3 shows the correction factor for determining the aerodynamic particle diameter for elevated temperatures. The aerodynamic diameter (D_p) as determined from Figure A-1 must be multiplied by the correction factor from Figure A-3 to determine the diameter for that temperature.

The run procedure was identical in every way to the EPA train measurements except that it was necessary to insure that particulate loadings were not too heavy so as to avoid re-entrainment problems. We usually tried to avoid collecting more than 10 mg. per plate. In very dusty stacks, this required a short sampling time at each point and/or fewer sampling points per run. Times per point as low as one minute were used. Seldom did we sample at fewer than one-half of the points, and in those few cases replicate runs were made at more points. In no case was there any significant difference in replicate runs.

The same balances used in the method 5 measurements were used to weigh the impactor samples and these weights were recorded along with the emission parameters obtained from the train analysis. A typical data sheet would be similar to Table B-1. The percent isokinetic sampling and the gas flow rates were calculated as shown in Table B-2, as was the D_p particle size for each collector plate, using Figures A-1, A-2, and A-3, and ultimately tabulated as shown in Table B-3. Sample densities, required to make density corrections, were estimated on the basis of the known composition of the sample.

2. OPTICAL DEVICES

A. White-Light Transmissometer

(1) Description

One of the optical monitoring systems studied throughout the entire course of the program was a white-light transmissometer. The specific unit evaluated was a "precision optical smoke and dust density measuring instrument" known as the Model RM-4 Optical Transmissometer manufactured by Lear-Siegler, Inc.[9]

The instrument employs a dual-beam technique to achieve self-correcting operation through a gain-stabilization process. A white-light source (i.e., broadband visible spectrum) is split into two beams, each of which is modulated at its own discrete frequency by a single chopper mechanism. A single detector is employed for both optical channels which can always be re-separated by virtue of their characteristic modulation frequency.

One of the beams, a reference beam, stays within the confines of the optical head, and is used to establish a "calibration-gain" level via feedback control of a preamplifier common to both channels. In the event of a change in characteristics of any component common to both beams or channels (i.e., lamp aging, chopped variations, pre-amp gain drift, line-voltage instabilities, etc.), the reference leg compensates by varying the gain of the preamplifier to thereby maintain a constant output level. The change in preamplifier gain will also serve to maintain the calibration of the moni oring beam.

This beam, which traverses the stack and is returned by a retro-reflector, can then be used to determine the overall opacity encountered in the path. A logarithmic amplifier converts this signal to density, and an output driver permits the recording of this data. An integral calibration-check feature is employed to periodically verify the zero-set level and the gain calibration of the system. The unit has an adjustable threshold setting which can be used to activate an alarm or other mechanism should a predetermined opacity level be exceeded.

(2) Readout

The output of the white-light transmissometer is in the form of a current that can be recorded on a strip chart as a linear function of optical density. The instrument's characteristics are such as to establish zero density at 2 mA, with the full scale density (20 mA)

established by internal gain selection. Since the design incorporates a double-pass optical path, the resulting single-pass scale factors for the five ranges available are 0.045, 0.09, 0.225, 0.45 and 0.9 (full scale densities). For purposes of this program, the data was recorded on a strip chart for high resolution information during data runs, and on a circular chart for continuous 24 hr/day records.

(3) Data Reduction

Data reduction for comparison with the gas train results involves averaging the densities recorded during the train sampling periods. Since the fluctuations in densities are often large, this can become a tedious and marginally accurate chore. To facilitate the analysis, an event marker system was incorporated to accurately establish the durations of gas train sampling. Manual techniques were then employed to establish average levels of the analog data. These techniques varied with the nature of the recording, from a straightforward visual process during quiet runs, to the summation of incremental averaging periods during runs involving large fluctuations due to blowing of the bags, shaking of precipitators, or other plant induced perturbations. Reproductions of typical raw data indicative of both extremes are shown in Figures A-4 and A-5. Also included is a typical example of data reduction, indicating the procedures and techniques employed. An example of reduced data is incorporated in the appendix, Table B-4.

B. Plume Opacity Instruments

(1) Description

As a second optical monitoring technique, plume opacity measurements were made using two different types of instruments[10,11]. One was a Sun Photometer and the other was a Telephotometer. At each site, the most appropriate instrument was selected and plume opacity measurements made with it.

The sun photometer was a hand-built unit furnished by the Environmental Protection Agency. The sun photometer is simply a device used to detect and measure incident radiation received by the instrument. Its field of view is limited to slightly less than that subtended by the sun ($\approx$ 9.3 milliradians, or 0.53 degrees). A gain adjustment control permits calibration during use.

To obtain an indication of plume opacity, it is only necessary to locate the shadow of the top of the stack. By observing the sun as seen just outside of the shadow of the plume, setting the

gain to any appropriate level, and then obtaining a similar reading through the plume (without readjusting the gain), the ratio of levels thus obtained is indicative of the attenuation provided by the plume, thereby defining the plume transmissivity/opacity characteristic. The logarithm of this ratio yields the plume's density.

The telephotometric instrument operates on a similar principle. In this case, however, direct viewing of the sun is not required, thus facilitating the measurement and removing the limitation imposed by stack-shadow accessibility. The unit which was used throughout the program is known as a "Spectra Brightness Spot Meter", made by Photo Research, a division of Kollmorgen Corporation.

The telephotometer is set up in a semi-remote location affording a view of the stack exit. The telescopic nature of the instrument permits accurate observation within the field-of-view established by its design. The field-of-view of the detector is indicated by a reticle in the telescope. Contrasting natural background targets are located such that the pair can be viewed both through the plume and to one side of the plume. This may necessitate translating the instrument. If man-made targets are used, they can be built in the form of two identical pairs and one pair can be seen through the plume and the other to one side of the plume.

The instrument measures the incident energy received from the diffuse targets. Readings from all four targets are necessary to make a determination of opacity. The readings can be used to calculate the plume's transmission, opacity, and optical density. One nice feature of the unit is that it permits different filters to be inserted while making measurements. Thus we were able to collect data with white light, blue light and red light.

(2) Readouts

The readout mechanism employed for both instruments is a simple micro-ammeter movement. The telephotometer which has a high gain amplifier also has an output that can drive a recorder. With either instrument, it is necessary to make a series of readings, alternating between background and plume in order to obtain a reliable data point.

(3) Data Reduction

With the sun photometer, the uncorrected transmission through the plume is obtained by finding the ratio of the readings through the plume to the direct readings of the sun. The uncorrected opacity is simply 1-T and the uncorrected optical density is log 1/T.

In order to use the data, it must be corrected for the slant distance through the plume and, if the data is to be compared with in-stack measurements, additional corrections must be made if the two optical paths are not the same length.

With the telephotometer, four measurements are needed to calculate the transmission. For simplicity, consider the target as white on black. The four measurements taken are of the white target through the plume (I_{WP}), the black target through the plume (I_{BP}), and the two target areas as referenced with no plume (I_{WR} and I_{BR}). The transmission is then given by

$$T = \frac{I_{WP} - I_{BP}}{I_{WR} - I_{BR}} \qquad (4\text{-}1)$$

Again, if there is an appreciable slant to the sighting path, a slant distance correction may have to be made. Typical examples of data reduction sheets are shown in the appendix in Tables B-5 and B-6.

C. Auxiliary Optical Measurements

(1) Description

In addition to the tasks specified in the statement of work, the Philco-Ford Corporation conducted independently funded measurements of their own, the results of which are included for the sake of completeness. The instrument employed was designed and developed as a company-funded project and has been undergoing tests for the past two years. The device is a laboratory model of a multi-wavelength transmissometer which has been adapted for field use.

The unit uses a broadband light source and the necessary optics to form a modulated beam that propagates across the stack. The beam is collected by receiver optics, then split into selected wavelength domains and focused through narrow band filters to detectors appropriate for the wavelength. The filters have been chosen so as to avoid the absorption bands associated with the common stack gases. The output of the detectors are fed to phase locked amplifiers which in turn drive multipen recorders. The system records the transmission through the stack at each of the selected wavelengths.

(2) Data Processing

The wavelength dependence of the transmission arises from the fact that the scattering efficiency (or more accurately the extinction efficiency) of a particle is a function of size and wavelength. For a mono-disperse system of particle

$$K(r,\lambda) = N\,Q\,(r,\lambda)\,\pi\,r^2 \qquad (4\text{-}2)$$

where K is the extinction coefficient; N, the number of particles per unit volume; Q, the extinction efficiency and $\pi\,r^2$ the geometric cross section of a particle. The transmission for a path length x is given by

$$K(\lambda) = \int_{r1}^{r2} N(r)\,Q(r,\lambda)\,\pi\,r^2\,dr \qquad (4\text{-}3)$$

Once the complex indicies of refraction of the material are known for each wavelength of interest, the Q functions can be calculated from Mie theory or found in tabulated form. If the size distribution is expressed as a function of 2 or 3 parameters, the best value of the parameters can be selected commensurate with the wavelength dependence of K. The calculation normally requires a computer program but much valuable size information can be inferred by direct observation of the K values.

A finished instrument will couple directly to a minicomputer which has been programmed with appropriate information about the system (i.e., Q function, distribution forms, material density, etc.). The computer will supply all required output data in any desired readout form. Currently, the data is manually read from the strip chart and fed to a time-share computer which performs the desired calculation. For example, if mass concentration is desired, the computer calculates

$$M_c = \rho \int_{r1}^{r2} N(r)\,4/3\,\pi\,r^3\,dr \qquad (4\text{-}4)$$

using the distributional parameters found which best fit equation 4-3. Here, ρ, is the density of the material which constitutes the particles.

In the next section, the data obtained at each site from the various monitoring systems will be illustrated and the key site characteristics discussed.

SECTION V

TEST RESULTS

1. ASPHALTIC CONCRETE PLANT

During the testing period at Site #1 we were able to obtain a total of 26 probe measurements. Four of the initial runs were considered preliminary and are not utilized for data comparison. Of the remaining 22, six were impactor runs and sixteen were train measurements.

A. Impactor Measurements

The results of five different impactor measurements with various simulated bag leaks are illustrated in Figure 5-1. The data is presented as a percent of mass smaller than a given particle diameter plotted on log normal paper. If the size distribution is truly log normal the points should lie on a straight line. This appears to be true in a general sense. The distributions all have a median particle diameter between 5 and 6 microns and are the results of averaging over both space and time. They represent the accumulation from each of the sampling points taken over a period of 1 to 2 hours of plant operation. The density was taken to be 28 gm/cm^3 based on the average of the densities of the constituents.

B. EPA Train Measurements

Of the sixteen train measurements, twelve were full traverses of both ports, two were traverses of the individual ports, and two were taken at the mid points of the traverses for each port. In each case, the samples were made only during periods of plant operation. The white light transmissometer was operational at all times. If the facility suspended operation for a period of 30 minutes, the probe run was also suspended.

It was generally observed that the right port yielded heavier samples than the left and that it would be safer to make full traverse of both ports even though it was very time consuming (i.e., because of the intermittent plant operation).

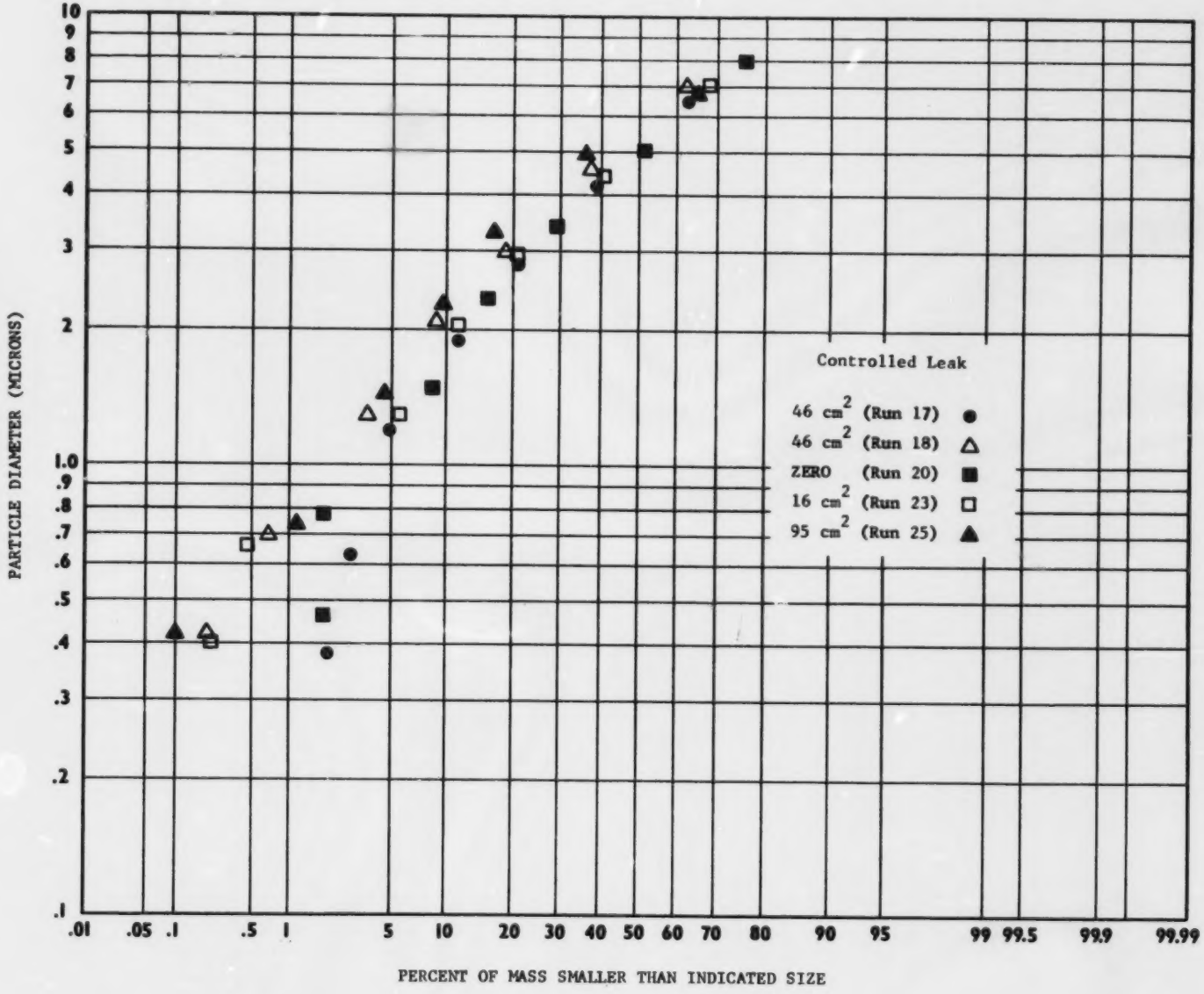

FIGURE 5-1

COMPARISON OF PARTICLE SIZE DISTRIBUTIONS IN THE EMISSIONS OF AN ASPHALTIC CONCRETE PLANT WITH CONTROLLED BAGHOUSE LEAKS

Figure 5-2 shows the average opacity recorded for each value of mass concentration measured with a full traverse of both ports. One run was not included because the optical data was unavailable. The general level of mass concentration was varied by introducing a fixed leak into the baghouse system. This was done by removing two bags and capping off the bag ports. The cap flanges were fitted with a variety of orifices that could be unplugged as desired. Total orifice area was varied between zero and 95 cm^2. The optical opacity observed depended not only on this area but on the type and quantity of asphalt being mixed at any given moment.

C. Plume Opacity Measurements

Because of the location and orientation of the facility, sun photometry appeared to be the most suitable way of measuring plume opacity. Because of overcast skies and varying sun brightness, only a few days during the period of data acquisition were suitable for the measurement, and then only those hours during the day when the plume was not obscured by steam and the stack shadow was accessible. The resulting data is shown in Figure 5-3 where the plume opacity is plotted as a function of the in-stack opacity. Nearly all of the sun photometry at this and succeeding sites was done with the unit furnished by the Environmental Protection Agency. We briefly obtained a unit manufactured by the Shell Corporation and used by the Los Angeles Pollution Control District. The unit is extremely simple to use because you can see the full field of view and read the meter simultaneously. No data from this instrument will be presented because of its limited use.

D. Multi-wavelength Transmissometer

The multi-wavelength transmissometer was in operation during all key periods of facility operation. The unit simultaneously measures the transmissivity of the stack at a number of different wavelengths selected by narrow band filters. This unit utilizes four different detectors covering a range from .4μ and 12μ. The filters employed have been selected to miss the absorption bands of the most common stack gases (i.e., H_2O, CO, CO_2, SO_2, etc.). Data was taken at .4μ, 1.25μ, 2.2μ, 11.6μ.

The single pass optical densities as measured on these four channels is shown in Figures 5-4, 5-5, 5-6, and 5-7 respectively. The data is obtained by measuring the transmissivity (or change in transmissivity) at a given point in time for one of the channels and comparing it to the optical density (or change in optical density) as measured by the white light transmissometer. This comparison can be made for any point in time since all channels are recorded on strip charts. The scatter in the data is probably due to particle size fluctuation.

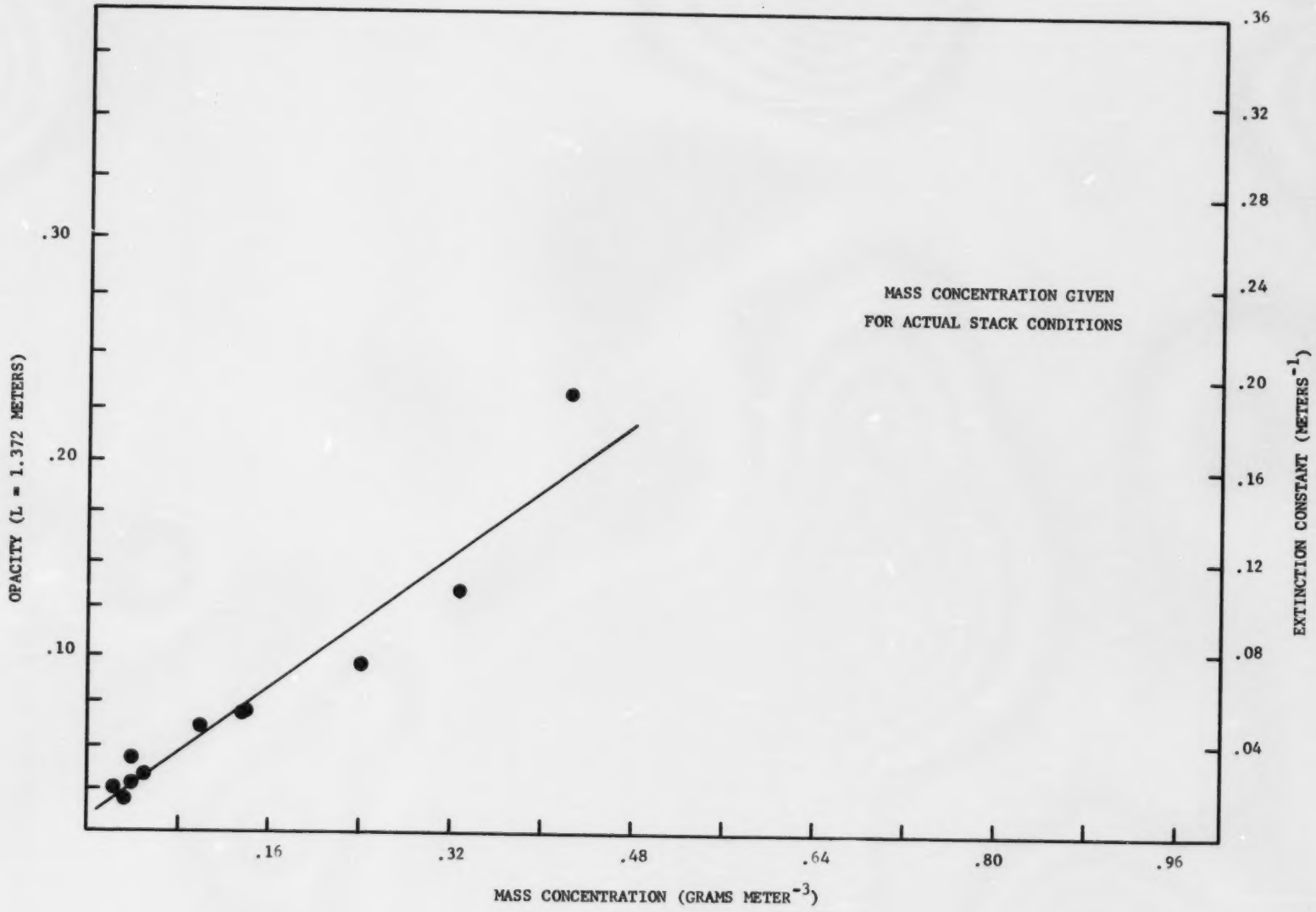

FIGURE 5-2

OPACITY - MASS CONCENTRATION RELATIONSHIP OF THE ASPHALTIC CONCRETE PLANT EMISSIONS

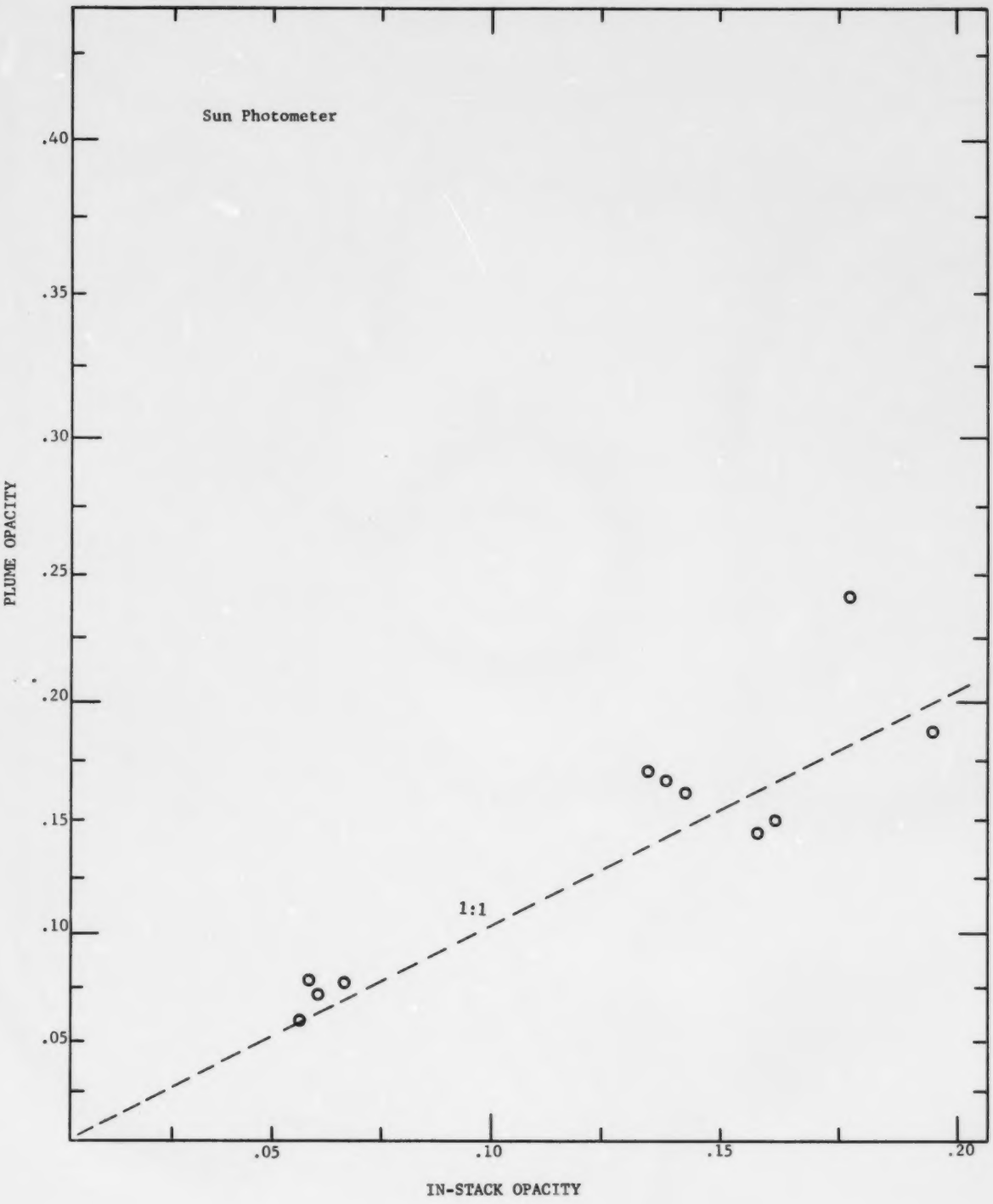

FIGURE 5-3

COMPARISON OF THE PLUME AND IN-STACK OPACITIES OF THE ASPHALTIC CONCRETE PLANT EMISSIONS

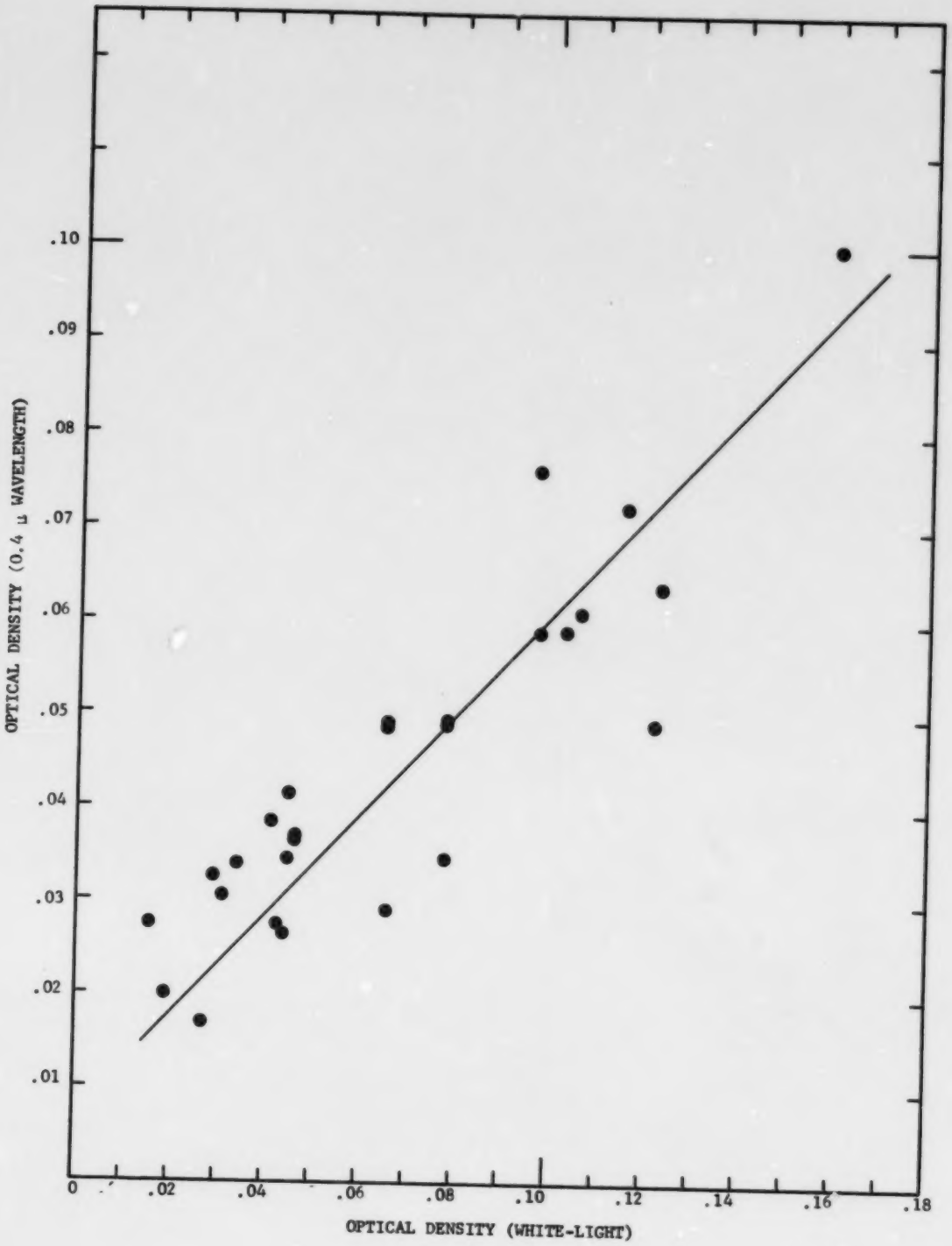

FIGURE 5-4

COMPARISON BETWEEN OPTICAL DENSITY MEASUREMENTS MADE WITH WHITE LIGHT AND MONOCHROMATIC RADIATION AT .4 MICRONS ON ASPHALTIC CONCRETE PLANT EMISSIONS

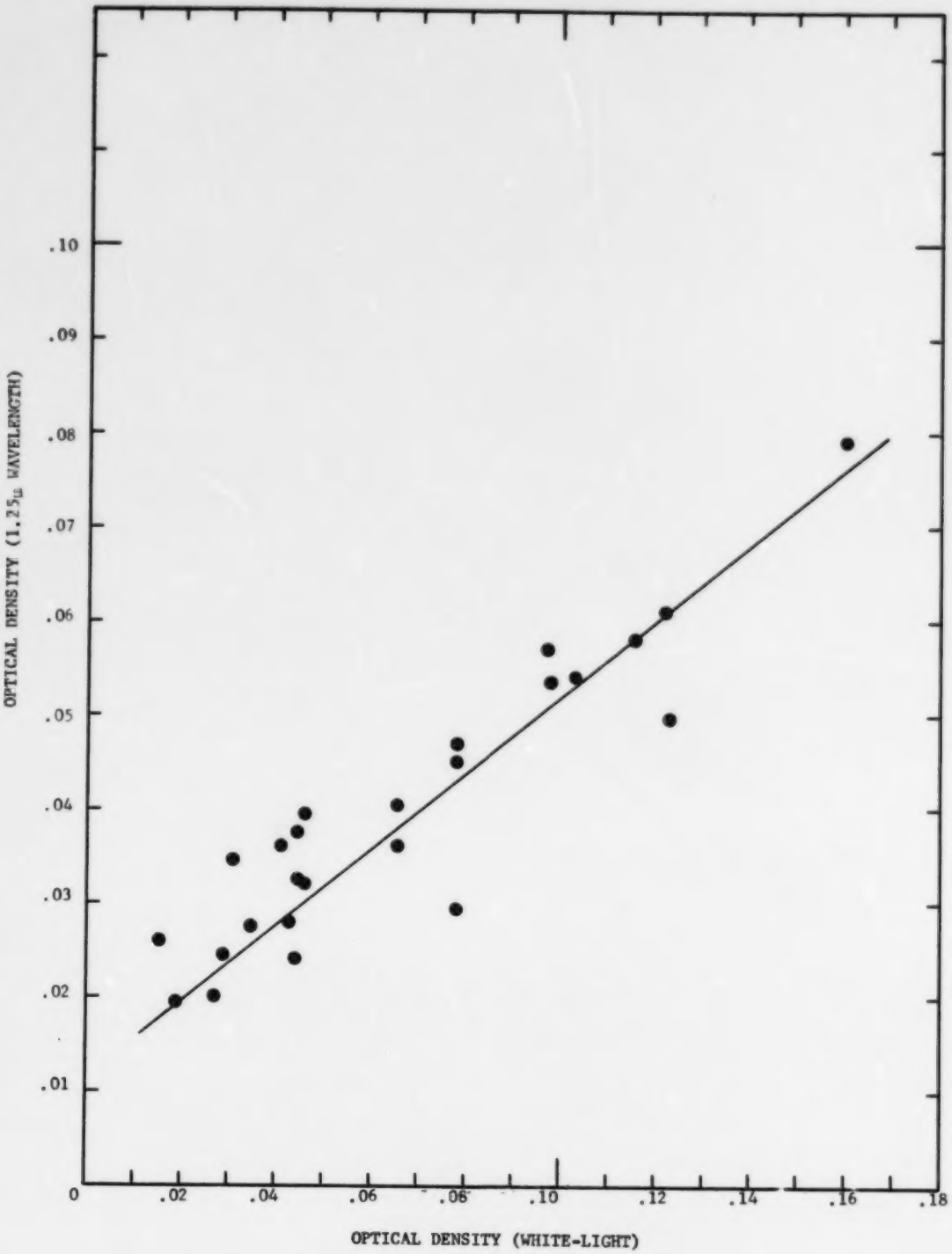

FIGURE 5-5

COMPARISON BETWEEN OPTICAL DENSITY MEASUREMENTS MADE WITH WHITE LIGHT AND MONOCHROMATIC RADIATION AT 1.25 MICRONS ON ASPHALTIC CONCRETE PLANT EMISSIONS

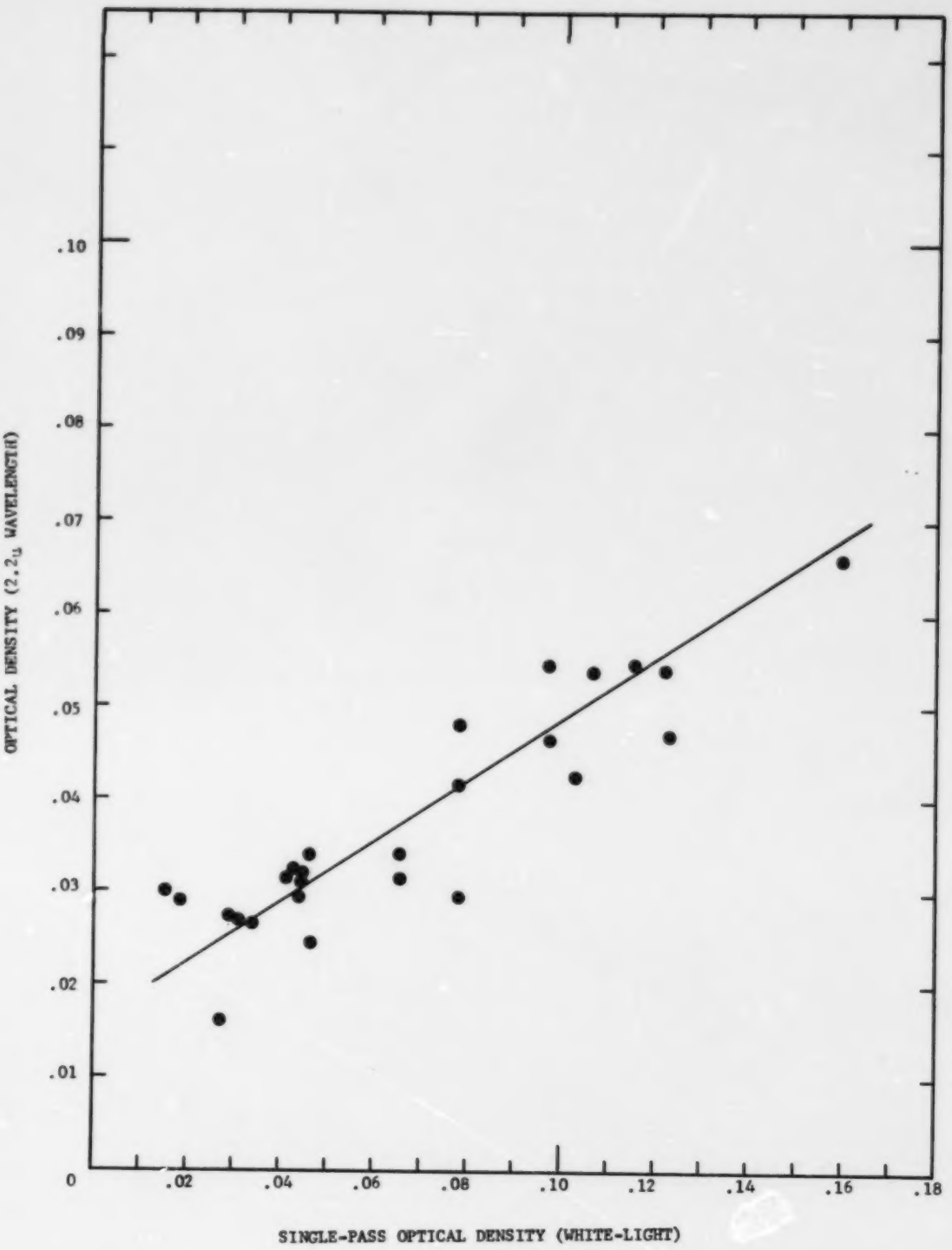

FIGURE 5-6

COMPARISON BETWEEN OPTICAL DENSITY MEASUREMENTS MADE WITH WHITE LIGHT AND MONOCHROMATIC RADIATION AT 2.2 MICRONS ON ASPHALTIC CONCRETE PLANT EMISSIONS

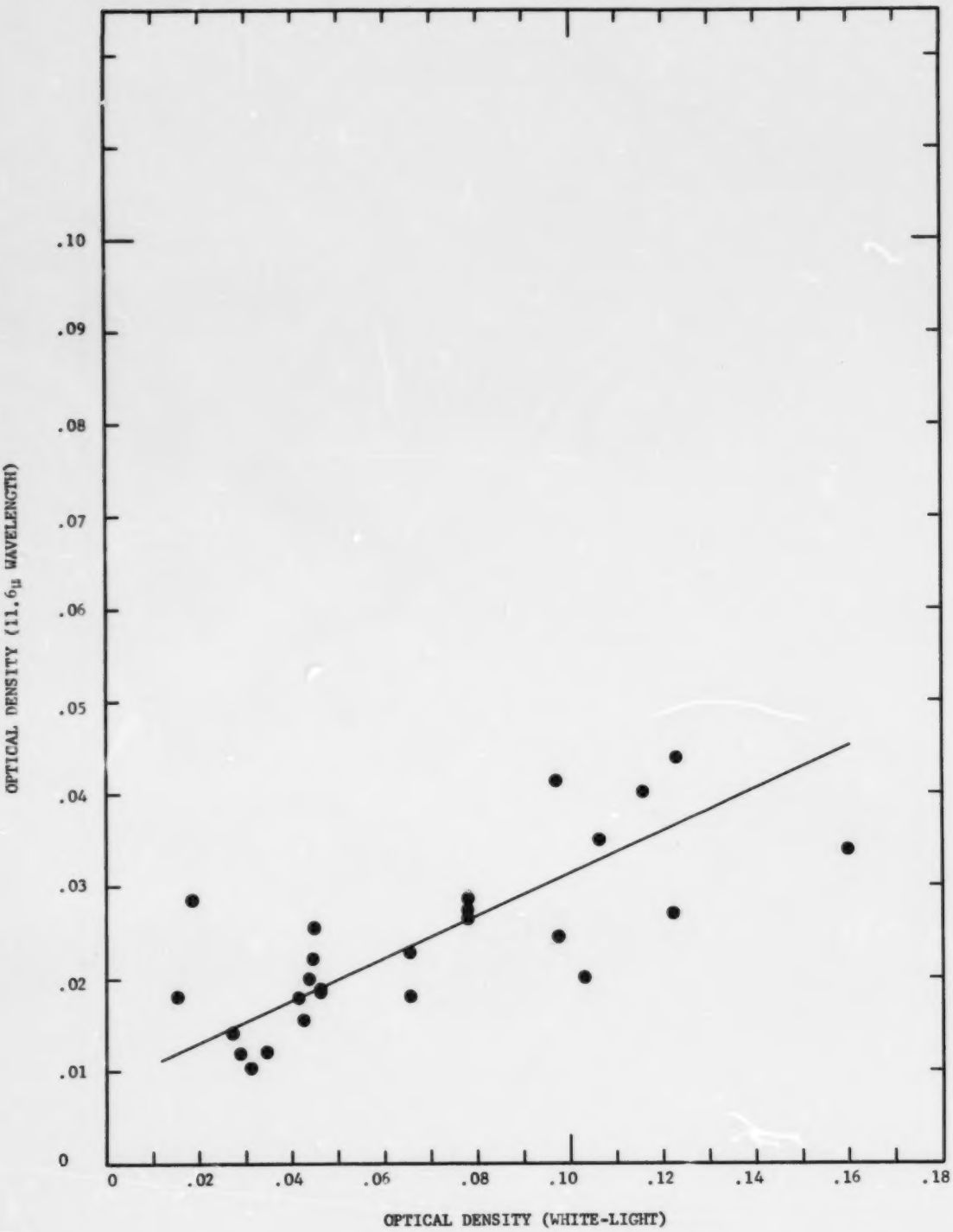

FIGURE 5-7

COMPARISON BETWEEN OPTICAL DENSITY MEASUREMENTS MADE WITH WHITE LIGHT AND MONOCHROMATIC RADIATION AT 11.6 MICRONS ON ASPHALTIC CONCRETE PLANT EMISSIONS

Figure 5-8 is a composite of the mean results at the four wavelengths. The data shows a gradual decrease in scattering efficiency with increasing wavelength. At 11.6 microns the efficiency is about 45% of what it is at .4 microns. The wavelength dependence is in close agreement with the optical dependence which would result from silica particles with a size distribution similar to those measured with the impactor.

Since the operational wavelengths of the multi-wavelength unit encompass that of the Lear Siegler unit, one might justifiably expect the optical densities to encompass the 1:1 line. The fact that this does not occur strongly suggests that the multi-wavelength unit is mounted at a point in the duct where it views lower emissions than the Lear Siegler unit. This supports the left-right asymmetry found in the probe samples. The reasons for this asymmetry and the geometry which forced us to accept it, can be inferred from the diagram of the ductwork and the constraints shown in Figures 3-1 and 3-2. This problem does not affect the size information from the multi-wavelength unit since this information is in the relative value of the slopes at the different wavelengths.

E. Material Analysis

Spectroscopic analysis was used on the collected samples to determine their composition. The dominant element was silicon (and oxygen presumably) with iron, aluminum, potassium, sodium, calcium and magnesium with a combined weight comparable to that of silicon. X-ray diffraction techniques indicate that the material was 50-75% α quartz, 15 to 35% feldspar and 5 to 15% amphibole. Microscopic examination was also made. Particles appear to be like fine granules of sand, mostly clear but some with pale color.

F. In-Stack Transmissometer Performance

The transmissometer was mounted directly on to the duct running from the baghouse to the exhaust fan. The duct had a rectangular cross section and was made from steel plate about 3 mm. thick (1/8"). Although the plate was structurally reinforced, it was subjected to heavy vibration during plant operation. This vibration was coupled to the transmissometer and caused a significant perturbation of the beam alignment. Since the instrument zero setting depended on this alignment, when the vibration began, the zero would suddenly shift to a new value and then slowly vary throughout the day. The shift in the zero was typically equivalent to double pass density shifts of about .005 - .010. The shifts throughout the day were about one third of these values and were thought to be caused by thermal deformation and differential expansion of the duct walls. In order to maintain a true zero, it was necessary to constantly check and adjust the alignment. A permanent transmisssometer installation at this site would require either strengthening of the duct

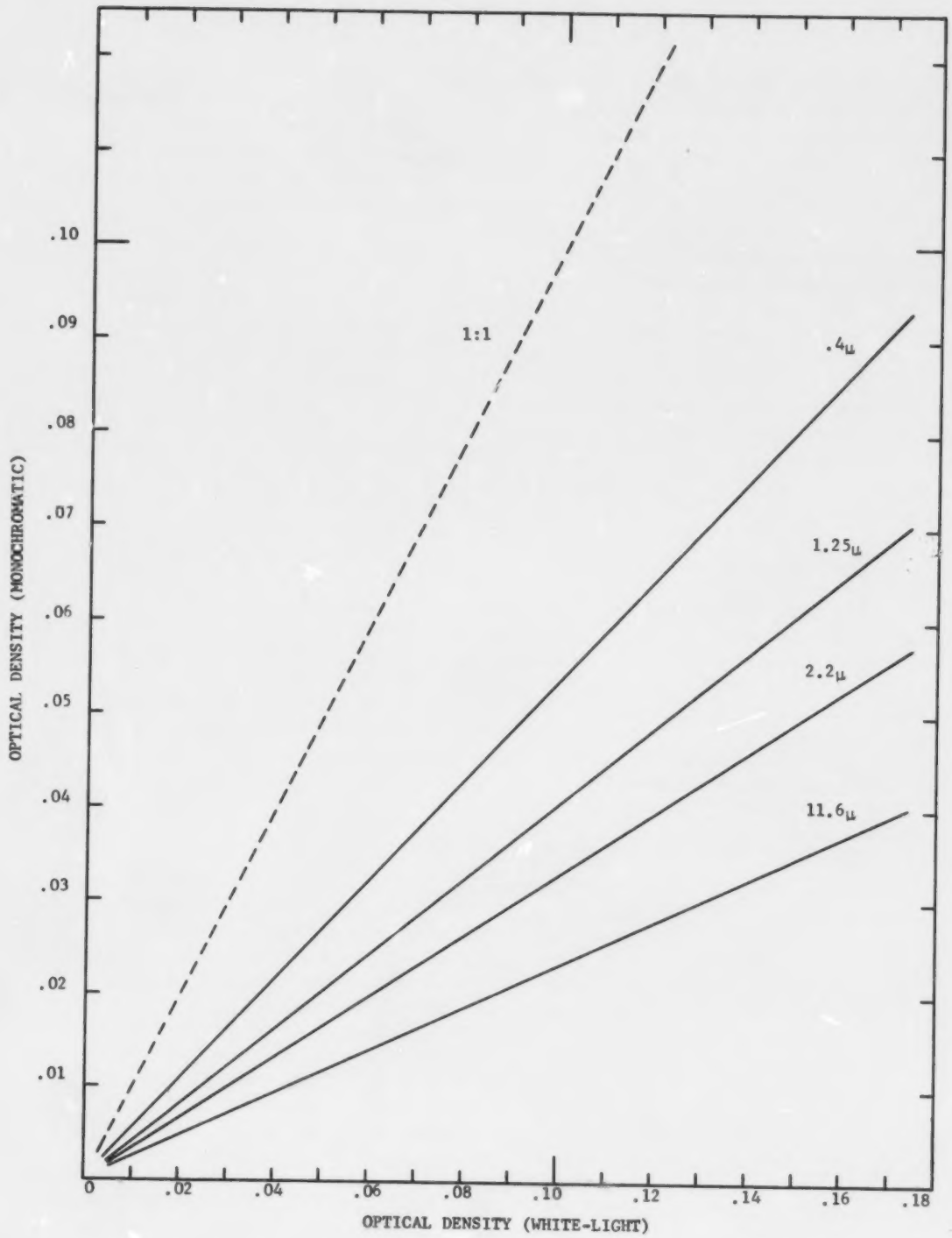

FIGURE 5-8

SUMMARY OF OPTICAL DENSITY MEASUREMENTS MADE ON ASPHALTIC CONCRETE PLANT EMISSIONS WITH WHITE LIGHT AND MONOCRHOMATIC RADIATION AT FOUR WAVELENGTHS

wall or support of the transmissometer by a stable structure external to the duct. The calibration zero was not particularly affected by the vibration and it varied about .002 optical density in a random fashion. The randomness appeared to be associated with the way the zeroing reflector seated and it occurred at every site.

2. SLUDGE INCINERATOR

The initial probe measurements revealed a very bad flow distribution in the stack. The velocity was very low except at back edge of the stack. This was due to the manner in which the ducts feeding the stack were designed. In order to improve the flow pattern, we designed and fabricated a truncated conical section to fit down inside the stack just above the feed ducts. The flow velocity was then uniform to about ± 50% instead of the previous factor of 10.

A second flow problem which we encountered was caused by a hood which was rigidly attached to the stack to protect the furnace from heavy rain. Not only did the hood interfere with the plume measurements but appeared to cause a recirculating flow which greatly affected the measured particulate characteristics of the stack. In the one case where we tried to make train measurements with the hood in place, the measured mass concentration was almost six times greater than that without the hood. The optical measurements were unchanged. We feel that this simply means that the recirculation affected the portions of the stack weighted heavily in the probe sampling pattern (i.e., the outer radii), but did not appreciably affect the opacity across the diameter. It is quite possible that for different hood and stack geometries, the results might have been significantly different. Because of these problems, we replaced the original fixed hood with an adjustable hood that could be quickly tipped out of the way and made all of our remaining measurements without the hood. The recirculation problem is one that should be considered anytime a sampling measurement is made or an optical instrument installed on a stack that is hooded.

The particle characteristics at Site #2 were entirely different from those of Site #1. The particles were smaller and appeared to be like amorphous carbon when collected. Although the furnace operated continuously, the transmissometer output varied in a cyclic fashion. The furnace was designed to be highly self regulating and automatically adjusts its dampers to control the operation. When we attempted to misadjust the burn in order to change the stack opacity, we had to constantly override the automatic control system. Originally we attempted to vary the stack opacity by reducing the efficiency of the scrubber but found

that when the furnace was operating efficiently the scrubber had very little influence on the particulates. The scrubber did not appear to be removing the particles nor did it appear to contribute to the plume opacity by adding moisture to the emissions. In fact, at no time did we observe a moisture plume at this site. We ultimately abandoned attempts to regulate the level of particulates using the scrubber in favor of misadjusting the burn.

During the test period at Site #2, we obtained a total of 13 probe measurements. Of the 13 measurements, two were impactor runs, one was exploratory and ten were full train measurements. These measurements covered the full range of operation over which the furnace could be manipulated (or more correctly, the range over which the crew were willing to deviate from normal operation).

A. Impactor Measurements

Two impactor runs were taken. The first was during normal furnace operation when the average stack opacity was about 2%. The majority of the particulates were too small for the impactor plates and were collected on the final filter. The results are shown plotted in Figure 5-9 where the percent of collected mass smaller than a given diameter is plotted on log normal paper. A second impactor run taken at a higher level of opacity (about 14%) is also shown. For the normal operation, the data shows that 90% of the mass is in particles whose diameters are less than .4μ. At the higher opacity the small particles still dominate. About 82% of the mass is in particles whose diameters are less than .4μ. It appears that the small particles are carbon and the large particles are fly ash. The density used in calculating D_p was taken to be that of an amorphous carbon, 1.95 gms/cm^3. This value is based on the chemical makeup of the samples.

B. EPA Train Measurements

The data for the train measurements are shown in Figure 5-10 where the in-stack opacity is plotted as a function of mass concentration. The run taken without the cone in place appears to fit will all the other runs in spite of its non-uniform flow. The run taken with the hood in place is grossly different than the rest.

C. Plume Opacity Measurements

A number of attempts were made to measure plume opacity using the sun photometer, but only limited data were obtained. We finally constructed a pair of black and white targets and proceeded to take

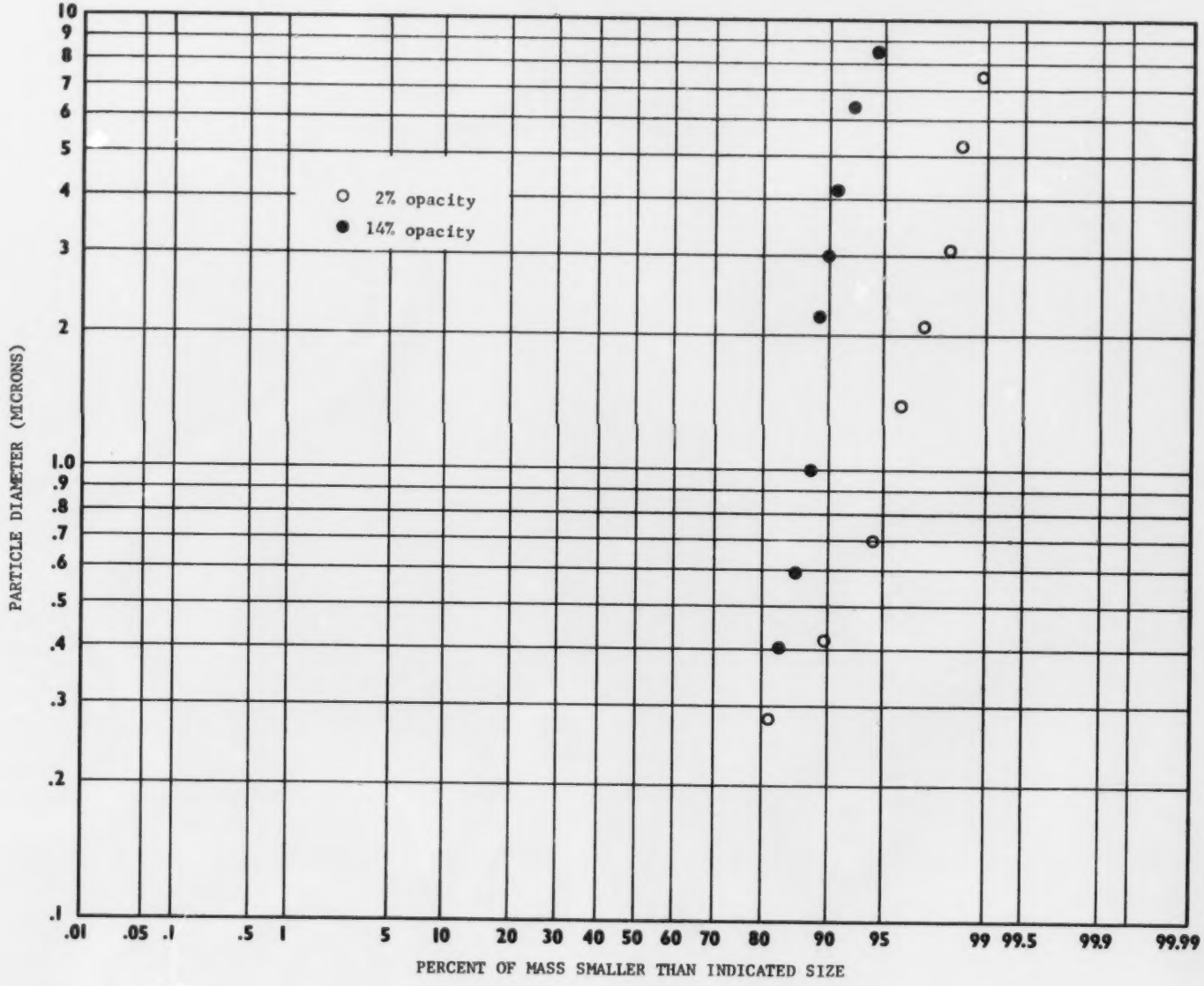

FIGURE 5-9

PARTICLE SIZE DISTRIBUTION OF THE SLUDGE INCINERATOR EMISSIONS

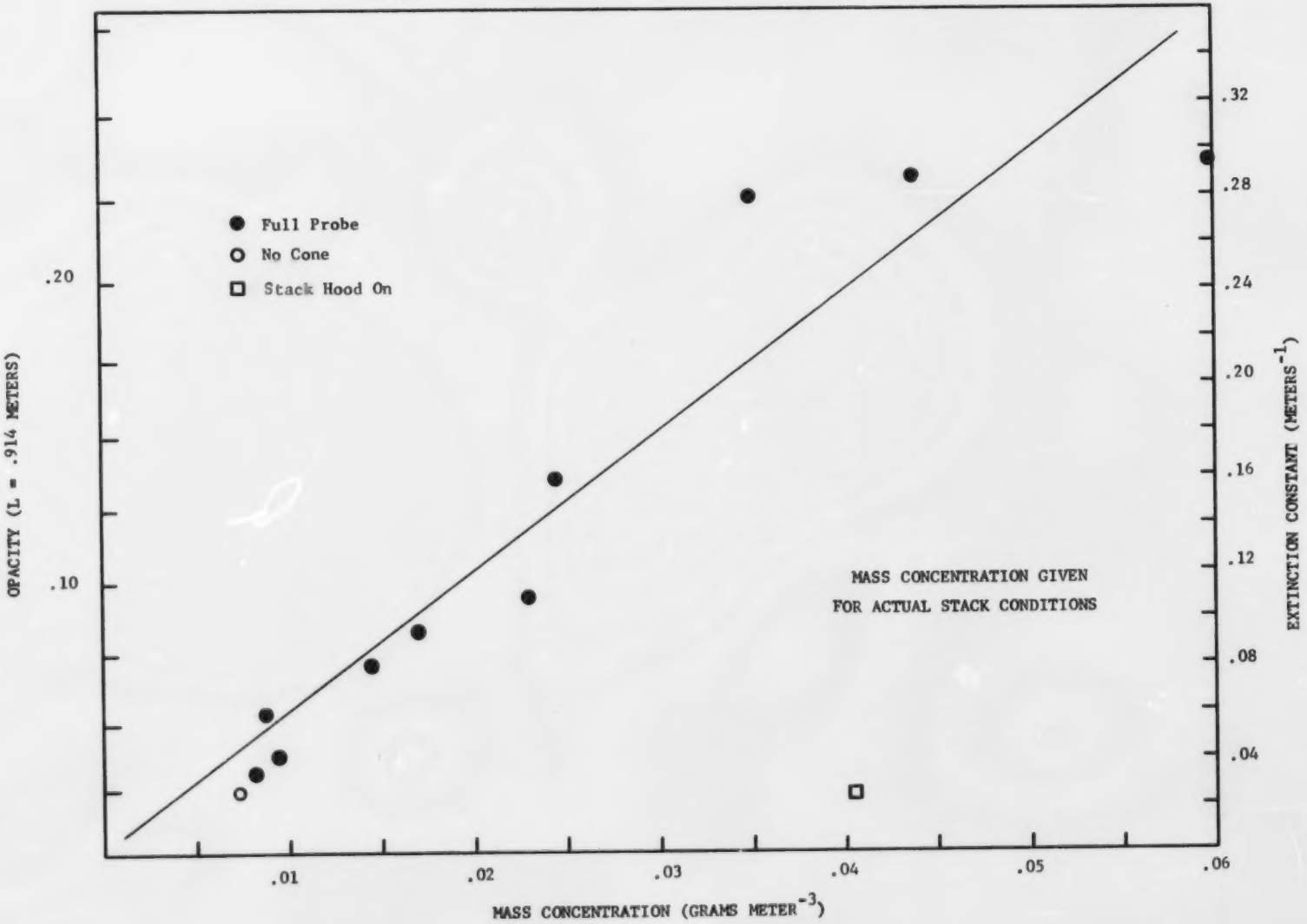

FIGURE 5-10

OPACITY - MASS CONCENTRATION RELATIONSHIP OF THE INCINERATOR PLANT EMISSIONS

telephotometer data for various levels of opacity. Over thirty measurements were obtained using this technique. The measurements were made with the blue filter, with the red filter and with no filter at all. Only the results taken without a filter were sufficiently repeatable to be used as data and these are shown in Figure 5-11. The data is slightly erratic. An attempt has been made to identify the uncertainty in the telephotometer readings due to fluctuations on the meter. It was felt that these uncertainties were about ± 5 divisions on any portion of the scale (e.g. full scale is 1000 divisions). These uncertainties are shown as error bars on figures.

D. Multiwavelength Transmissometer

Data was again taken at .4μ, 1.25μ, 2.2μ and 11.6μ. The single pass optical densities at these four wavelengths are shown in Figure 5-12. The data shows a steady decrease in scattering efficiency (i.e., extinction efficiency) with increasing wavelength. At 1.25μ the efficiency is about 1/4 of that at 0.4μ and 2.2μ is one-half of that at 1.25μ. These values agree well with those that arise from carbon particles about 0.2μ in diameter. The efficiency at 11.5μ is higher than expected. Experimentally it is about one-half that at 2.2μ whereas a value of about one-sixth was anticipated. The deviation is possibly due to the behaviour of the index in that region (for example, see Twitty and Weinman[12].

E. Material Analysis

The material collected was predominantly carbon with an ash content of 11%. The principle ingredients in the ash were zinc, lead, silicon, tin and phosphorus in that order of importance.

F. In-Stack Transmissometer Performance

The transmissometer behaved very well at this site. The true zero was stable to an equivalent density of .004; the calibration zero was stable to about .002. At no time did we see the calibration vary (i.e., there was a constant density change each time the calibration filter was activated in the Lear Siegler unit). There was very little vibration at this site.

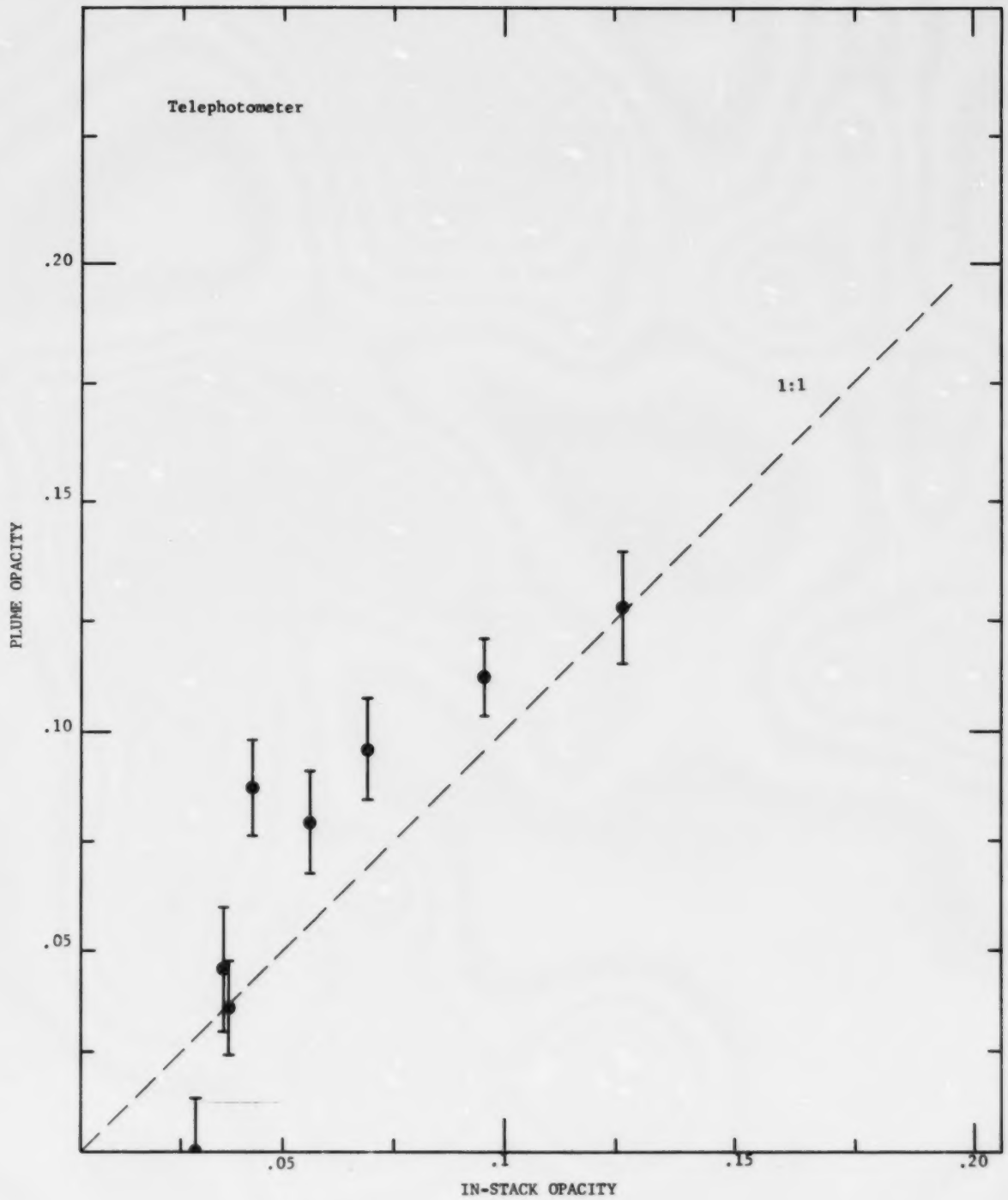

FIGURE 5-11

COMPARISON OF THE PLUME AND IN-STACK OPACITIES OF THE SLUDGE INCINERATOR EMISSIONS

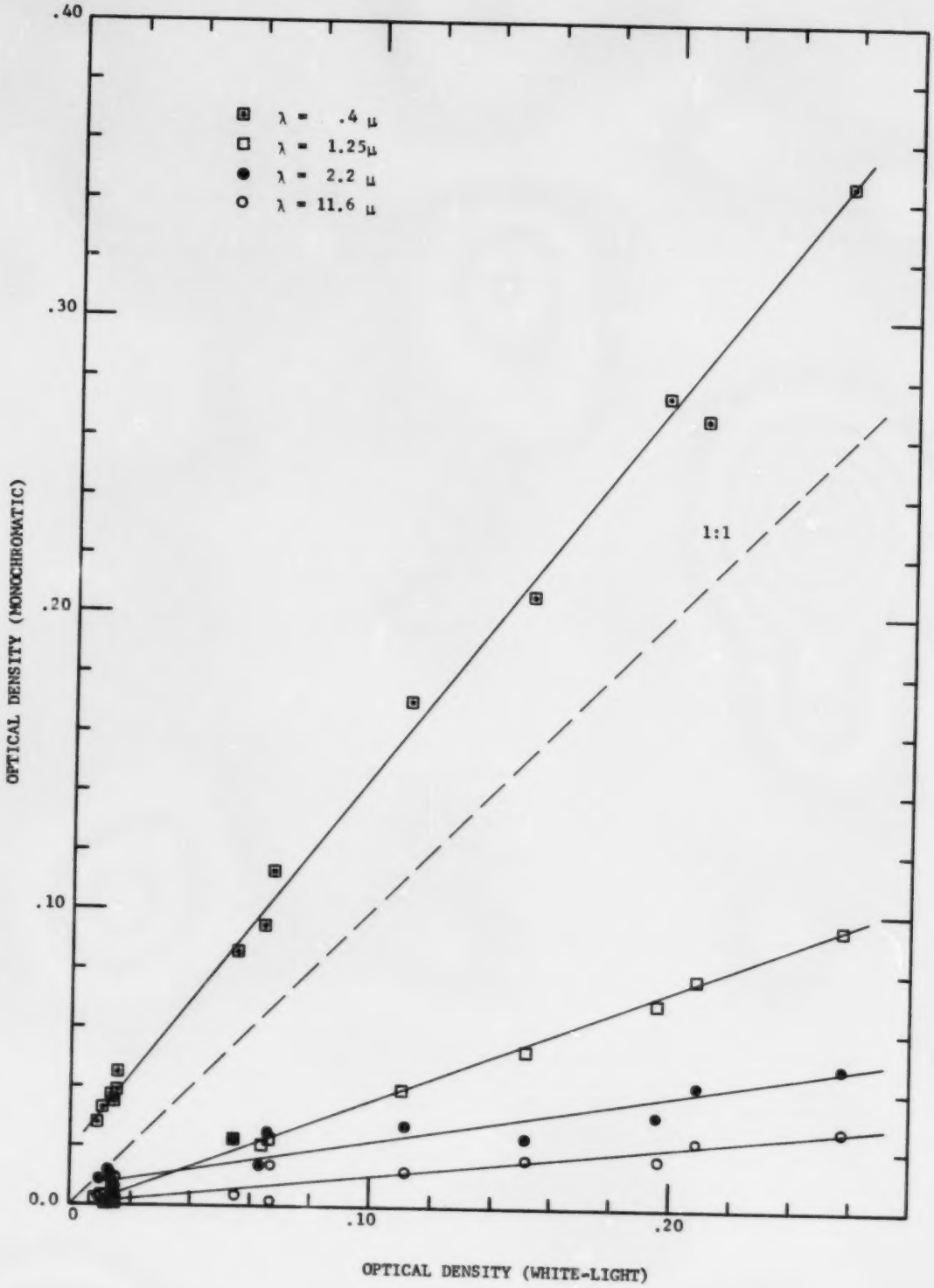

FIGURE 5-12

SUMMARY OF OPTICAL DENSITY MEASUREMENTS MADE ON SLUDGE INCINERATOR EMISSIONS WITH WHITE LIGHT AND MONOCHROMATIC RADIATION AT FOUR WAVELENGTHS

3. REFINERY CATALYTIC CRACKER REGENERATOR

During the testing period at Site 3, a total of seventeen probe measurements were made. Five of these were impactor runs for purposes of determining size distributions during the various modes of precipitator operation. The runs fully spanned the opacity range which the refinery management permitted us to explore.

A. Impactor Measurements

Of the five impactor measurements made, two were taken under normal conditions with the precipitator sections all on. One was taken with sections 2 and 3 turned off, one with section 1 turned off and one with sections 1 and 3 turned off. We were not permitted to turn all the sections off because of the excessive plume opacities which would result. The results of the measurements are shown in Figure 5-13. The data is again plotted on log normal paper and forms an approximation to a straight line in each case. The median particle diameter falls between 1 and 2 microns. The particulate is an aluminum silicate in the form of a zeolyte which has been doped with rare earth oxides. We have taken the density to be 2.3.

B. EPA Train Measurements

The data from the train measurements are shown in Figure 5-14 where the in-stack opacity is plotted as a function of mass concentration. Run #1 has not been included because it appears to be anomolous in that the mass concentration is abnormally high. This might be due to an unrecoverable weighing error. The data shows more scatter than that of either Site 1 or Site 2.

C. Plume Opacity Measurements

Several attempts were made to measure the plume opacity using the sun photometer. Except for a few minutes late in the afternoon, the shadow of the stack was inaccessible as it was continually intercepted by other stacks and other structures. Attempts were also made to set the telephotometer on one of the levels of the catalytic cracker and sight through the plume to naturally occuring ground targets. This method also proved to be unsatisfactory as the areas which were viewable were very structured and small pointing errors in the telephotometer produced variation in readings which exceed the stack opacities.

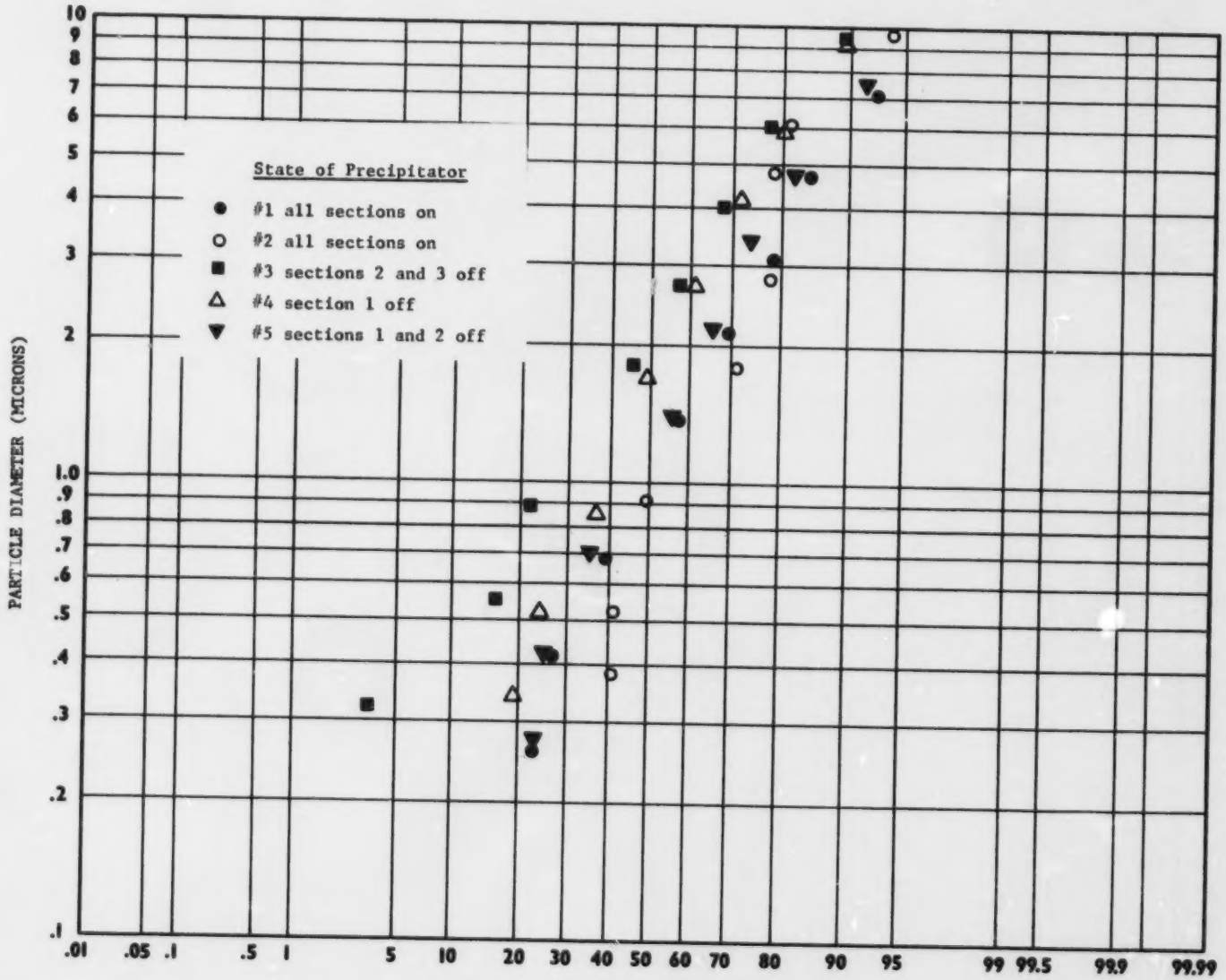

FIGURE 5-13

PARTICLE SIZE DISTRIBUTIONS OF THE REFINERY CATALYTIC CRACKER REGENERATOR EMISSIONS

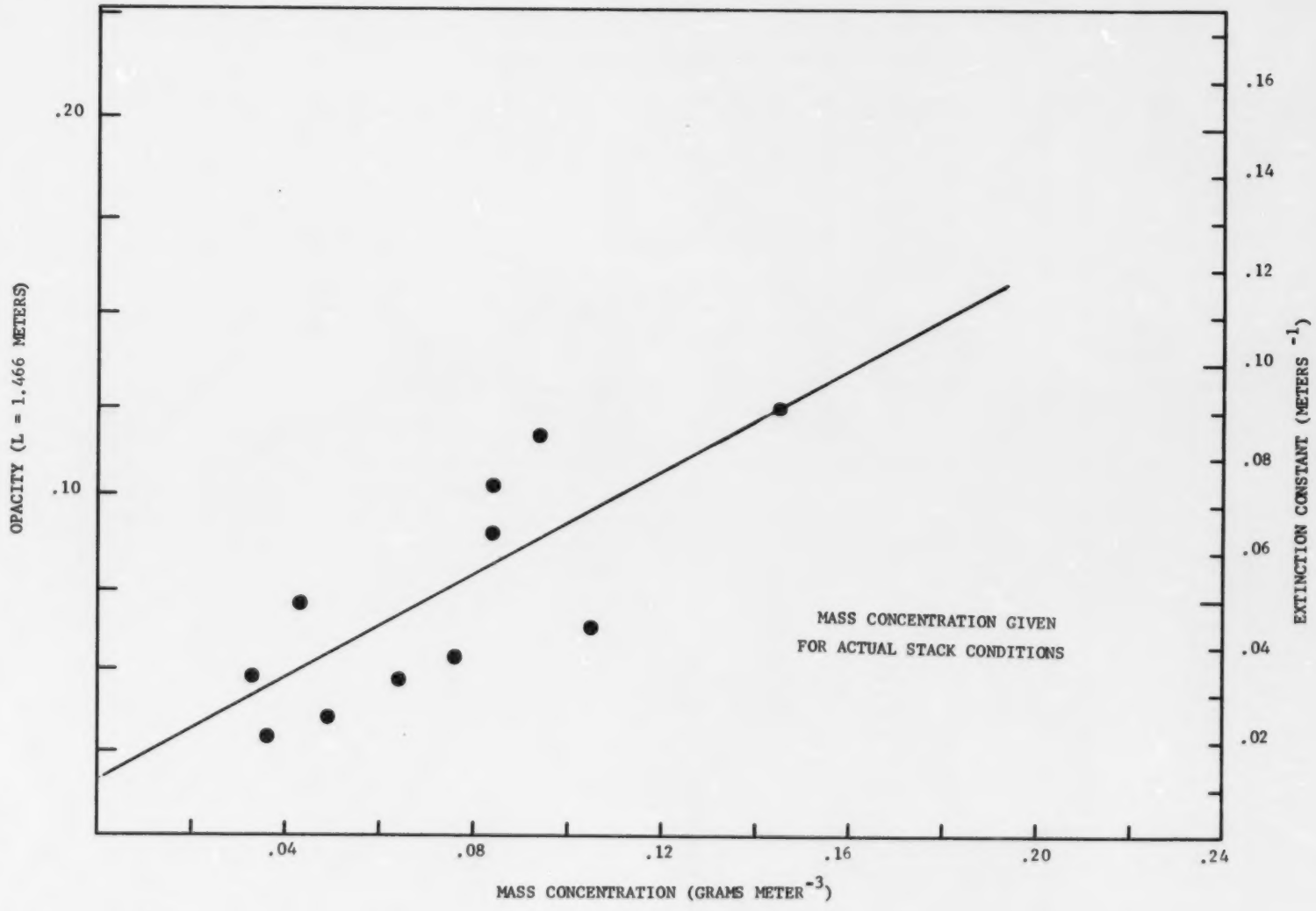

FIGURE 5-14

OPACTIY-MASS CONCENTRATION RELATIONSHIP OF THE REFINERY CATALYTIC CRACKER REGENERATOR EMISSIONS

The most consistent plume opacity data was obtained by working at night and using a light placed on an adjacent stack. The light was viewed both through the plume and to one side of the plume. It would have been ideal to switch the light on and off but safety regulations prohibited this because of the potential explosion hazard. Instead, a black shadow area immediately above the lamp was also viewed. Readings were taken with the various filter options previously described, however, only the data taken without the filter are presented (Figure 5-15).

D. Multiwavelength Transmissometer

Data was again taken at .4μ, 1.25μ, 2.2μ and 11.6μ. One fact that became evident by the time we had reached the third site was that surges in opacity were, in general, accompanied by changes in the size distribution. This could not be sensed by the white light transmissometer alone and some times not by the visible or near visible channels of the multiwavelength unit. At the far IR wavelength, these size differences were much more significant. We generally selected our data points in three different ways. If the opacity were staying at a constant level or was varying slowly so that an average value could be ascertained, we would record the average and refer it to 100% transmission. If superimposed on this average were an occasional spike, we could do one of two things. We could take the opacity peak and refer it to 100% transmission or refer it to the base of the spike. This latter approach will produce the most significant effect whenever there is a size change associated with the peak. Naturally, whatever procedure is used, it is used at all wavelengths.

At the asphaltic concrete plant, the opacity was constantly fluctuating making it difficult to determine average values. Almost every reading was associated with a violent increase or decrease in opacity and particles of a different size on a different portion of the size distribution. If "best fit" slopes are drawn through these points (a pseudo time averaging technique), then the results should agree with the distribution obtained from a time average monitoring technique (as in the impactor data). If, however, a single set of points are looked at, then it is apparent that the fall off of opacity with increasing wavelength varies from data point to data point. This suggests that the distribution is not constant over short times even though the long time average is very stable.

At the sludge incinerator site, the distribution appears to be very stable for both long and short periods and so the data falls into a pattern of well defined straight lines of decreasing slope. The ratios of the slopes were characteristic of carbon particles in the .1 to .2μ range.

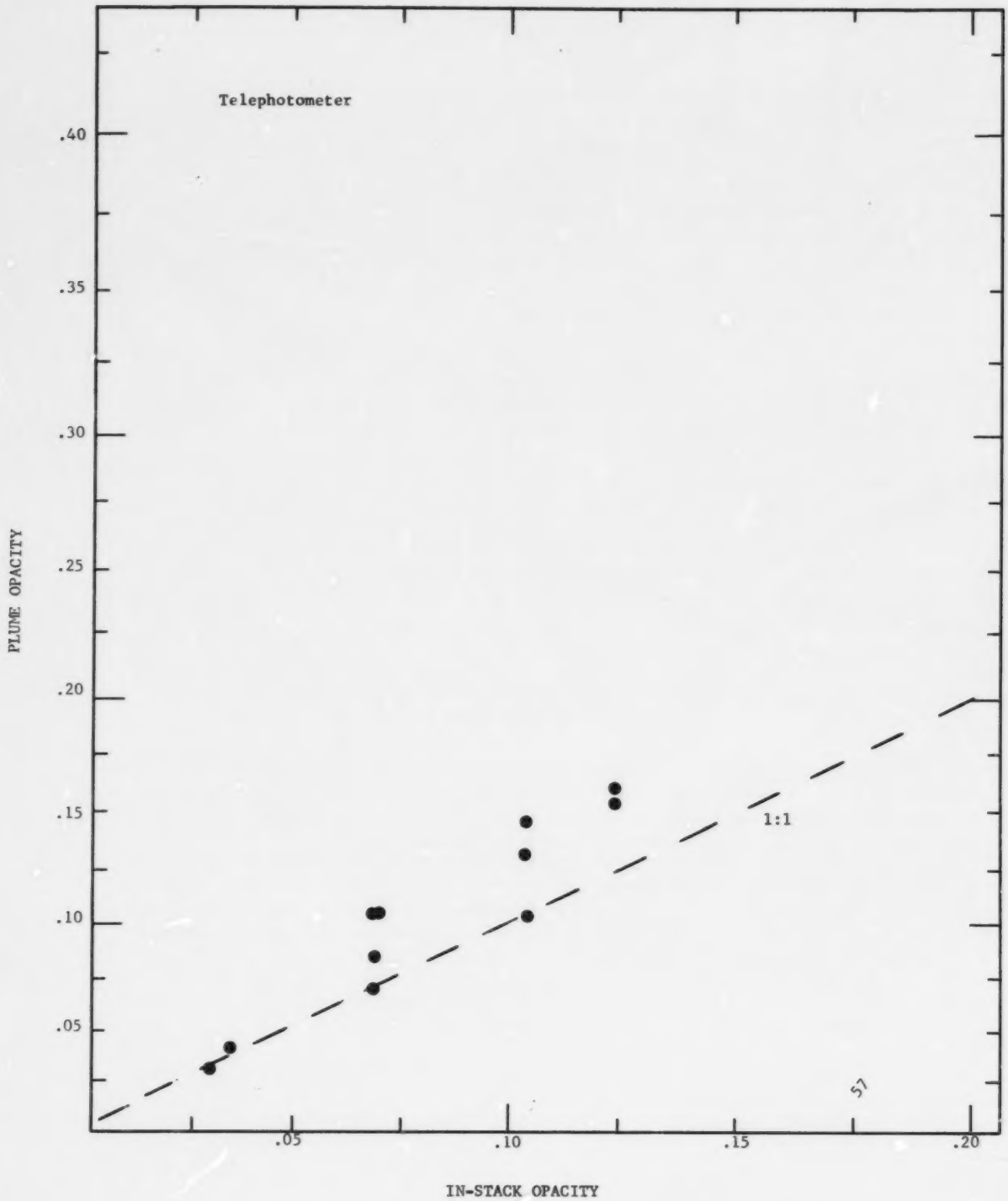

FIGURE 5-15

COMPARISON OF THE PLUME AND IN-STACK OPACITIES
OF THE REFINERY CATALYTIC CRACKER REGENERATOR EMISSIONS

At the refinery catalytic cracker regenerator site, changes in opacity were brought about by shutting off various combinations of sections in the precipitator. This initiates the release of material trapped in the precipitator. The initial release is very heavy and then gradually slows down. Every time the shut down unit is shaken or rapped by its automatic equipment, there is a further release of material. The visual results of the size changes are only slightly evident at .4 and 1.25μ but cause a considerable spread in the data at 2.2μ. The data at 11.6 was not presented because the detector appears to have suffered from a thermal problem. The data at .4μ is shown in Figure 5-16, that at 1.25μ in Figure 5-17 and that at 2.2μ in Figure 5-18. Figure 5-19 is a composite of the three slopes. The slope data agrees with the time averaged distribution observed in the impactor. The instantaneous data points (particularly at 2.2μ) show fluctuations in particle size.

E. Material Analysis

Spectroscopic analysis showed that the material collected in the probe was predominently silicon and aluminum with small amounts of neodymium and only traces of other metals. This is quite reasonable since the material is an aluminum silicate in the forms of a zeolite. A few percent of depleted rare earth oxides have been added to the zeolite as a cracking catalyst.

F. In-Stack Transmissometer Performance

The transmissometer behaved very well and showed drifts similar in magnitude to those reported at the previous sites.

4. BRASS AND LEAD SMELTER

During the testing period at Site 4/5, a total of 18 probe runs were made plus a series of other preliminary traverses to determine temperature and velocity profiles. Of the 18 runs, six were impactor measurements and the remaining twelve were mass concentration measurements. Although, on occasion, the plant activity was dominated by either the brass operation or the lead operation, generally the plant schedule was such as to provide combined lead and brass operations throughout most of our stay. The installation of controlled leaks in the separate baghouses permitted us to cause one or the other to be predominant, with

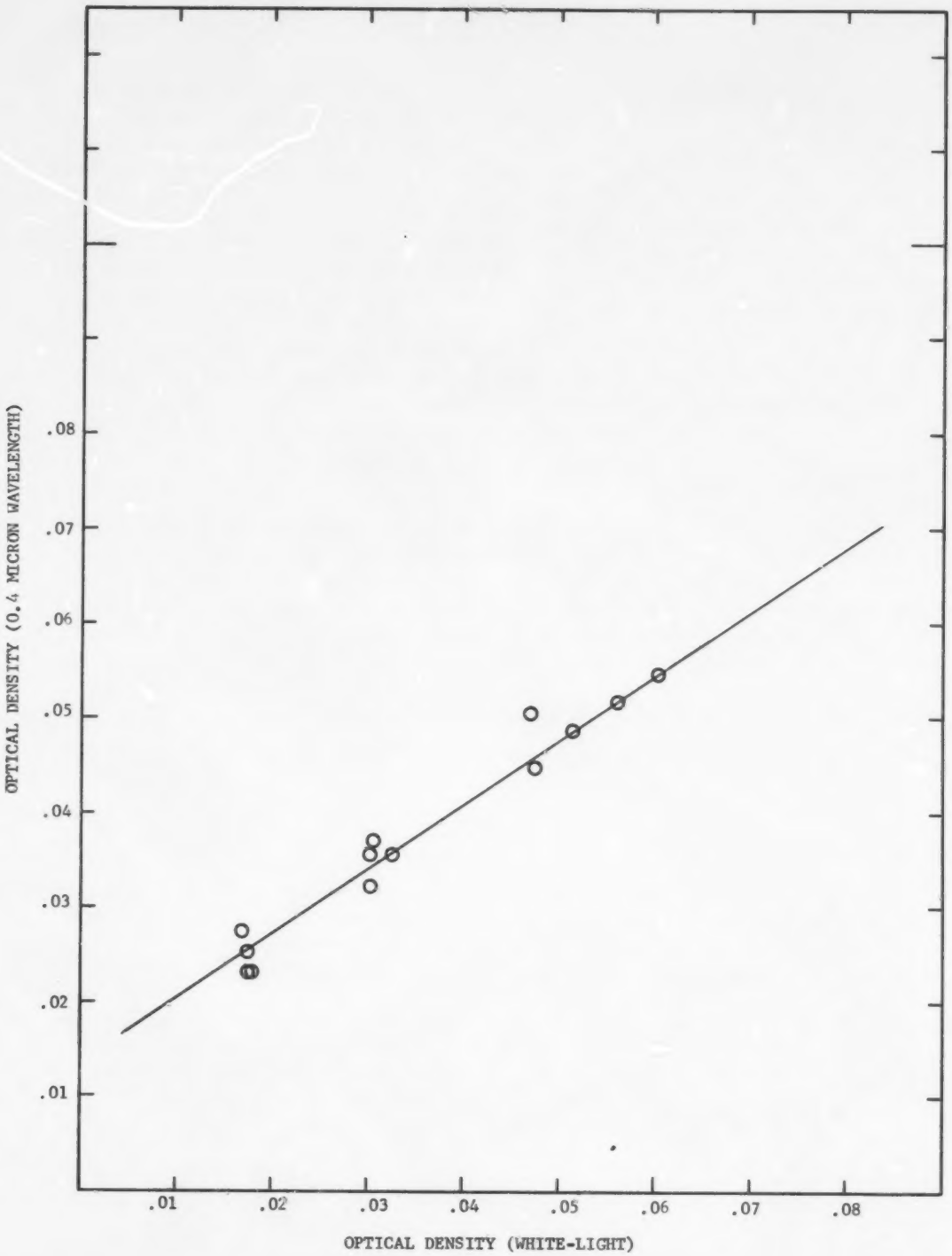

FIGURE 5-16

COMPARISON BETWEEN WHITE-LIGHT AND 0.4 MICRON MONOCHROMATIC
OPTICAL DENSITY MEASUREMENTS OF THE REFINERY CATALYTIC CRACKER REGENERATOR EMISSIONS

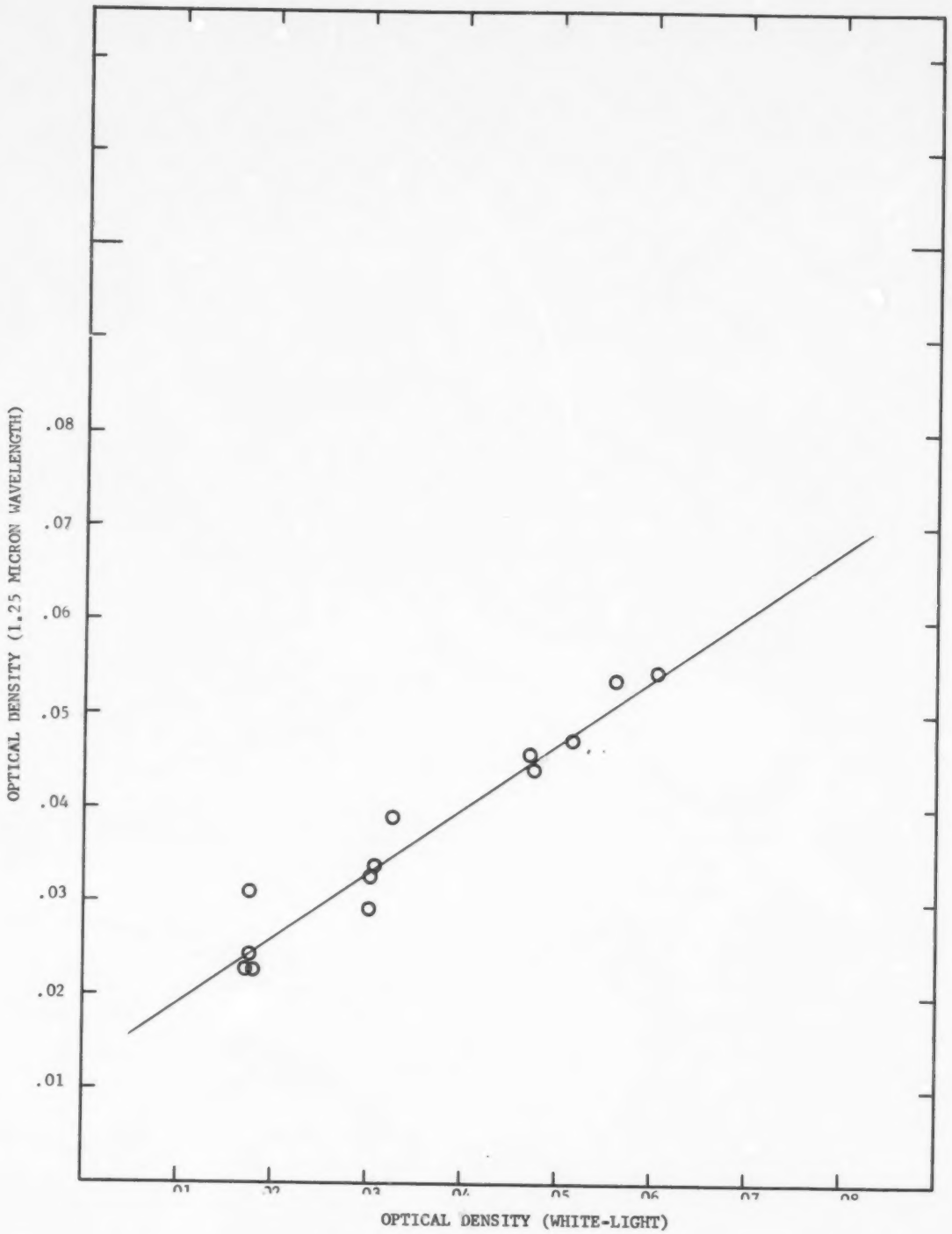

FIGURE 5-17

COMPARISON BETWEEN WHITE-LIGHT AND 1.25 MICRON MONOCHROMATIC
OPTICAL DENSITY MEASUREMENTS OF THE REFINERY CATALYTIC CRACKER REGENERATOR EMISSIONS

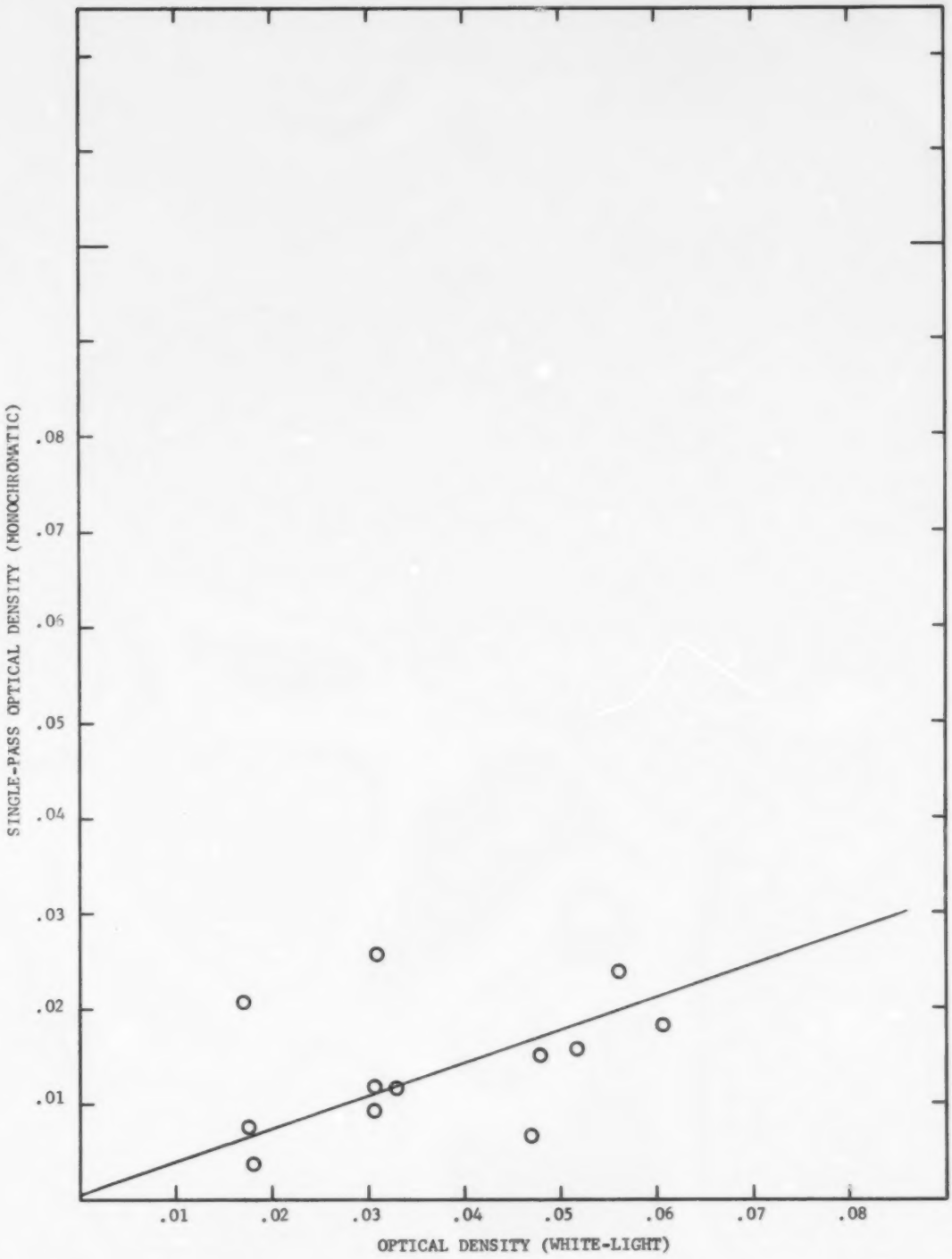

FIGURE 5-18

COMPARISON BETWEEN WHITE-LIGHT AND 2.2 MICRON MONOCHROMATIC
OPTICAL DENSITY MEASUREMENTS OF THE REFINERY CATALYTIC CRACKER REGENERATOR EMISSIONS

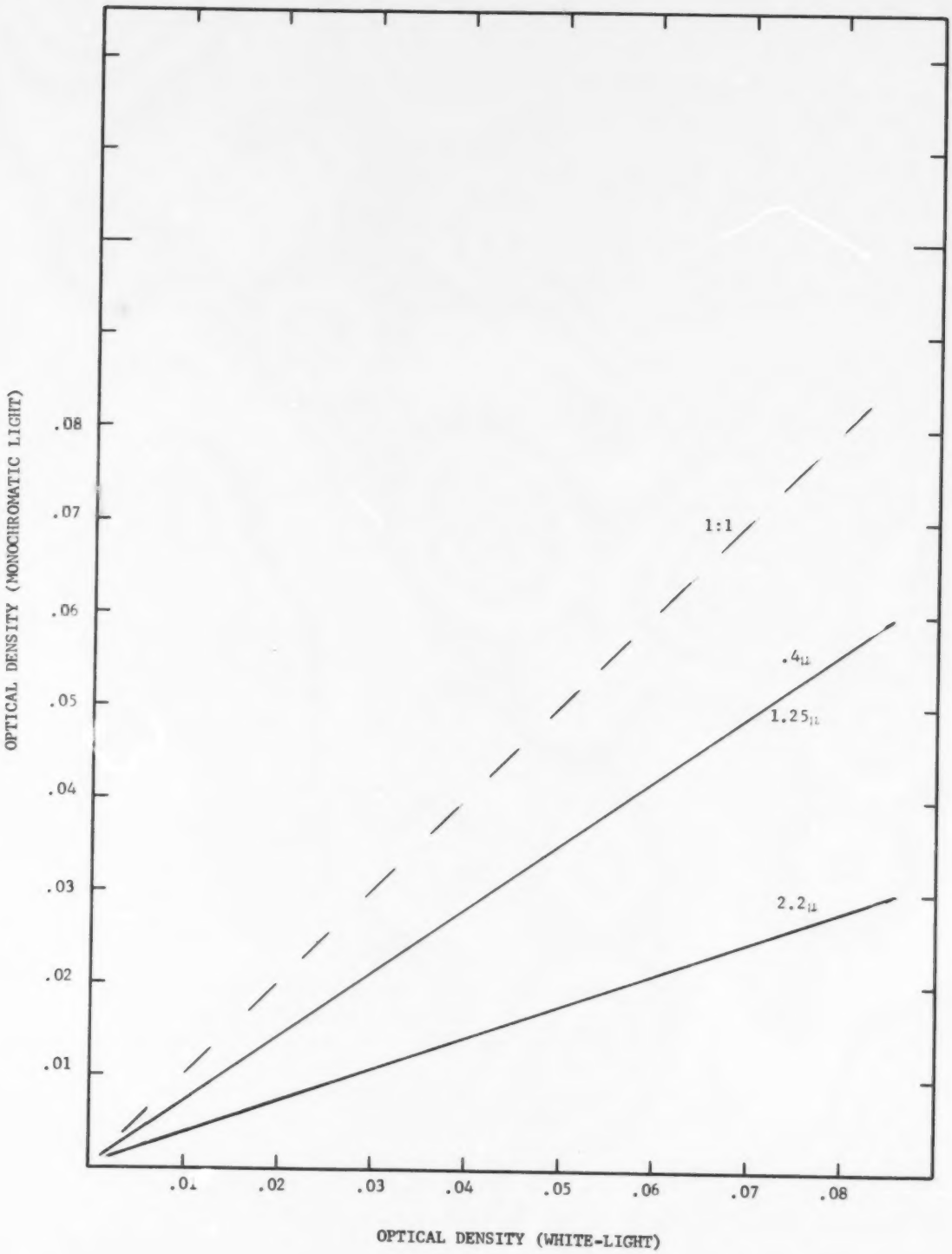

FIGURE 5-19

SUMMARY OF OPTICAL DENSITY MEASUREMENT MADE ON REFINERY CATALYTIC CRACKER REGENERATOR EMISSIONS WITH WHITE LIGHT AND MONOCHROMATIC RADIATION OF THREE WAVELENGTHS

the capability of varying the levels of mass concentration of either. While we might be able to determine which side of the house was responsible for the emission, it was very difficult, on a minute by minute basis, to determine exactly what was happening at the furnace. For example, if a twelve hour period was scheduled for charging the brass smelter, the crew might be physically dumping scrap (which varied widely from billet to billet), agitating the scrap into the melt, or just sampling the composition of the melt. In all cases, they would be opening doors and dampers, turning the heat on and off and otherwise varying the air flow through the stack.

A. Impactor Measurements

Of the six impactor measurements made, two were dominated by the lead operation, three by the brass operation and one was a mixture of both. The dominant particulate of the lead operation is lead oxide. We have used a density of 9.5 for these particles. The dominant particulate of the brass operation is zinc oxide which has a density of 5.6.

The size distribution data for the two samples of lead particulates are shown plotted on log normal paper in Figure 5-20. In the first case, there is no leak and a total sample of approximately 4.4 milligrams was collected. The distribution is bimodal with most of the particles less than .18μ in diameter (i.e., 35% of the mass) and a major portion of the remainder of the mass centered near a diameter of 3μ. There is almost no mass between .2μ and 1.0μ. The second sample had a total weight of about 50 milligrams and was collected with a baghouse leak orifice set primarily at 95 cm^2*. The points lie closer to a straight line (but a poor straight line). What appears to have happened is that the size region that was void of mass in the sample taken without a leak has picked up a majority of the additional mass. The small particles (i.e., less than .17) have increased in mass by a factor of 3 and the large particles (a diameter greater than 2μ) have increased by a factor of 4 and the mid-range, by a factor of 50 to several hundred, depending on the definition of "range", representing about 70% of the collected mass. Both runs were made during the charging phase of the operation.

The values of the median diameters are slightly deceptive in the two cases. In the first case, it is at 1.8μ because the mass in the large particle mode is slightly greater than the small particle mode. Shifting some of the mass from one to the other would produce the median close to .2μ. When the leak is operational, the presence of the particles between the modes shifts the median to .4μ.

*The orifice was sometimes changed in the middle of a measurement in order to control the plume opacity. If, for example, the furnace emissions became excessive, the orifice size would be reduced.

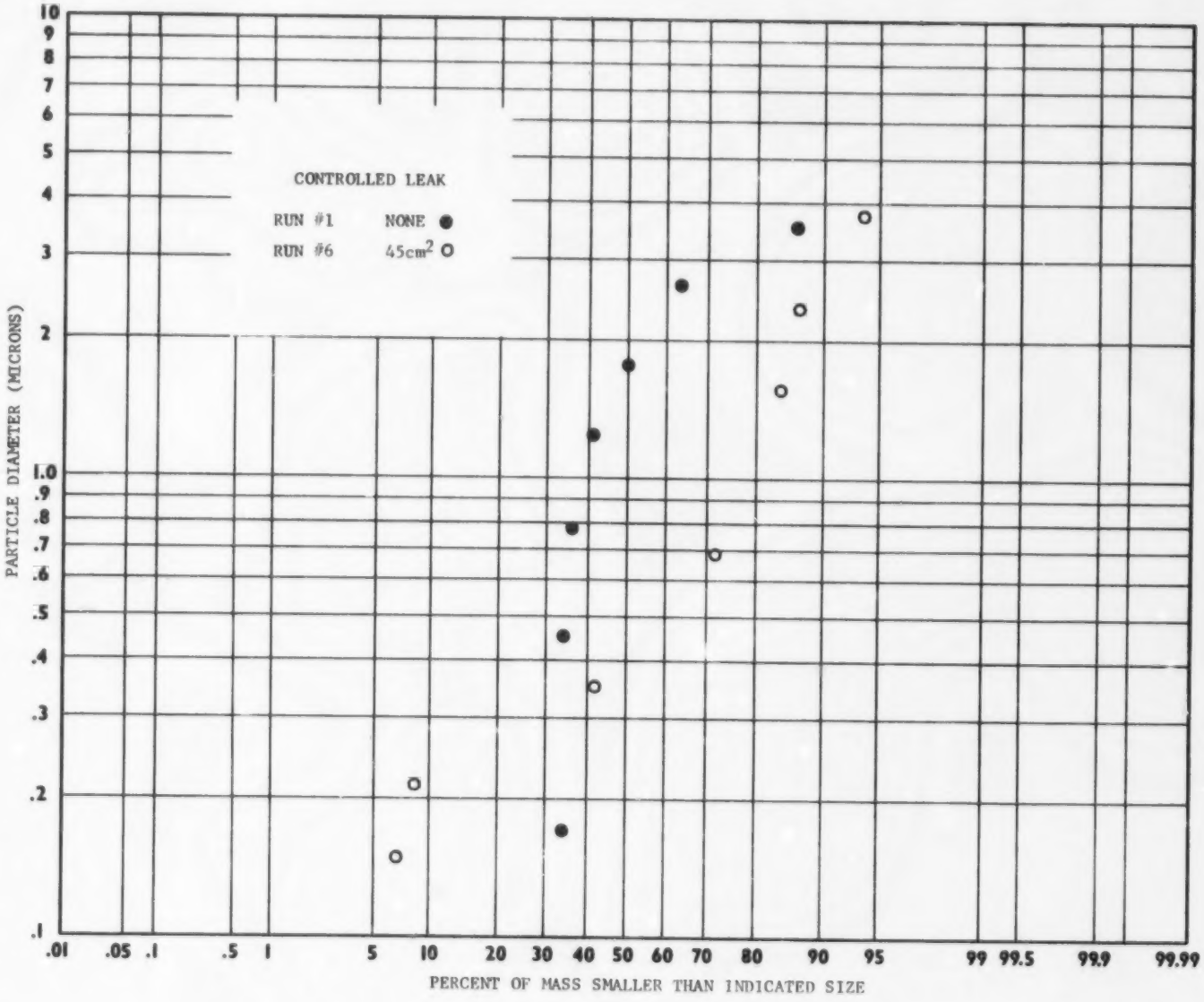

FIGURE 5-20
PARTICLE SIZE DISTRIBUTION OF THE LEAD SMELTER EMISSIONS

The size distributions for three examples of brass particulates are shown in Figure 5-21. The data taken with no baghouse leak might be considered as log normally distributed with a median diameter of 2μ. The total sample was 4.2 mg taken when the large brass smelter was operating but not charging.

The data in the second curve was taken when there was a controlled leak 136 cm^2 in area on the brass side of the baghouse. The median diameter is $.4\mu$. The mass of the sample is 44.0 mg taken immediately after a charging period but at a time when the emissions were low. The data in the third curve was taken when there was a controlled leak 90 cm^2 in area. Almost all of the mass (i.e., 93%) is in the form of particles less than $.24\mu$ in diameter. There are essentially none from .4 to 2.0 microns. In fact, 70% of the particles fall between $.17\mu$ and $.24\mu$. The sample size was 30 mg. There was very little plant activity and were it not for the leak, there would be essentially no emissions at the time the sample was taken.

B. EPA Train Measurements

In spite of the diverse nature of the impactor data, the mass concentration data forms a very smooth, straight line. Figure 5-22 shows the in-stack opacity plotted as a function of the mass concentration for brass emissions. Figure 5-23 shows a similar plot for the lead emissions. One lead run which resulted in a mass concentration of .0088 gm/m^3 is not plotted because an electrical problem caused the loss of the transmissometer data.

C. Plume Opacity Measurements

Opacity measurements were made through both lead and brass plumes using the sun photometer. The results of both sets are plotted in Figure 5-24. The error bars on the in-stack opacity readings are due to fluctuating transmissometer readings and the uncertainty in placing the event marker on the transmissometer strip chart. In both cases, the plume data has been reduced to a path equivalent to that of the transmissometer.

D. Multiwavelength Transmissometer

Data was again taken at $.4\mu$, 1.25μ, 2.2μ and 11.6μ for both the brass and lead operations. Figure 5-25 shows the result for brass. The scattering efficiency is very high at $.4\mu$, about twice that recorded by the white light transmissometer. At 1.25μ, the scattering efficiency has dropped by about a factor of 10. No data is shown at the larger wavelengths because the scattering efficiency is so small no reliable measurement could be made.

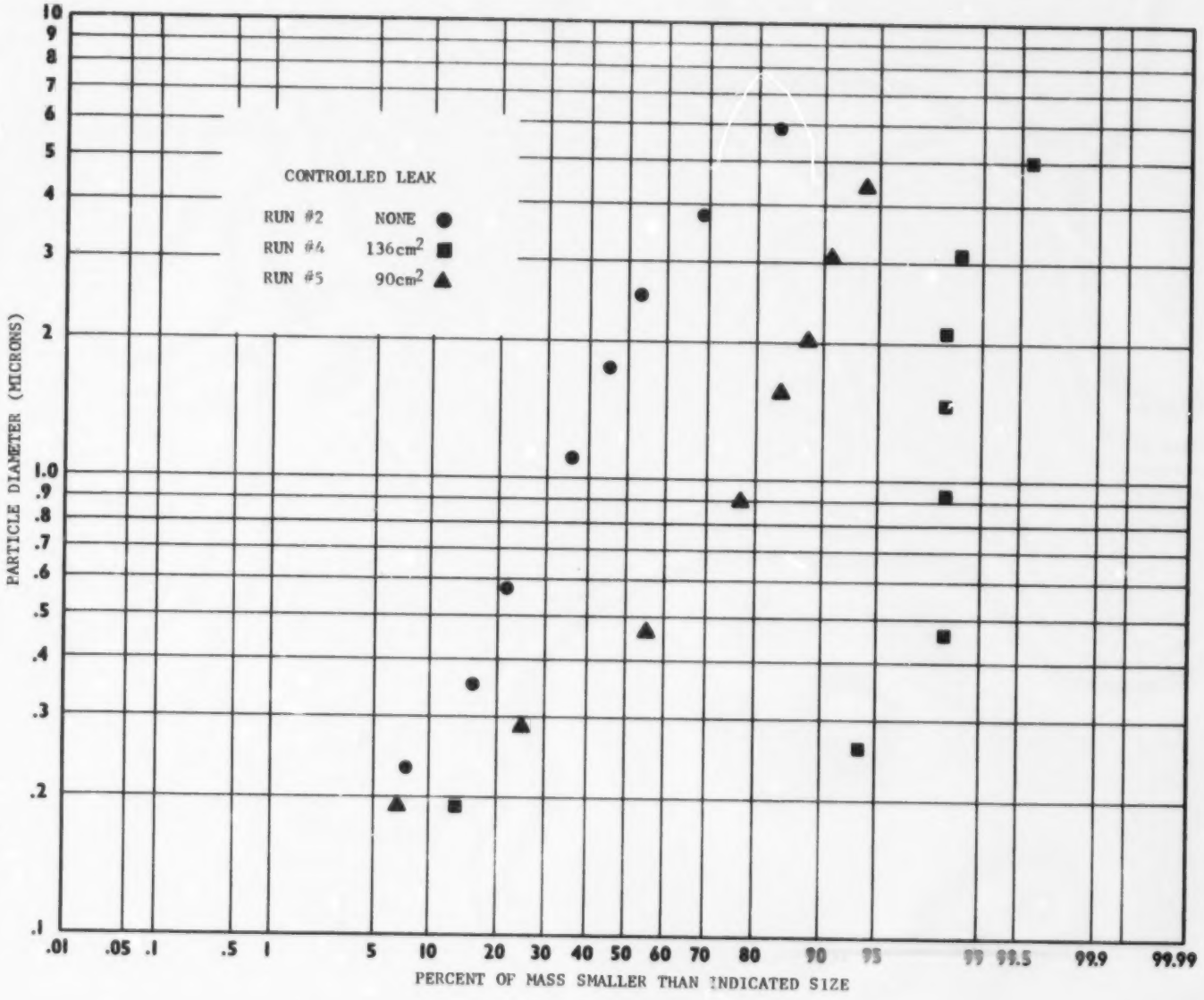

FIGURE 5-21
PARTICLE SIZE DISTRIBUTION OF THE BRASS SMELTER EMISSIONS

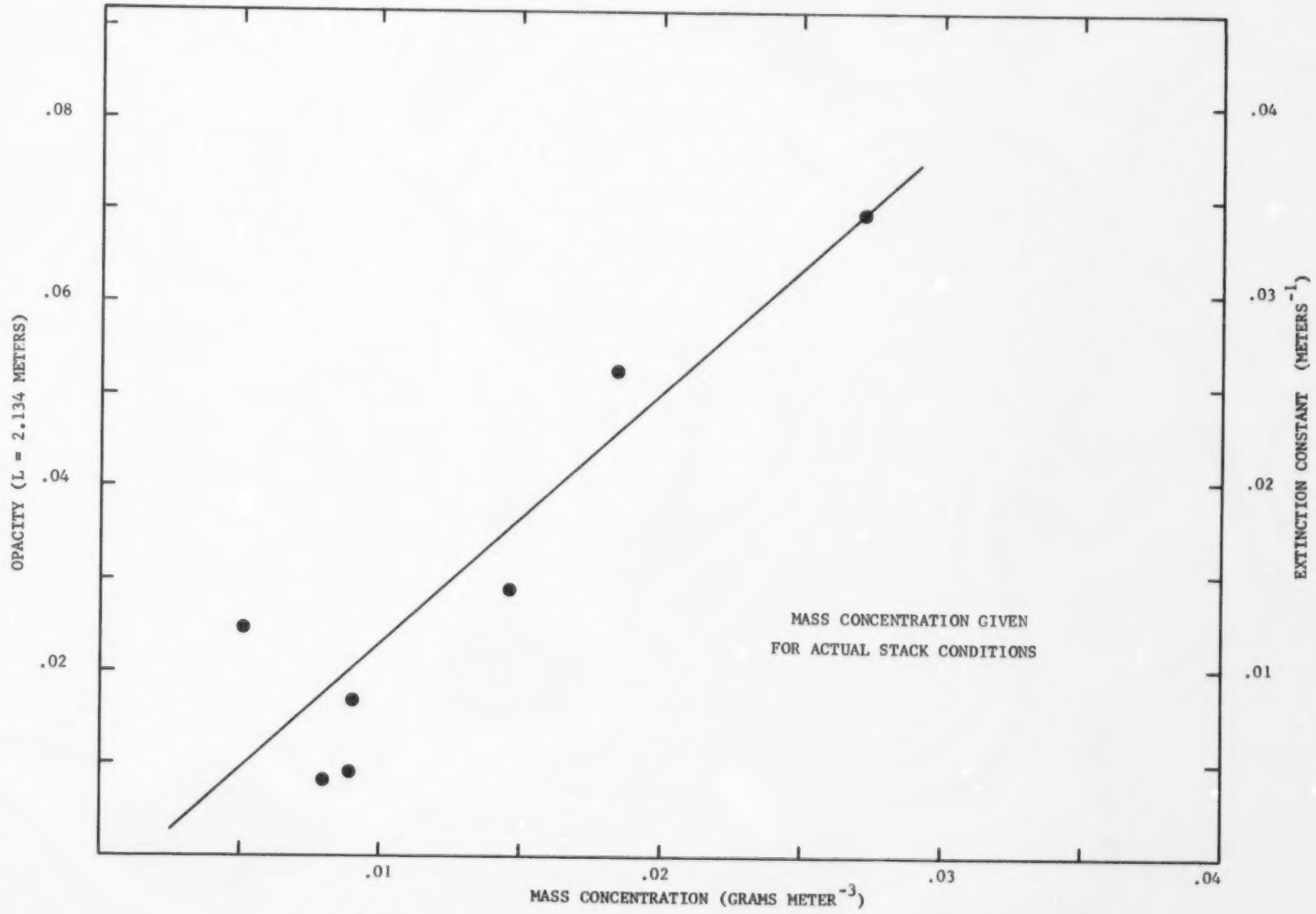

FIGURE 5-22
OPACITY - MASS CONCENTRATION RELATIONSHIP OF THE BRASS SMELTER EMISSIONS

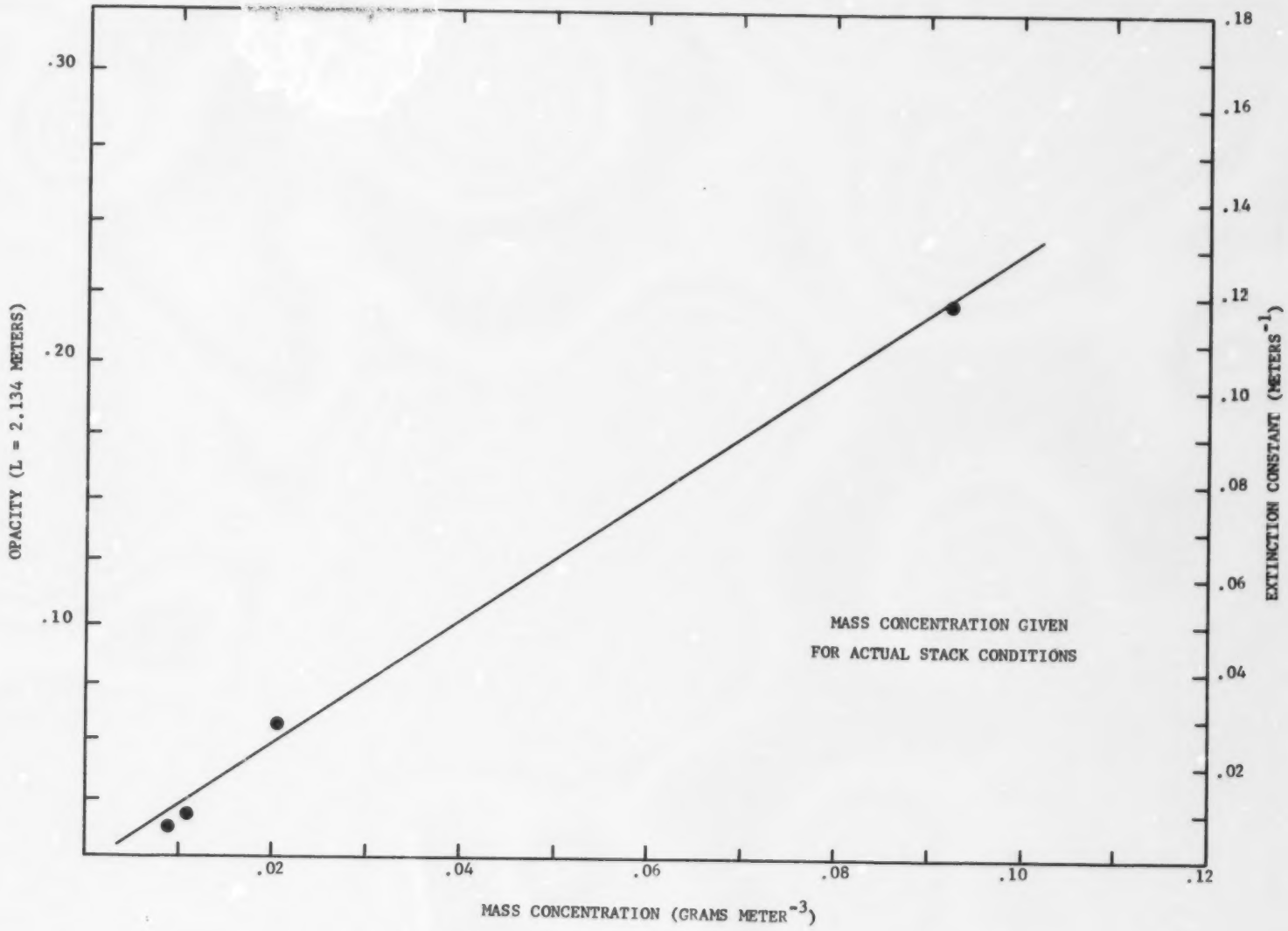

FIGURE 5-23

OPACITY - MASS CONCENTRATION RELATIONSHIP OF THE LEAD SMELTER EMISSIONS

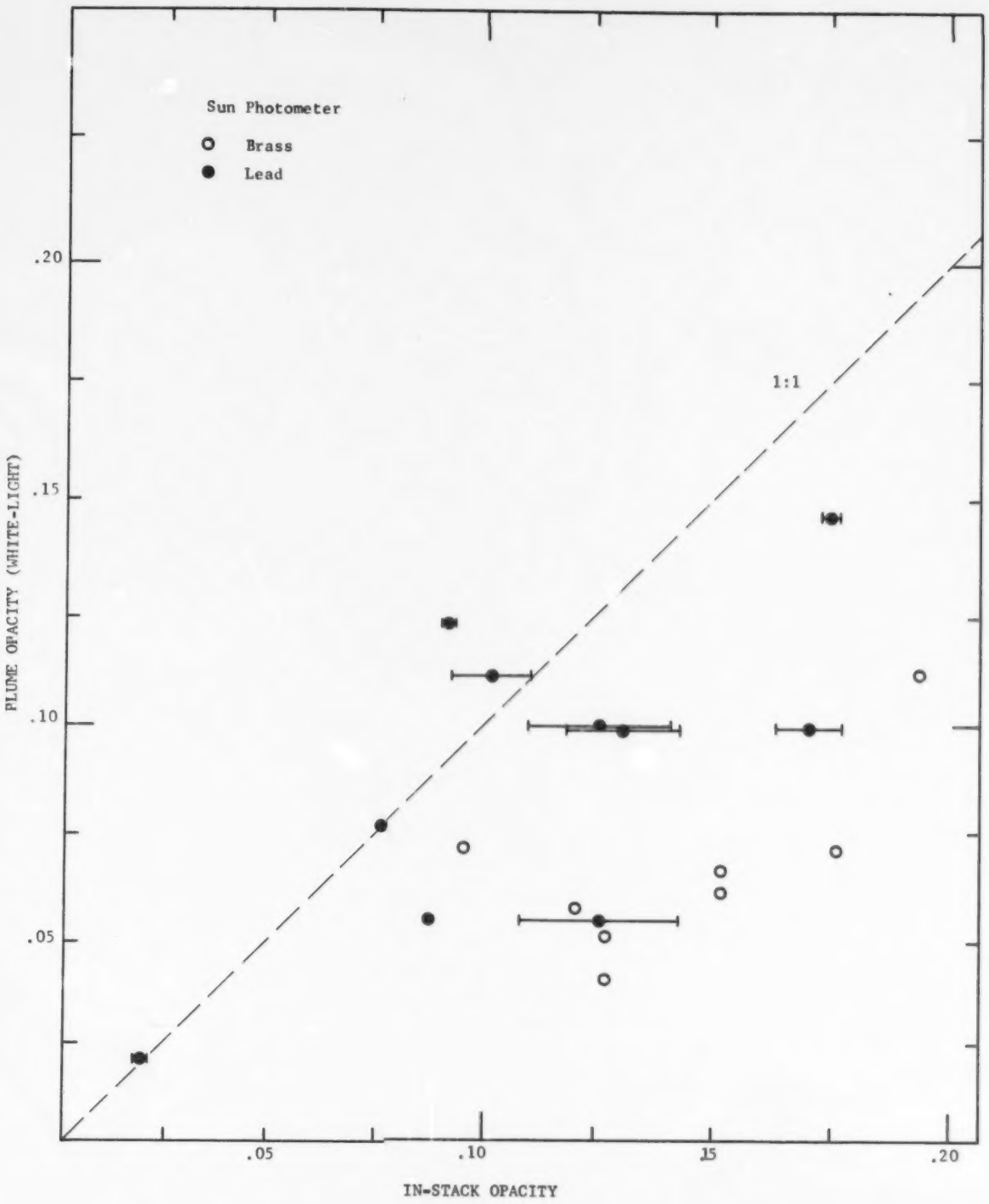

FIGURE 5-24

COMPARISON OF THE PLUME AND IN-STACK OPACITIES OF THE BRASS AND LEAD SMELTER EMISSIONS

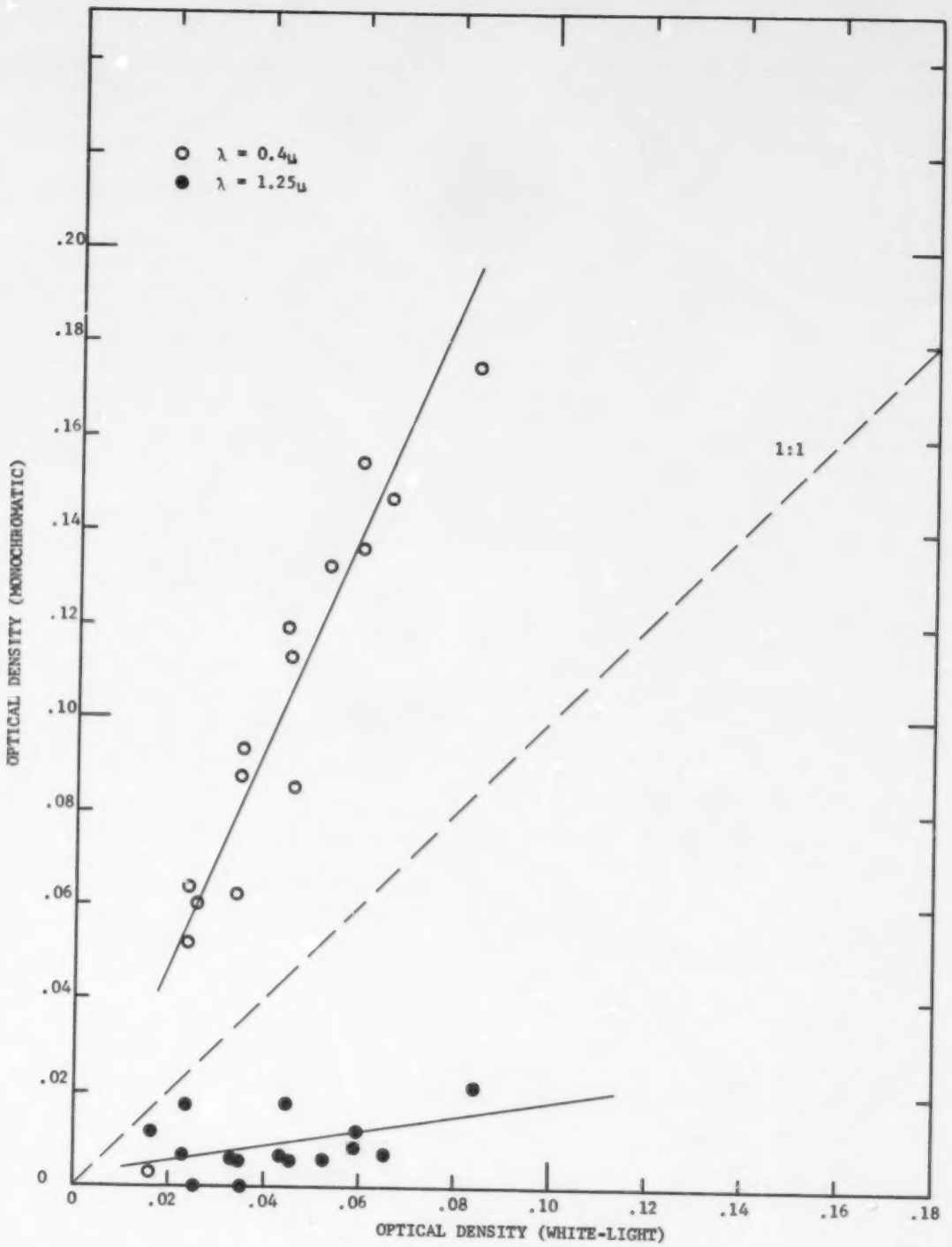

FIGURE 5-25

COMPARISON BETWEEN MONOCHROMATIC AND WHITE-LIGHT OPTICAL DENSITY MEASUREMENTS OF THE BRASS SMELTER EMISSIONS

The lead data is shown in Figure 5-26 where we have included some of the spiking data which is common at all the sites and very dominant at some. The average data represented by the unfilled symbol behaves in the following way. At .4μ, the scattering efficiency is similar to that recorded by the white light transmissometer. At 1.25μ, it has dropped to 25% of the .4μ value and at 2.2μ to 10% of the .4μ value. The data is not shown at 11.6μ as the scattering efficiency is too small to permit a reliable measurement. The data taken from the spikes behaves differently. At .4μ the scatter efficiency represented by the spikes is similar to that recorded by the white light transmissed. At 1.25μ it has dropped to about 40% of its .4μ value and at 2.2μ to about 25% of .4μ value. Thus, the scattering efficiency at 2.2μ of the particles causing the spiking data is about 2.5 times greater than those giving rise to the average data for comparable efficiencies in the visible range. Without detailed knowledge of the wavelength dependence of the optical index it is difficult to make accurate size determinations but a fair estimate would be that the particles giving rise to the spike are about twice the diameter of the others.

From the wavelength dependence, it can be inferred that both the lead and brass particulate distributions are dominated by very small particles, most of which are below .2μ in diameter. The scattering efficiency of the lead particles appears to fall off slower than that of the brass particles with increasing wavelength. This could be because the lead particles are more absorbing than those of the brass, or because the lead particle size distribution encompasses more large particles than the brass. In either case, if the wavelength dependence of the complex optical refractive index were known, a much more definitive statement of size would be possible.

E. Material Analysis

No material analysis was made at the site because it was felt that the nature of the particulates was the same as that collected at the baghouses. The powder from the lead side of the baghouse was predominantly lead oxide while that from the brass side was mostly zinc oxide. The material is usually bagged and shipped to the appropriate refinery for reprocessing.

F. In-stack Transmissometer Performance

This was a low vibration site as were the last two sites. The transmissometer operated perfectly with only the low drift previously noted.

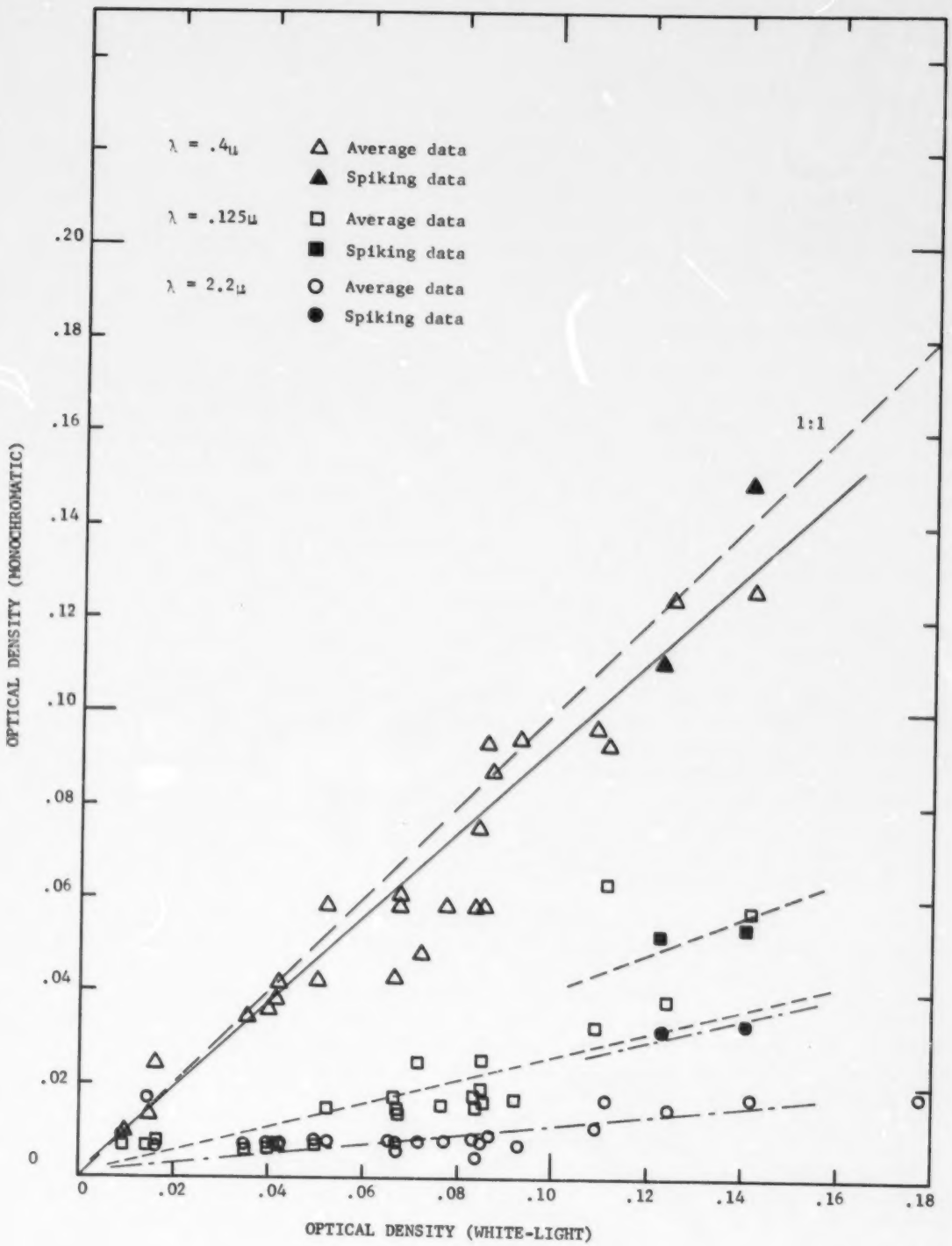

FIGURE 5-26

COMPARISON BETWEEN MONOCHROMATIC AND WHITE-LIGHT OPTICAL DENSITY MEASUREMENTS OF THE LEAD SMELTER EMISSIONS

5. OIL FIRED POWER PLANT

The sixth site was undoubtedly the most troublesome of all. The particulate level was consistantly low. The stack gas was hot and corrosive and frequently under positive pressure. The power output of the unit was almost always under the control of the central dispatcher and could not be varied significantly except during the transition from night load to day load.

A. Impactor Measurements

Four impactor measurements were made, the results of which are ambiguous. Upon checking aqueous extracts of the sample plus filter paper from the train measurements, significant amounts of both sulfate and sulfite were found to be present. The ratio of sulfate to sulfite was approximately nine to one. It was not immediately obvious whether the sulfate was a part of the particulate sample or whether it had been adsorbed on the filter paper and sample from the stack gas. Analysis of the water in the impingers, which are downstream from the filter, also showed the presence of sulfate and sulfite. This rules out metallic sulfates as the sole source of sulfate on the filters since no metallic sulfate is volatile at the temperature of the filter. From a titration of the acid in the impinger solution, it appeared that the sulfate in the impinger resulted from the adsorption of H_2SO_4 (plus SO_3). We have assumed that there is only one sulfate-bearing species present in the stack. The stack conditions - temperature range 300-335°F, water vapor 10-14% by volume, and SO_3 less than one ppm (0.2-0.5 ppm) - exceed the dew point of sulfuric acid so that the principal sulfate species is presumed to be gaseous sulfuric acid (and sulfur trioxide). Whether or not a fraction of sulfuric acid has reacted with the fly ash to form a soluble sulfate is unknown. We have treated it as a gaseous species which has adsorbed on the glass filter paper.

The sulfate content of the sample-filter paper extracts and the impinger solutions was estimated from a gravimetric determination as $BaSO_4$ and calculated as H_2SO_4. The sulfite was determined by reacting with excess iodine and back titrating with thiosulfate. For the train results, reasonable blank corrections could be made for the sulfate content of the paper. The blanks amounted to less than one ppm as H_2SO_4 per circle. This low blank may have been because this glass filter paper inherently has a low sulfate content or it may be that the sulfate was removed during the extensive washing with dilute HCl and deionized water. The filter papers used with the impinger were too fragile to wash extensively and these tended to have a relatively high sulfate content. Typically 5-10 mg of sample were collected per plate and the

blank correction turned out to be 5-10 mg per circle. Therefore, no attempt was made to correct the sample weights on the impactor papers for adsorbed sulfate, unlike the case with the train measurements. However, it was noted that the entire exposed surface of each impactor paper sustained a tan discoloration. The usual impactor plate hole pattern was superimposed on this tan background in black, as if it were carbon.

Instead of presenting the data in graphic form as was done for the other sites, it is probably more significant to tabulate the sample weights. This is down in Table 5-1. The final filter has an area about 5 times that of the impactor filters. Thus, a deposition by chemical reaction should leave five times the residue on the final filter as on the impactor filters.

Samples 1, 2 and 3 were taken with the facility operating normally (i.e., 1 to 2% opacity). Since the final filter appears to have collected about 5 times more mass than each impactor filter, the material collected on run numbers 1 and run number 3 could be predominantly sulfate. Run number 2 appears anomalous since each impactor filter shows a weight increase of twice that found in runs 1 and 3, but the weight increase of the final filter is essentially unchanged. To the eye, the black deposits in the impactor patterns are not grossly different from run to run.

The fourth impactor run was taken during a morning start-up after an extended period of complete shut-down. The opacity exceeded 10% during the early portion of the run. Many of the impactor plates (those collecting small particles) show very little change; however, those collecting large particles definitely shown increased sample weights which visually appear to be in the block of the impactor patterns. The final filter shows a weight increase about twice that of previous runs but does not appear any different in color from its predecessors. About all that can be said in summary is that the impactor always shows the presence of a black particulate in all stages. At start-up, the dominant particulate is greater than 4 microns in diameter and is probably a sooty fly ash. In order to calculate the diameter of the particles, a density value of 1.95 g/cm^3 was assumed. This corresponds to the assumption that the particulate matter was primarily amorphous carbon.

TABLE 5-1

WEIGHT GAIN PER IMPACTOR STAGE FROM OIL FIRED POWER PLANT EMISSIONS

Diameter Microns	.36	.36-.54	.54-.92	.92-1.75	1.75-2.9	2.9-4.2	4.2-6.2	6.2-9.8	9.8
1. Weight (mg)	22.6	3.8	5.0	4.5	5.2	4.8	3.5	5.0	5.8
2. Weight (mg)	23.7	9.0	9.6	8.4	9.2	9.2	10.1	9.2	10.1
3. Weight (mg)	23.0	5.2	5.7	5.5	5.3	5.6	5.0	5.0	6.3
4. Weight (mg)	43.5	5.4	5.4	5.4	6.4	7.2	8.6	12.4	19.7

B. EPA Train Measurements

The data from the train measurements suffers from problems similar to those of the impactor measurements. Fortunately, the sulfate content of the filters is low initially so that it is possible to perform a sulfate analysis and subtract the mass from the total collected. The reason this is done is that both SO_2 and SO_3 are gasses at the collection temperature, and are being collected via an adsorption process. They therefore should not be considered as particulates.

Of the total of 14 probe measurements made, 10 were train measurements, 9 of which resulted in usable data. The data is widely scattered and does not present a good correlation between opacity and mass concentration. This is due in part to the very low opacities and mass concentrations which were obtained at the source. It may also be due to the fact that the nature of the particulate varies from run to run. Instead of presenting the data as graph, we will follow the guide set for the impactor data and present the data in tabular form. The results are shown in Table 5-2.

C. Plume Opacity Measurements

Several attempts were made to measure the plume opacity using the sun photometer. This could only be done during the late afternoon when the shadow of the stack was accessible. Unfortunately, at that time of day the opacity rarely exceed 1%. Every time a measurement was made, there was excellent agreement. The photometer reading was always 1% or better. In order to obtain readings during the morning load increase when the opacity frequently became significant, it was necessary to use the telephotometer. The stack was one of the highest points in the area and the only place providing a view across it to a terrestrial target was from another stack. Access was essentially impossible. During our stay, the weather was such that no cloud or other target of opportunity drifted by our field of view. We were thus unable to make significiant plume opacity measurements at this site.

D. Multiwavelength Transmissometer

Originally, because of the consistently low stack opacities, we decided against installing the multiwavelength unit. However, when the furnace was shut down for repairs, it seemed like an excellent opportunity to have an additional instrument observing the start-up characteristics. We also felt that since the impactor measurements were all suspect, an optical sizing technique might provide useful information. Accordingly, we abandoned the long wavelength capability to make use of some

TABLE 5-2

OPACTIY-MASS CONCENTRATION MEASUREMENTS OF THE OIL FIRED POWER PLANT EMISSIONS

Run	Mass Concentration (Grams Meter^3)	Opacity (L=3,86 Meters)	Extinction Constant (Meters^{-1})
2	.0103	005	.00113
3	.0085	010	.00263
4	.0227	0114	.00295
5	.0151	0083	.06214
6	.0069	0113	.00294
7	.0103	0187	.00485
8	.0050	0102	.00264
9	.0165	0172	.00445
10	.0179	0101	.00261

inexpensive plate glass windows to isolate the instrument from the stack. We were not able to equip the system with blowers on this short notice but had to protect the equipment from the stack gases. The erratic blasts of hot gases coming from the stack brought moisture and oil vapor to the windows and tended to mask any valid data.

E. The Second Transmissometer

During the period of extended shutdown, we were able to install a second white light transmissometer identical to the first, in the breaching below the stack. When the furnace started up again, both transmissometers were operational. They produced almost identical records implying that at least for this facility a duct mounted unit would be satisfactory. Their high degree of correlation is shown in Figure 5-27.

F. In-Stack Transmissometer Performance

Both transmissometers behaved exceptionly well. The old transmissometer showed only the minor drifts mentioned previously. The new unit showed drifts of comparable magnitude.

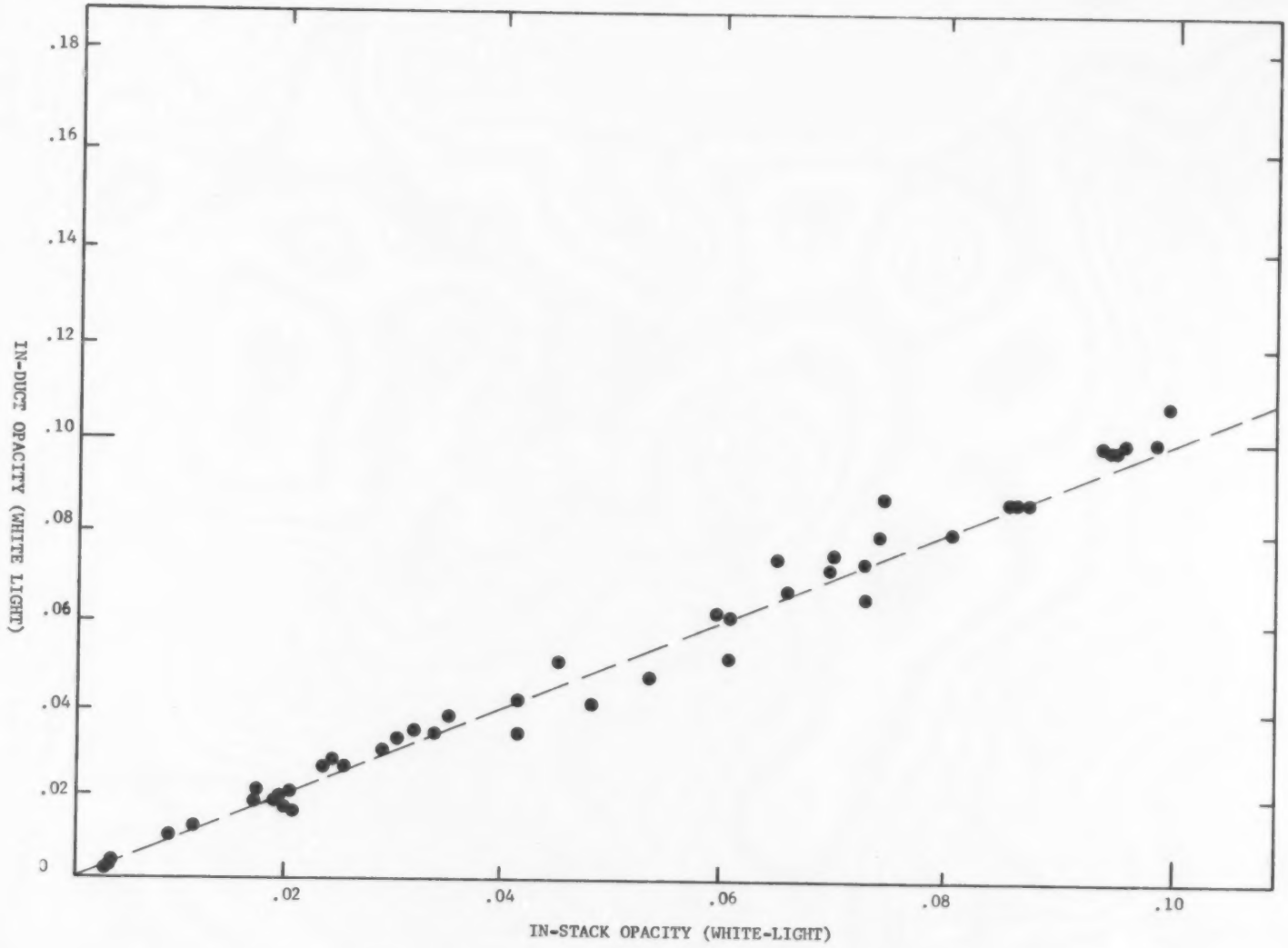

FIGURE 5-27

COMPARISON OF IN-DUCT AND IN-STACK OPACITY MEASUREMENTS OF THE OIL-FIRED POWER PLANT EMISSIONS

SECTION VI

SUMMARY AND CONCLUSIONS

In the course of conducting this program, we have had an opportunity to observe a number of different approaches to stack monitoring. The instruments and techniques have been utilized at six different industrial sites over the past year. Every approach has both good and bad features and those which dominate may depend strongly on the characteristics of the site.

The easiest site to monitor is one which produces a specific size, or size distribution, of particles that are uniformly distributed throughout the cross-section of the duct and stack. If the changes that take place are slow and involve only the number of particles, almost any approach will work, and sampling or monitoring can be done almost anywhere in the duct or stack. However, when the changes are rapid and involve varying size and spacial distributions, almost any approach runs into problems.

Consider, for example, the EPA train and the standard sampling procedure. It does nc. require that there be a uniform spacial distribution since many points in space are sampled, but it does require that very little change take place during the full sample run. This can be accomplished by having changes which are very slow compared to a full run, or very fast compared to the time required to sample a point. In the latter case, only the average must be constant over the full run. Alternatively, if the spacial distribution is uniform, then any reasonable temporal fluctuation is allowable.

A similar set of constraints can be placed on the impactor; however, the fact that the impactor is measuring aerodynamic size and not just mass concentration creates additional complications. The particle specie or size may change with time without altering the mass concentration. A duct with a uniform mass concentration might have a size or specie gradient across it. Unless the nature and state of the sample are very simple, interpretation of the impactor data can be very complicated.

The most obvious criticism of both the EPA train and the impactor (even if their results were 100% perfect) is their inability to make real time measurements. Often (particularly in smelting) a very dirty phase of the operation may start and stop during the time the probe is being moved

from one port to another, and thus go completely unrecorded. If monitoring systems are to reach their full potential as safety systems or as operation controllers, they need a response time that is much closer to real time.

Before passing on to optical systems, it is perhaps worth mentioning that several of the west coast pollution control agencies have adopted a sampling procedure where they sample at one fixed point in the stack. Although the project required that full sampling be the standard procedure, we were asked to examine the possibility of using a reduced procedure to see if there were sites and conditions that would give the same results for full and partial sampling. Our general conclusion was that there was too much variation from point to point. Although reduced sampling greatly simplifies the taking of data, we concluded that the convenience was not worth the risk. We therefore continued to sample over the full stack cross-section.

The in-stack optical techniques are superior to a single point sampling technique in that they integrate the effects over the full optical path. They obviously cannot detect a right-left asymmetry and, hence, must be rather carefully located where there is no asymmetry or where they are monitoring the mean value of the asymmetry. If the location selected, either by change or circumstance, is less than ideal, it may still be possible to determine the proper factor to relate their reading at the site selected to that which would have been obtained at an ideal location. This could be done by comparing the results of a full sampling measurement with sample measurements made by traversing along the selected line of sight.

The Lear-Seigler transmissometer was in operation at every site for at least 30 days and was considered the primary optical monitoring system. In the course of a year we have become very familiar with the instrument and have formed some definite opinions. The instrument is well designed and well engineered. It performed reliably and accurately, requiring only a minimum of attention. It appears to have good long-time stability and does not exhibit serious temperature drifts, etc. During the entire year of operation, we encountered only three problems that required service. The first occurred immediately after installation at Site #1. The high vibrational levels caused the alignment screws to move, continually misaligning the instrument and causing it to become inoperative. We solved that problem by putting "lock-tite" on the threads. A positive locking mechanism would be very helpful. The second and third problems involved electrical component failures that were serviced in the field and probably were not due to vibration.

The floating, non-groundable output tends to restrict the readout systems which can be employed and, at some locations, appeared to be vulnerable to noise. In areas where there was a high noise level carried on the power lines, we found noise in the chart recordings and a zero level which was noise dependent. The range switch that is now available greatly enhanced the versatility of the instrument. Unfortunately, the instrument must be opened and deactivated to change ranges. A way of changing the range remotely would be very beneficial. The periodic zero and calibration check system works very well. For all sites but the first, the zero drifts were very small and generally cycles in form. Typically, the true zero was stable to an equivalent density of .004 and the calibration zero was stable to about .002, although both might occasionally vary beyond these bounds by 50 to 100%. The drift appeared to follow a day-night pattern. It was never determined whether this was due to thermal or line voltage differences. It was obviously not due to dust. There were also very small negative drifts in both true and calibration zeros over the 30 day period. It is hard to estimate their magnitude because we would correct about once a week. The drop probably was about the same magnitude (over a month) as the daily variation. The span calibration was always perfect. At the first site the high vibration level created a need for continual check of the alignment. The drifts were 2 to 3 times greater than at any other site.

The instrument, in its present form, is an excellent device which very accurately measures in-stack opacity in the visual range. It can readily detect density changes of 001. Like all optical devices, it only measures the characteristics of the particulates it encounters. If water droplets are present because the temperature of the stack is below the dew point, the instrument records their presence as a particulate. If SO_3 is present in vapor form because the stack temperature is high, the instrument will be unaffected and indicate that there is no particulate matter. Problems of this nature require special consideration and may need additional instrumentation.

One of the main conclusions we reached after watching hundreds of hours of data being recorded is that the size of the particles can be constantly changing depending on the type of operation and the process in effect. Most of this information was obtained using the multiwavelength transmissometer which was designed to monitor this type of occurance. If changes in particle size are not properly taken into account, significant errors can be introduced when optical techniques are used to monitor mass concentration. To examine this more completely, it is necessary to introduce two simple equations which define the mass concentration and extinction coefficient for a simple monodisperse system of particles,

$$M_c = No\ \rho\ 4/3\ \pi\ r^2 \qquad 6.1$$

$$K(\lambda) = No\ Q\ (\lambda/r)\ \pi\ r^2 \qquad 6.2$$

where M_c is the mass concentration (gm/cm^3), N_o is the number of particles (cm^{-3}), ρ is the density of the material (gm/cm^3) and r is the radius of the particles. K is the extinction coefficient (cm^{-1}) and Q is the extinction efficiency, a dimensionless number relating observed cross-section with geometric cross-section. If the particles are always of one type and are constant in size, both M_c and K are proportional to N_o. If one is plotted as a function of the other, a straight line results, the equation for which is,

$$M_c = \frac{4/3\ \rho\ r\ K}{Q} \qquad 6.3$$

If r is constant then the slope which is dependent on size through r and Q is constant and hence a measurement of K gives M_c.

If we now consider the plots of opacity vs. mass concentration made for every site, we see that, in general, there was a good functional relationship between the two. In some cases, the relationship was almost definable by a straight line. The behavior is compatible with fluctuations in particle size because both the opacity and mass concentrations are obtained by averaging data over the sampling period. If the period is long enough so that the distribution of the particles does not change during the interval, K and M_c will still be linearly related. The departures of the data from a straight line is a measure of the degree to which the averaging is fulfilled.

When the mass concentration is plotted against the extinction coefficient (or the opacity) the strong dependence of both on N_o sometimes disguises the fact size changes may also be involved. If N_o is changing by orders of magnitude, then both M_c and K change by orders of magnitude. A factor of two due to a size change may pass unnoticed, however, values of M_c deduced from K will still be off by a factor of two.

At site #1, the instantaneous optical data fluctuated widely. This could be due to fluctuation in N_o or in r. The N_o dependence, however, can be eliminated from the multiwavelength data by taking ratios [i.e., $K(\lambda_2)/K(\lambda_1)$, $K(\lambda_3)/K(\lambda_1)$ etc]. If the ratios are fluctuating, it means that the sizes are fluctuations. This was the case at site #1. The integrated data, however, appears to be very stable. The five impactor runs have very similar size distributions indicating that over a period of 2 to 4 hours the average distribution is almost constant. This also means the train sample data should correlate well with the transmitter data if the latter is averaged over the sample period. It does.

One question that has been raised is why the impactor run without a bag leak, is not significantly different than those runs made with simulated holes. Since the bags preferentially remove the large particles, the run made with its bags intact should exhibit a distribution shifted on toward the small particles. The reason is that there are always many small leaks in the total bag area and these mask the performance of the perfect bag which probably would pass the small particles preferentially.

The particle size fluctuations were very evident at all sites except #2 where the size ranged between 0.10 and 0.15μ for the dominant particles (carbon). In selecting multiwavelength data at most sites, we attempted to find data which most closely resembled the average when the facility was running smoothly. Had we wanted to demonstrate size fluctuation we would have studied the ratio of the site and was the subject of comment in Section 5.

In general, a real time optical monitor of mass concentration must be able to identify change in particle size even when accompanied by changes in number density.

The multiwavelength transmissometer is a device which attempts to monitor the instantaneous particle size by continuously monitoring the wavelength dependence of the extinction. It then uses the size information, coupled with the opacity information, to determine the mass concentration. This added feature of real-time size determination makes the device a potentially more effective real time monitor of mass concentration.

Plume opacity measurements suffer from a variety of complications. Irrespective of the type of instrument used, the following problems occurred repeatedly:

(1) Steam, either from the stack under investigation or from a nearby vent, constantly obscured the optical path, making meaningful determination impossible.

(2) The wind either blew the plume into tatters, or whipped it back and forth so that it was impossible to determine the length of path through the plume.

(3) With the sun photometer, the wind direction was generally such that the plume was bent toward the sun.

(4) Continuously varying conditions of brightness and cloud cover caused gross fluctuations in readings.

In general, the atmospheric complications, coupled with the random, nonhomogeneous inconsistent nature of the plume, acted to limit the viability of any measurements. The hand-held sun photometer was found to be awkward and usually required two men to obtain moderately accurate data; one aligning the instrument, and one reading the meter. The possibility of a steam plume made it desirable to work close to the top of the stack where it was impossible to judge if the instrument was clear of the penumbra portion of the shadow of the stack. A sun photometer built by Shell Research, and used only briefly during the program, was considered a vast improvement in all of these respects because of its see-through design. In both cases, however, plant layouts usually precluded usage except during very short specific times of the day when the stack shadow was accessible. Unfortunately, this often coincided with periods of cloud cover or lack of plume.

The telephotometer permits viewing directions not available to the sun photometer, but it places stringent conditions on the targets which may be used. It requires that four measurements be made in quick succession so that two contrasts are determined; one of a target pair alongside the plume, and one of a target pair through the plume. The implication is that if the plume were absent, the contrast would be identical, that is,

$$\frac{I_{WP} - I_{BP}}{I_{WR} - I_{BR}} = 1. \qquad 6\text{-}4$$

Where the subscripts W, B, P and R stand for white, black, plume and reference, respectively.

This implies that the lighting conditions are the same in the four areas and remain constant during the measurement. It further implies that the illumination angles and viewing angles are such as to make $I_{WP} = I_{WR}$ and $I_{BP} = I_{BR}$ in the absence of a plume. Measurements made at Site #2 on identical targets indicated that the latter condition could not be met, except under very special geometries.

The unit requires two men to operate it properly. Its weight and optical magnification make the use of a tripod mandatory. The simplest targeting occurred when the instrument was used at night with a dominant light source far enough behind the stack so as to be accessible for both through-plume and reference measurements. The general feeling was that the instrumental plume opacity

measurements were imprecise and at best can give only a general level of opacity. Even so were able to obtain some degree of correlation between in stack opacity and plume opacity at every site.

REFERENCES

1. Nader, J. S., Conner, W., and Jaye, F., "Performance Specifications for Stationary-Source Monitoring Systems for Gases and Visible Emissions," NO. EPA-650/2-74-013, National Environmental Research Center.

2. Crim, J. A., and Snowden, W. D., "Atmospheric Emissions Study," No. APTD-0936, Valentine, Fisher and Tomlinson Asphaltic Concrete Plants (1 November 1971).

3. "Sewage Sludge Incinuation," No. EPA-R2-72-040W72-12631, Environmental Protection Agency (August 1972).

4. Kalen, B., and Zenz, F. A., "Pollution Control Operations: Filtering Effluent from a Cat Cracker," The Duson Co., Inc., Chemical Engineering Progress (Vol. 69, No. 5) (June 1973).

5. Rozovsky, H., Lead and the Environment at the Smelting Division of Brunswick Mining and Smelting Corp., Can Min & Met Bull 61.50-60 (April 1974).

6. Ehrenfeld, J. R., Bernstein, R. H., Carr, K., Goldish, J. C., and Orner, R. G., "Systematic Study of Air Pollution from Intermediate-Size Fossil-Fuel Combustion Equipment," No. APTD-0924, Walden Research Corporation (July 1971).

7. Federal Register 36, No. 247, pp 24088-9, Thursday, December 23, 1971 (Method 5).

8. Bird, A. N., Jr., and McCain, J. D., "Particle Sizing Techniques for Controlled Device Evaluation," Southern Research Institute, Birmingham, Alabama; Also D. Bruce Harris, E.P.A. Research Triangle Park.

9. Beutner, H. P., "Measurement of Opacity and Particulate Emission with an on-Stock Transmissometer," Air Pollution Control Association Journal, Vol. 27, #9, P 865 (September 1974).

10. Conner, W. D., and Hodkinson, J. R., "Optical Properties and Visual Effects of Smoke-Stack Plumes," PUB-999-AP-30, Public Health Service, National Center for Air Pollution Control (1967).

11. Walker, R. A., "Optical Systems for Defining the Viewing and Measuring Fields in Liminance/Radiance Meters," Applied Optics, Vol. 11 #9 (September 1972).

12. Twitty, J. T., and Weinman, J. A., "Radiative Properties of Carbonaceous Aerosols," Journal of Applied Meteorology, P 725 (August 1971).

APPENDIX A

RAW DATA AND NOMOGRAPHS

The figures which follow are examples of transmissometer data as it records on the circular and strip chart. Also shown are the nomographs used to process the impactor data.

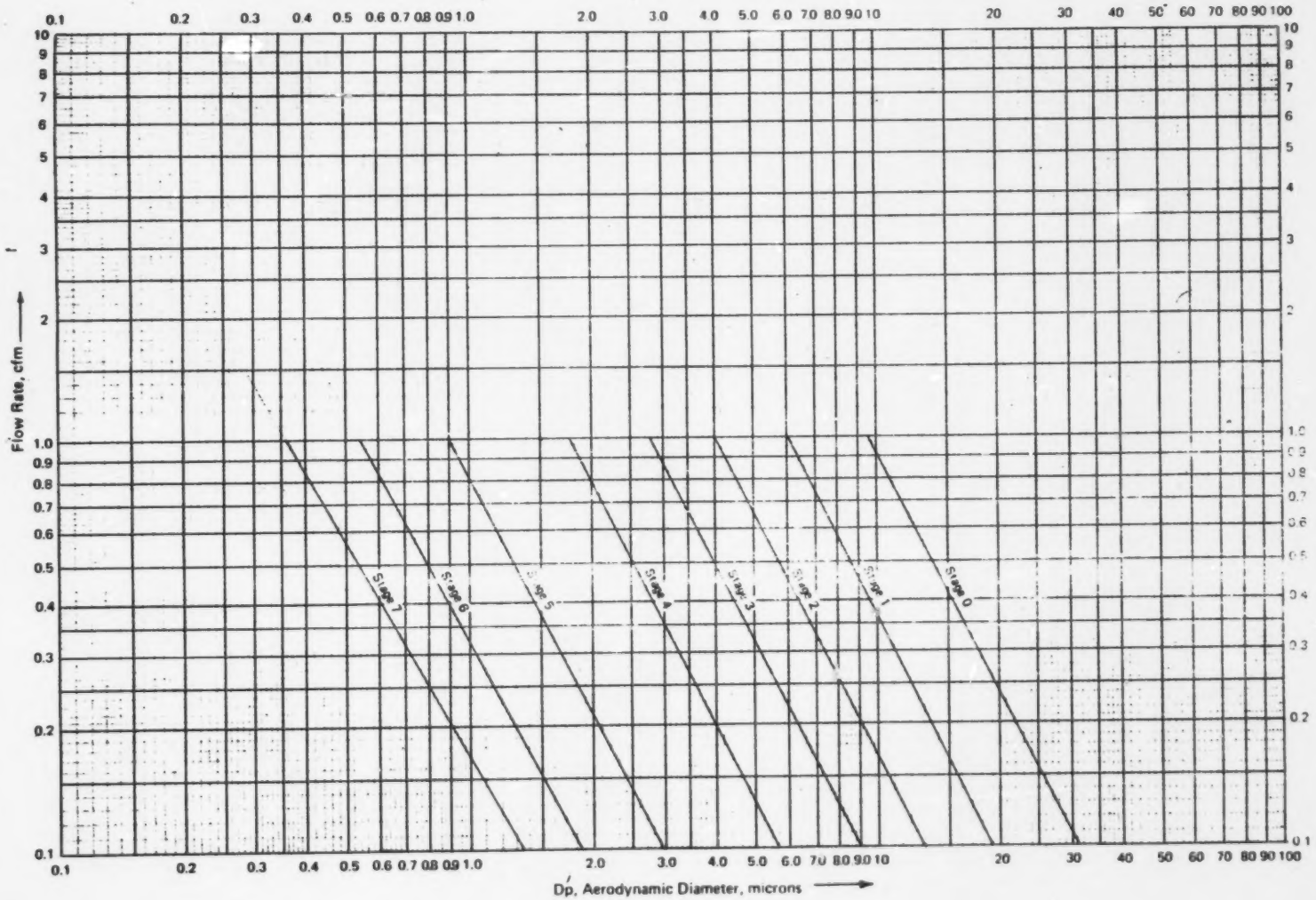

FIGURE A-1

AERODYNAMIC DIAMETER NOMOGRAPH OF ANDERSON IMPACTOR

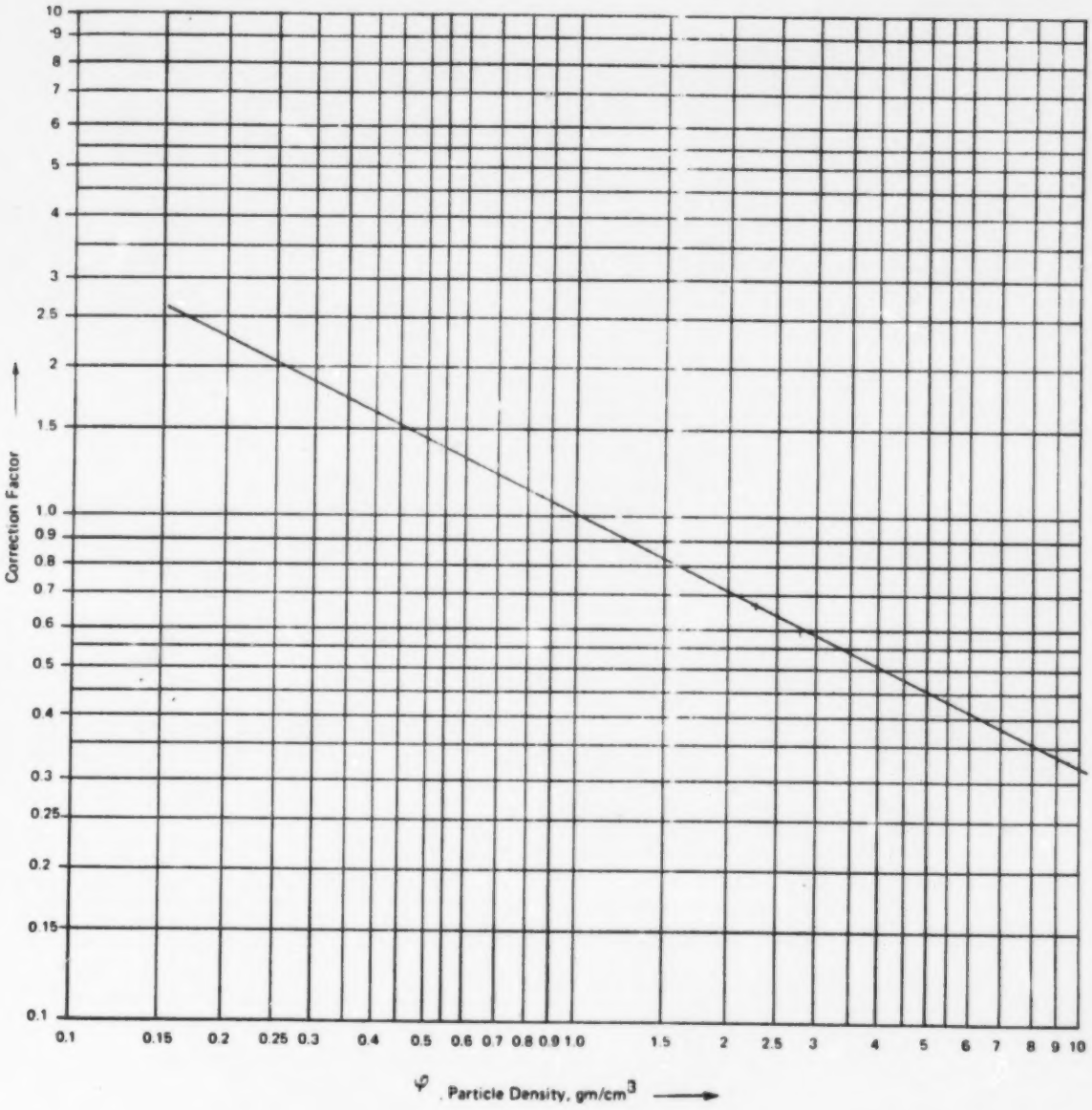

FIGURE A-2

IMPACTOR DENSITY CORRECTION NOMOGRAPH

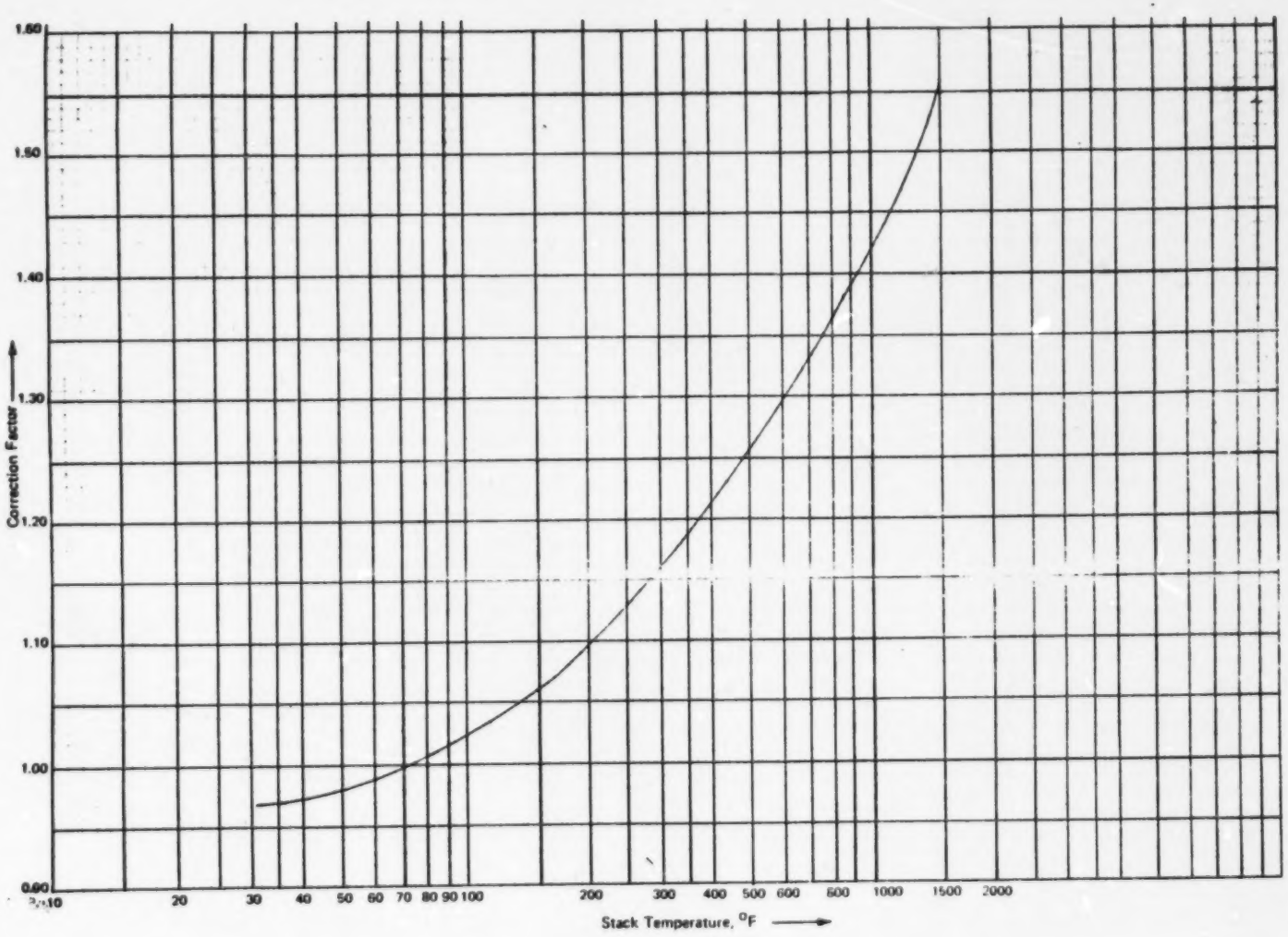

FIGURE A-3

TEMPERATURE CORRECTION NOMOGRAPH OF ANDERSON IMPACTOR

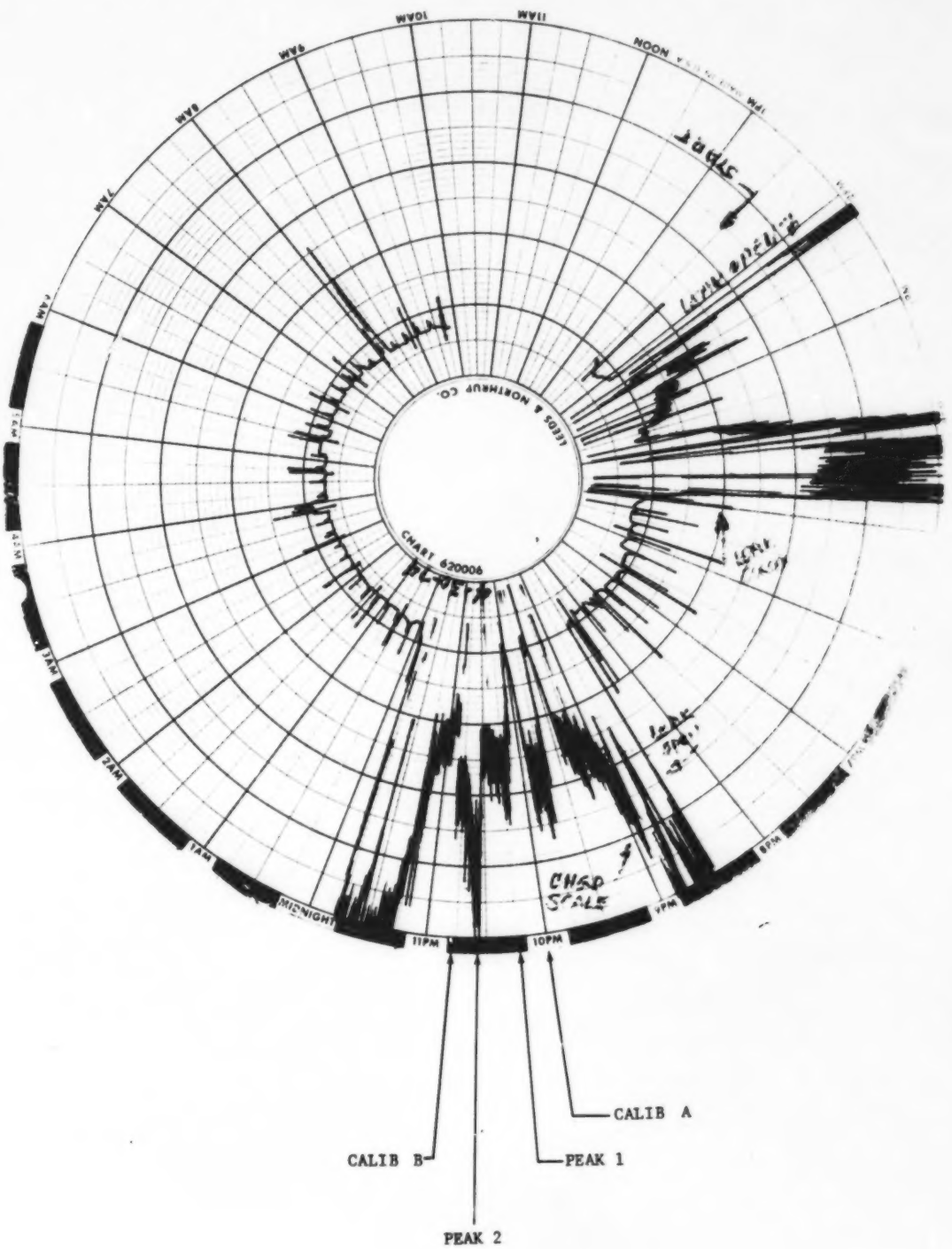

FIGURE A-4

TYPICAL TRANSMISSOMETER RECORDING FROM CIRCULAR CHART

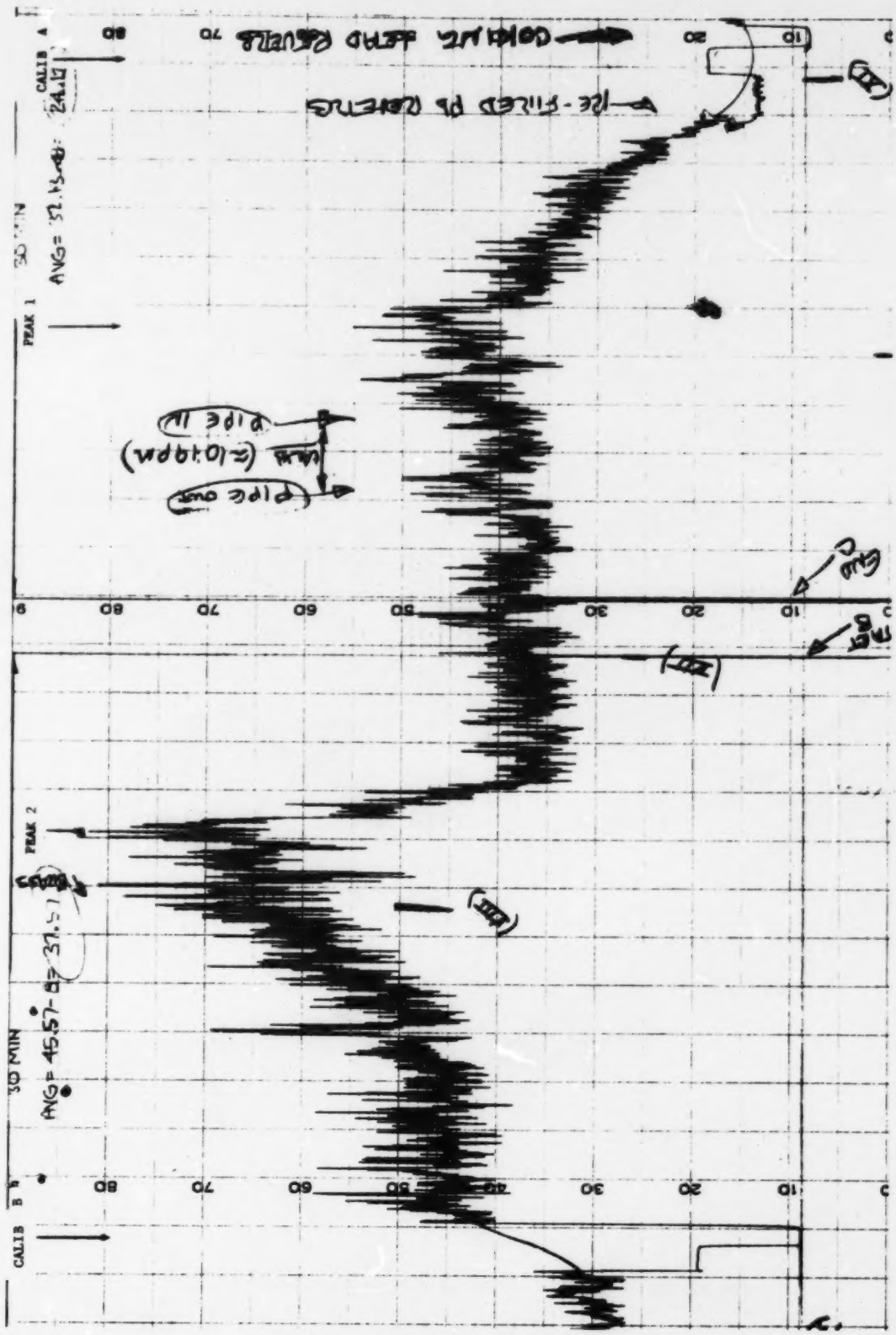

TYPICAL TRANSMISSOMETER RECORDING FROM LINEAR CHART

APPENDIX B

TABULATION FORMS

The tabulation forms which follow are the ones used to record and reduce data. They are also used to record the key parameters

TABLE B-1

EXAMPLE TABULATION OF PROBE DATA

PROBE DATA

(1 of 2)

PLANT Brass & Lead Smelter — BAROMETRIC PRESSURE 30.17 IN. Hg

TEST NO. & DATE SF-12-PM 4/30/74 — STACK PRESSURE -0.25 IN. H_2O

INITIAL VOLUME 4943.77 CU. FT. — Nozzle size 3/8 IN. — Start time 8:35 PM

MTL: LEAD (ALL LEAKS OPEN)

POINT No.	ELAPSED TIME	Sample Volume	VELOCITY HEAD $\sqrt{P_s}$	ORIFICE ΔP	TEMPERATURES: STACK	PROBE	OVEN	IMPING. IN	IMPING. OUT	METER
E-1	0	4943.77	.33	.86	100	270	210	120	55	60
3	5	—	.83	.76	160	280	265	190	55	62
5	10	4951.31	.30	.66	155	273	273	190	53	62
7	15	4954.58	.30	.64	140	248	252	200	52	65
9	20	4957.88	.23	.91	130	255	212	173	49	69
11	25	4960.57	.20	.42	120	258	209	170	49	70
	30	4963.18								
D 2	0	4963.18	.35	.95	150	253	205	149	49	75
4	5	4966.[illegible]	.38	1.00	160	245	210	170	49	75
6	10	4970.32	.38	1.00	155	260	230	178	49	78
8	15	4974.76	.32	.74	160	263	225	185	49	82
10	20	4978.29	.26	.50	155	255	233	189	50	85
12	25	4981.16	.26	.58	150	255	230	170	99	88
	30	4984.10								
C-1	0	4984.00	.35	.91	130	245	225	155	49	85
3	5	4987.50	.40	1.14	140	243	220	175	48	85
5	10	4991.70	.32	.72	155	260	222	175	48	83
7	15	4995.—	.32	.72	100	260	225	178	ok	85
9	20	4998.52	.23	.40	155	270	230	188	ok	88
11	25	5001.43	.26	.50						
	30	5003.88								
B-2	0	5003.05	.32	.72	140	255	228	155	49	89
4	5	5007.05	.30	.64	150	250	223	172	48	90
6	10	5011.23	.33	.76	155	← ok →				
8	15	5013.58	.28	.56	160	← ok →				
10	20	5016.49	.26	.50	155	← ok →				
12	25	5019.22	.26	.50	155	← ok →				
	30	5022.—								
A-1	0	5022.—	.26	.50	100	250	228	135	50	91
3	5	5024.67	.28	.64	120	← ok →		170	← ok →	
5	10	5027.56	.28	.60	160	245	223	170	49	93
7	15	5030.60	.22	.38	160	253	228	173	50	93
9	20	5033.02	.22	.38	160	265	230	167	49	95
11	25	5035.40	.25	.74	160	← ok →				
		5037.95								
	WATER: 15ml			WASH: 0.0[illegible]435		grams				
				FILTER: 0.1928		grams				

FINAL VOLUME 5037.95 Cu. FT.

(2 of 2)

EXP. NO. SF-12-P6 DATE 9-30-74

A. Baro. Press, _____ 30.17

B. ΔP, Orifice _____ .651

C. Gas Press. @ Meter, A + B/13.6 _____ 30.22

D. Vol. Water Collected 15 + (17) _____ 32 ml.

E. ~~D~~ * 1/15 _____ 1.5 Cu Ft.

F. Volume Gas Metered _____ 94.18 Cu. Ft.

G. E + F _____ 95.68 Cu. Ft.

H. % water in gas, (E/G) * 100 _____ 1.57 (.9843)

I. Ave. Mol. Wt. /28.95 _____ 1

J. Static Stack Pressure _____ .25 In H_2O

K. Abs. Stack Pressure, A + J/13.6 _____ 30.15 In Hg

M. Flue Gas Temp 147 °F _____ 607 °R

N. Sq. Rt. Velocity Head _____ .297 $\sqrt{In H_2O}$

O. Flue Gas Velocity, $2.9 * 0.87 * N * \sqrt{\frac{29.92 * M(°R)}{K * I}}$ (:562.8°) _____ 16.31 Ft/sec

P. Flue Area _____ Ft^2

Q. Actual Gas Flowrate, O * P * 60 54,800 CFM R. *STD $Q * \frac{530}{M} * \frac{K}{29.92}$ 48200 SC

S. II (DRY, STD) R * (100 - H) 47500 DSCM

T. Vol. Sampled @ Stack Conditions (WET) G * C/K * M/530 109.47 CF

U. " " " Stand. Cond. (DRY) F * C/2992 94.81 DCF

V. Wt. Particulates .2866 grams

W. Particulate conc. - Stack (WET) 15.43 * V/T = 0.0404 GRAINS/FT³

Z. Sampling Time 150 min. a. Probe tip diameter .375 in.

b. % isokinetic Sampling, $\frac{305.6 * T}{O * Z * a^2}$ 97.26 %

Y. Emission Rate = $Q * \frac{V}{T} * 0.1323$ = 18.99 lbs/HR.

TABLE B-3

EXAMPLE TABULATION OF IMPACTOR PARTICLE DATA

EXPERIMENT NO. SF-4-(i)-B DATE 4-23-74

IMPACTOR

PLATE NO.	PROBE TIP	0	1	2	3	4	5	6	7	FILTER	Σ
WEIGHTS											
GROSS (g)	.0013	.1831	.1746	.1822	.1663	.1842	.1786	.1821	.1799	.0038	
TARE (g)	—	.1805	.1732	.1812	.1644	.1813	.1687	.1690	.1712	—	
SAMPLE (mg)	—	.0026	.0014	.0010	.0019	.0029	.0099	.0123	.0087	.0030	43.7mg
D_p' (μ)	—	10.2	7.0	4.65	3.55	2.08	1.05	0.65	0.43	<0.4	
d (μ)	—	4.07	2.82	1.87	1.43	.837	.423	.260	.173	—	
%	—	5.95	3.2	2.3	4.4	6.6	22.65	28.1	19.9	6.8	
CUM. %	—	99.9	93.95	90.75	88.45	84.05	77.45	54.8	26.7	—	

FLOW-RATE = "VOL. SAMPLED @ STACK CONDITIONS" / "SAMPLING TIME" - 55.87CF / 75MIN =

= 0.745 CFM

DENSITY = 5.6 g/cm³

TEMPERATURE (AVE.) = 112 °F

TABLE B-4

EXAMPLE TABULATION OF TRANSMISSOMETER DATA

LSI
DATA REDUCTION

SITE: BRASS/LEAD SMELTER
DATE: 9-20-74
RUN: 12-SF-Pb
SCALE: 2 & 3

D_{LSI}

$k = \frac{(SCALE)}{(2)(ZL)} = \frac{(.00150)}{(2)(150)} = [0.0000083]$ SCALE 2

$= \frac{(.00625)}{(2)(150)} = [0.0000208]$ SCALE 3

RUN SEG	SCALE	TIME	AVG LASE	k	BxLxk
PORT A	3	30 MIN	50.63	.0000208	0.03153
" B	3	30 "	37.57	.0000208	0.02344
" C	3	30 "	24.13	.0000208	0.01506
" D	3	30 "	29.36	.0000208	0.01832
" E	2	16.2 "	64.32	.0000083	0.00811
" E	3	14.8 "	41.70	.0000208	0.01284
			$(D_{AVG}) = \Sigma =$		0.10930

$(M_c = 0.0404$ GRAIN/FT^3 PROBE (12-SF-Pb) $= .092516$ gm/m^3)

$\Sigma(t) =$ 150 MIN.

DENSITY AVG TOTAL = 0.10930
(SINGLE PASS)

NOTE: EXTINCTION CONSTANT = $\left[\frac{(D)(2.3025)}{L}\right] = (D)(1.079)$
$(L = 2.134\,m)$

∴ EXT. CONST. = 0.11794

ARO-1027

AERONUTRONIC—DEVELOPMENT SKETCH

TABLE B-5

EXAMPLE TABULATION OF SUN PHOTOMETER OPACITY DATA

I.D	L.S.I		PLUME									
	DIVS.	(x scale/2) D	T/T_o RATIO	$\log \frac{T}{T_o}$ D	SUN $\angle$ = 0 TAN^{-1}	COSθ	$(\frac{K_{ext}}{K_{sea}})$ D^*	$\frac{I_{DILUT}}{I_{SEA}}$	$(\frac{I_o}{I_s})$ D_{PL}	L.S.I OPACITY	PLUME OPACITY
3:19	30	.09375	.786	.1046	45°	.707	.0789	0.7	.0517	.195	.214
3:23	27	.08438	.760	.0655	45°	"	.0463	"	.0324	.177	.140
3:24	14	.04375	.760	.0655	45°	"	.0463	"	.0324	.096	.140
3:26	23	.07188	.870	.0555	45°	"	.03925	"	.0275	.153	.120
3:32	18	.05625	.787	.0521	45°	"	.0368	"	.0258	.122	.113
3:35	19	.05938	.920	.0362	45°	"	.0256	"	.0179	.128	.080
3:37	19	.05938	.900	.0458	45°	"	.0324	"	.0227	.128	.100
3:45	19	.05938	—	—	—	—	—	—	—	—	—
3:47	35	.10938	.880	.0555	45°	"	.0392	"	.0275	.223	.120
3:50	23	.07188	.870	.0605	45°	"	.0428	"	.0300	.153	.130

AERONUTRONIC—DEVELOPMENT SKETCH

PREPARED BY / CHECKED BY / APPROVED BY — NAME / DATE / PROJECT — TEMPORARY / PERMANENT

REMARKS: SIZE — DATE 4-28-64 — RUN — SCALE

ARD-7027

TABLE B-6

EXAMPLE TABULATION OF TELEPHOTOMETER OPACITY DATA

PLANT OPERATING CONDITION

I.D.	LSI (mils) DIVS.	LSI (% SCALE/L) D	TELEPHOTOMETER STACK WHITE$_S$	STACK BLACK$_S$	STACK WH$_S$-BLK$_S$	REFERENCE WHITE$_R$	REFERENCE BLACK$_R$	REFERENCE WH$_R$-BLK$_R$	WH-BLK / WH-BLK	D_{TELE}
A (F)	11.75	.01469	680	0		710	0		.958	.01864
A (R)			340			370			.895	.04818
A (B)			220			230			.956	.01954
B (F)	12.25	.01531	680			700			.970	.01323
B (R)			340			350			.970	.01323
B (B)			210			210			1.00	—
C (F)	24.75	.03094	690			715			.395	.04818
C (R)			340			370			.92	.03621
C (B)			210			240			.875	.05799
D (F)	25.—	.03125	640			715			.895	.04818
D (R)			330			370			.892	.04964
D (B)			200			240			.833	.07918
E (F)	37.25	.04781	610			715			.853	.06905
E (R)			320			370			.865	.06299
E (B)			200			235			.809	.09205
F (F)	38.25	.04781	620			715			.867	.06198
F (R)			320			370			.865	.06298
F (B)			185			235			.787	.10403
G (F)	46	.0575	600	0		715	0		.939	.07624
G (R)			315	0		370	0		.851	.07007
G (B)			190	0		230	0		.826	.08302
H (F)	46	.0575	450	0		715	0		.629	.20135
H (R)			—	0		370	0		—	—
H (B)			—	.0		230	0		—	—

AERONUTRONIC — DEVELOPMENT SKETCH

APPROVED BY | PREPARED BY | CHECKED BY | NAME | DATE | PROJECT | PERMANENT | TEMPORARY

REMARKS: GM AUTOMAY SITE CONN. COACH CO. DATE 3-26-74 AIR SCALE AQ.-3 2

APPENDIX C

SUMMARY TABELS OF METHOD 5 TEST DATA

The tables which follow summarize for each site the key stack characteristics monitored during the method 5 tests.

TABLE C-1

SUMMARY OF METHOD 5 TEST DATA, ASPHALTIC CONCRETE PLANT

Run	Stack Gas Temp (°F)	Ave. Gas Velocity (m/s)	Stack Pressure (In. Water)	Water Vapor (% by Vol.)	Mass Concentration		Average Opacity L = 1.37 m
					Actual (g/m^3)	Standard Condition (Dry Gas) (g/m^3)	
5	205	15.3	-15.2	14.0	.040	.061	.028
6*	217	16.6	-15.2	16.4	.027	.041	.029
7	206	15.9	-17.0	17.5	.040	.063	.044
8*	210	15.1	-17.2	20.7	.047	.078	.059
9	213	18.8	-15.5	16.4	.052	.084	.033
10*	193	13.9	-15.5	15.4	.145	.220	.053
11*	160	17.8	-16.0	19.3	.088	.134	.071
12	237	16.8	-14.4	19.4	.100	.150	.061
13	226	17.3	-14.5	19.3	.136	.227	.068
14**	202	16.2	-14.8	16.4	.213	.333	**
15	217	17.0	-14.8	18.3	.241	.388	.097
16	213	17.2	-15.2	20.4	.328	.545	.134
19	238	13.0	-15.5	19.5	.032	.056	.0192
22	218	18.9	-17.9	15.5	.024	.038	.0255
24	238	18.5	-15.4	17.6	.140	.234	.070
26	235	15.8	-14.0	19.5	.418	.707	.232

*Incomplete Traversal
**Optical data unavailable

TABLE C-2

SUMMARY OF METHOD 5 TEST DATA, SLUDGE INCINERATOR

Run	Stack Gas Temp (^{o}F)	Ave. Gas Velocity (m/s)	Stack Pressure (In. Water)	Water Vapor (% by Vol.)	Mass Concentration		Average Opacity L = .914 m
					Actual (g/m^3)	Standard Condition (Dry Gas) (g/m^3)	
1	192	2.90	0 ± 1/2	2.8	-	-	-
2	202	3.96	0	4.1	.0405	.0518	.022
3	198	3.21	0	3.7	.0073	.0094	.023
4	192	4.02	0	3.3	.0096	.0120	.037
5	190	3.45	0	3.5	.0089	.0110	.052
6	196	3.20	0	3.5	.0082	.0105	.031
7	201	3.27	0	2.85	.0232	.0292	.095
8	195	2.91	0	2.0	.0146	.0181	.071
9	209	2.24	0	2.4	.0245	.0311	.135
10	220	3.25	0	2.2	.0595	.0767	.236
11	218	2.77	0	2.2	.0168	.0219	.083
12	217	2.10	0	1.9	.0350	.0451	.225
13	223	2.20	0	1.9	.0437	.0570	.232

TABLE C-3

SUMMARY OF METHOD 5 TEST DATA, REFINERY CATALYTIC CRACKER REGENERATOR

Run	Stack Gas Temp °F	Ave. Gas Velocity (m/s)	Stack Pressure (In. Water)	Water Vapor (% by Vol.)	Mass Concentration		Average Opacity L = 1.466 m
					Actual (g/m^3)	Standard Condition (Dry Gas) (g/m^3)	
1	515	15.4	-.4	13.3	.169*	.358*	.051
2	553	18.8	-.18 ± .1	11.3	.064	.137	.047
3	540	17.2	-.62 ± .17	12.0	.076	.162	.054
4	550	19.0	-.6	12.4	.049	.106	.036
5	563	19.4	-.6	5.0	.033	.067	.048
6	565	19.4	-.6	13.2	.105	.234	.063
7	580	20.9	-.6	13.1	.036	.081	.030
8	590	21.5	-.6	14.0	.043	.098	.070
9	612	21.7	-.2	15.1	.084	.198	.103
10	580	21.8	-.6	14.7	.084	.191	.089
14	570	21.6	-.5	13.9	.145	.328	.124
15	568	20.8	-.5	15.9	.094	.214	.117

* Mass concentration too high. Must have unrecoverable weighing error.

TABLE C-4

SUMMARY OF METHOD 5 TEST DATA, BRASS AND LEAD SMELTER

Run	Stack Gas Temp (°F)	Ave. Gas Velocity (m/s)	Stack Pressure (In. Water)	Water Vapor (% by Vol.)	Mass Concentration Actual (g/m^3)	Mass Concentration Standard Condition (Dry Gas) (g/m^3)	Average Opacity L = 2.134 m
1 Pb	136	3.72	-.25	1.5	.0109	.0123	.0201
2 Pb	142	3.31	-.25	1.7	.0091	.0104	.0140
3 Pb	128	3.78	-.25	1.4	.0094	.0105	-
4 B	126	3.84	-.3	1.6	.0082	.0091	.0091
5 B	112	3.68	-.2	1.1	.0092	.0099	.0173
6 B	118	3.82	-.25	1.1	.0092	.0100	.0092
7 B	125	3.56	-.25	1.2	.0054	.0060	.0267
8 B	105	3.82	-.25	1.8	.0186	.0199	.0536
9 B	114	4.68	-.25	1.4	.0272	.0299	.0711
10 B	116	4.95	-.25	1.2	.0149	.0158	.0293
11 Pb	148	3.93	-.25	2.0	.0206	.0222	.0584
12 Pb	147	4.97	-.25	1.6	.0925	.107	.223

TABLE C-5

SUMMARY OF METHOD 5 TEST DATA, OIL-FIRED POWER PLANT

Run	Stack Gas Temp (°F)	Ave. Gas Velocity (m/s)	Stack Pressure (In. Water)	Water Vapor (% by Vol.)	Mass Concentration* Actual (g/m^3)	Mass Concentration* Standard Condition (Dry Gas) (g/m^3)	Average Opacity L = 3.86 m
2	337	19.8	-.6	10.2	.0104	.0174	.0050
3	335	19.7	-.8	10.3	.0086	.0144	.0101
4	329	19.5	-.6	10.8	.0227	.0329	.0114
5	304	15.2	-.6	10.2	.0151	.0243	.0083
6	319	18.9	-.6	10.3	.0069	.0114	.0113
7	294	15.1	-.2	10.1	.0103	.0163	.0187
8	311	15.7	-.3	14.0	.0050	.0085	.0102
9	308	14.5	-1.0	9.9	.0165	.0266	.0172
10	324	17.8	-.2	9.8	.0118	.0184	.0101

* Corrected for Soluble Sulfate-Sulfite